UCLA
UCLA Electronic Theses and Dissertations

Title

To Define the Mechanistic Basis for the Effect of RECK Alternative Isoform Expression on Cell Migration

Permalink

https://escholarship.org/uc/item/4nh7m1vx

Author

Lee, Ha Neul

Publication Date

2019

Peer reviewed|Thesis/dissertation

eScholarship.org Powered by the California Digital Library
University of California

UNIVERSITY OF CALIFORNIA

Los Angeles

To Define the Mechanistic Basis for the Effect of RECK Alternative Isoform Expression on Cell Migration

A dissertation submitted in partial satisfaction of the

requirements for the degree Doctor of Philosophy

in Molecular Biology

by

Ha Neul Lee

2019

© Copyright by

Ha Neul Lee

2019

ABSTRACT OF THE DISSERTATION

To Define the Mechanistic Basis for the Effect

of RECK Alternative Isoform Expression on Cell Migration

by

Ha Neul Lee

Doctor of Philosophy in Molecular Biology

University of California, Los Angeles, 2019

Professor Hilary Ann Coller, Chair

For many types of animal cells, migration is essential for their physiological function. Long distance crawling is required for the development of a nervous system and for the ability of macrophages to accumulate at sites of infection. In response to a wound, resident fibroblasts migrate to the wound site and promote the wound healing process. Furthermore, cancer metastasis involves the ability of cancer cells to transform their morphology and acquire an ability to migrate. A better understanding of cell migration would have implications for normal development and

could yield therapies for multiple different disease states, including fibrosis, atherosclerosis, and metastasis.

Alternative polyadenylation (APA) is the process by which the same genetic locus can produce multiple transcripts ending at different polyadenylation sites. Coding sequence APA can change the length of the amino acid and can also switch the function of the protein. Proliferating cells, cancer cells, and stem cells in the early stages of mouse development and tumors tend to use proximal polyadenylation sites and commonly show rapid cell migration. Our laboratory has discovered that fibroblast migration can be regulated through polyadenylation site selection. To date, however, no studies have been performed to research how cell migration and invasion can be controlled by APA.

Reversion-inducing-cysteine-rich protein with kazal-like motifs (RECK) suppresses cell migration. Previous studies have documented a role for RECK on the cell surface in inhibiting MMP activity via its Kazal-like motifs. RECK has also been implicated in tubulin dynamics and in anterior-posterior polarity. Our lab discovered through an RNA-Seq-based screen that there are short and long RECK isoforms that are generated by coding region alternative polyadenylation.

In this dissertation, I explain how cell migration and invasion can be controlled by APA via alternative isoform expression of the RECK protein. I show that the short RECK isoform promotes cell migration and that this result is mediated by short RECK and long (canonical) RECK interaction. Furthermore, I propose that RECK APA can regulate cell migration not only through its established role of modifying matrix metalloproteinases but also via its roles in affecting tubulin post-translational modifications (PTMs). These studies provide a much more detailed and mechanistic model for the biological functions of RECK alternative isoform use.

The dissertation of Ha Neul Lee is approved.

Luisa M Iruela-Arispe

Tracy L Johnson

William Edward Lowry

Jorge Torres

Hilary Ann Coller, Committee Chair

University of California, Los Angeles

2019

DEDICATION

This dissertation is dedicated to my grandmother,

Ilsoon Park, who is in heaven.

TABLE OF CONTENTS

Abstract of the Dissertation		ii
Committee Page		iv
Dedication Page		v
List of Figures		vii
Acknowledgements		ix
Vita		xi
Chapter 1:	Introduction	1
	References	14
Chapter 2:	RECK isoforms have opposing effects on cell migration (Lee *et al.*, Mol Biol Cell 2018)	24
	References	37
Chapter 3:	RECK isoforms differentially regulate fibroblast migration by modulating tubulin post-translational modifications. (Lee *et al.*, Biochem Biophys Res Commun. 2019)	51
	References	59
Chapter 4:	Conclusions and future studies	60
	References	65

LIST OF FIGURES

Chapter 1:

No figures.

Chapter 2:

Figure 2-1:	Short RECK isoform levels are elevated in proliferating and TGF-β–treated fibroblasts and cancer cells.	28
Figure 2-2:	The short RECK isoform is essential for cell migration.	30
Figure 2-3:	The short RECK isoform interacts with the long RECK isoform.	31
Figure 2-4:	A short RECK–long RECK complex is localized in the perinuclear region and on the cell surface.	32
Figure 2-5:	The Kazal-like motif domain is important for short RECK binding to long RECK.	33
Figure 2-6:	The short RECK isoform competes with MMP9 for binding to the long RECK isoform.	34
Figure S2-1:	Validation of the short RECK-specific antibody.	44
Figure S2-2:	RNA-Seq read counts from The Cancer Genome Atlas were compiled for different types of cancer for the short and long isoforms of RECK.	44
Figure S2-3:	RECK isoforms do not affect cell proliferation and RECK isoform overexpression does not affect migration through Matrigel.	45
Figure S2-4:	RECK isoforms do not activate AKT, ERK, or JNK pathways.	46
Figure S2-5:	Long RECK interacts with itself and short RECK interacts with itself.	47

Figure S2-6: Further validation of the interaction between the short and long RECK isoforms at the cell surface. 48

Figure S2-7 The portion of long RECK residing between amino acids 635 and 773 is important for binding to short RECK, while the C terminus of long RECK is important for long RECK dimerization. 49

Figure S2-8: The short RECK isoform does not affect dimerization of the long RECK isoform. 50

Chapter 3:

Figure 3-1: RECK isoforms differentially regulate cell migration and tubulin PTM levels. 54

Figure 3-2: Tubulin PTMs can regulate cell migration. 55

Figure 3-3: Knockdown of αTAT and TTL reverts faster migration with long RECK knockdown. 56

Figure 3-4: MMP9 and the integrin signaling pathway regulate levels of acetyl-tubulin. 57

ACKNOWLEDGEMENTS

I was able to complete the doctoral program at UCLA with the help of many people. I would like to take this opportunity to express my gratitude.

I would first like to thank Dr. Hilary Coller, my thesis advisor and research mentor for her support and excellent guidance over the past five years. Luckily, I was able to have the chance to be her first graduate student at UCLA. She has given me the chance to grow as a scientist as well as a nice person. She was always sharp in data analysis but warm to her students. Especially, every time I was in trouble, the comfort she gave me has raised me up. I also thank her for her advice and support for my career path.

I would like to thank the members of my committee: Dr. Luisa M. Iruela-Arispe, Dr. Tracy L. Johnson, Dr. William Edward Lowry, Dr. Jorge Torres for their critical evaluation and valuable suggestions. Special thanks go to Luisa, Bill, and Jorge who wrote me recommendation letters whenever I asked.

I would also thank all Coller lab members for their support. I believe that my project was able to move forward with the many advice I got from the lab meeting and lab management by David. In Particular, I appreciate Dr. Mithun Mitra and undergraduate students (Oye Bosompra, Nadin Rashed, and Linda Ho) who passionately participated in the RECK project.

I must also thank Dr. Jeffrey A. long (confocal microscopes and real-time PCR machine), Dr. Jose Rodriguez (Duo flow), The Center of Excellence in NanoBiophysics, University of Southern California (MALS), and The Broad Stem Cell Research Center (confocal microscopes and Incucyte) for allowing me to use their instruments. The research contained in

this thesis was funded by Life Science Innovation Fund, the Whitcome Fellowship, and the UCLA Dissertation Year Fellowship.

I, who had never taken a class in English, was able to finish my coursework at UCLA with the help from my classmates, ACCESS XX. Special thanks to Calvin Leung, Adriana Corvalan, Jane Seo, and Hanjun Kim.

I would also like to extend my sincere thanks to those who have supported me mentally from outside of the UCLA. Thanks to my parents in Korea who always prayed for our family. I would also like to thank members of the Calvary Faith Church. Finally, I would also thank my lovely wife Lily and daughters Luri, Elli, and Cali from the bottom of my heart.

VITA

EDUCATION

09/2013 – 03/2019	University of California, Los Angeles, Molecular Biology Interdepartmental Ph.D. Program (expected)
09/2006 – 08/2008	Seoul National University, Dept.of Medicine, Graduate School**,** Seoul, South Korea Degree: Master of Science in Medicine Thesis: Derivation of mesenchymal stem cells from human embryonic stem cells
03/1999 – 02/2003	Yonsei University, College of Liberal Arts and Sciences, Seoul, South Korea Degrees: Bachelor of Science Distinction: Graduated with High Honors

AWARDS

2018-2019	Dissertation Year Fellowship ($36,818.77)
2017	ASCB Travel Award
2017-2018	The Philip Whitcome Pre-doctoral Fellowship ($23,376)
2016-2018	Life Science Innovation Fund ($10,000)

PUBLICATIONS

1. **HN Lee*,** O Bosompra* and HA Coller: RECK isoforms differentially regulate fibroblast migration by modulating tubulin post-translational modifications. **Biochem Biophys Res Commun.** 2019 Jan 28. pii: S0006-291X(19)30077-4. doi: 10.1016/j.bbrc.2019.01.063. **(*equally contributed)**
2. **HN Lee,** M Mitra, O Bosompra, DC Corney, EL Johnson, N Rashed, LD Ho, and HA Coller: RECK isoforms produced via alternative polyadenylation have opposing effects on cell migration. **Mol Biol Cell.** 2018 Jun 6:mbcE17120708. doi: 10.1091/mbc.E17-12-0708.
3. M Mitra, **HN Lee** and HA Coller: Determining genomewide transcript decay rates in proliferating and quiescent human fibroblasts. **J Vis Exp.** 2018 Jan 2;(131). doi: 10.3791/56423.
4. J Yoo *, **HN Lee***, I Choi, D Choi, HK Chung, KE Kim, S Lee, B Aguilar, J Kang, E Park, YS Lee, YS Maeng, CJ Koh and YK Hong: Opposing regulation of PROX1 by Interleukin-3 receptor alpha and NOTCH directs a differential host cell fate reprogramming by Kaposi Sarcoma Herpes Virus. **PLoS Pathog.**, 2012 June 8(6):e1002770 (*equally contributed) (PMID: 22719258)

5. EJ Lee*, HJ Kang*, **HN Lee**, SK Kang, KH Kim, SW Lee, G Lee, YB Park, HS Kim: New culture system for human embryonic stem cells: Autologous mesenchymal stem cell feeder without exogenous fibroblast growth factor 2. **Differentiation**, 2012 Jan;83(1):92-100. (*equally contributed) (PMID: 22099180)

6. I Choi, YS Lee, HK Chung, D Choi, T Ecoiffier, **HN Lee**, KE Kim, S Lee, EK Park, YS Maeng, NY Kim, RD Ladner, NA Petasis, CJ Koh, L Chen, HJ Lenz, and YK Hong: Interleukin-8 reduces post-surgical lymphedema formation by promoting lymphatic vessel regeneration. **Angiogenesis**, 2012 Sep 4. (PMID: 22945845)

7. B Aguilar, I Choi, D Choi, HK Chung, S Lee, J Yoo, YS Lee, YS Maeng, **HN Lee**, E Park, KE Kim, NY Kim, JM Baik, JU Jung, CJ Koh, and YK Hong: Lymphatic Reprogramming by Kaposi Sarcoma Herpes Virus Promotes the Oncogenic Activity of the Virus-Encoded G-protein Coupled Receptor. **Cancer Res.** 2012 Aug 31. (PMID: 22942256)

8. I Choi*, HK Chung*, S Ramu, **HN Lee**, KE Kim, S Lee, J Yoo, D Choi, YS Lee, B Aguilar, and YK Hong: Visualization of lymphatic vessels by Prox1-promoter directed GFP reporter in a bacterial artificial chromosome-based transgenic mouse. **Blood**. 2011 Jan 6;117(1):362-5 (*equally contributed) (PMID:20962325)

9. J Yoo, J Kang, **HN Lee**, B Aguilar, D Kafka, S Lee, I Choi, J Lee, S Ramu, J Haas, CJ Koh, YK Hong: Kaposin-B enhances the PROX1 mRNA stability during lymphatic reprogramming of vascular endothelial cells by Kaposi's sarcoma herpes virus. **PLoS Pathog.** 2010 Aug 12;6(8):e1001046. (PMID:20730087)

10. EJ Lee*, **HN Lee***, HJ Kang, KH Kim, J Hur, HJ Cho, J Lee, HM Chung, J Cho, MY Cho, SK Oh, SY Moon, YB Park, and HS Kim: Novel embryoid body-based method to derive mesenchymal stem cells from human embryonic stem cells. **Tissue Eng Part A**. 2010 Feb;16(2):705-15. (*equally contributed) (PMID:19895342)

ORAL PRESENTATIONS

1. RECK isoforms produced via alternative polyadenylation have opposing effects on cell migration 2018 UCLA Biological Chemistry seminar

2. Alternative Polyadenylation, a Novel Mechanism of Cell Migration and Invasion: A Focus on RECK 2016 ASCB, San Francisco

3. Alternative Polyadenylation, a Novel Mechanism of Cell Migration and Invasion: A Focus on RECK 2016 UCLA MCDB retreat, Arrowhead

CHAPTER 1:

Introduction

Cell Migration

Mechanisms of Cell Migration

Cell migration is an evolutionarily conserved mechanism critical for proper development and the function of uni- and multicellular organisms (Mayor and Etienne-Manneville, 2016). For many types of animal cells, migration is essential for their physiological function. For example, long-distance crawling is required for the development of a nervous system (Lake and Heuckeroth, 2013) and for the ability of macrophages to accumulate at sites of infection (Verollet et al., 2011).

To facilitate cell migration, cells change their intracellular and extracellular environment at the same time (Friedl and Wolf, 2003). In the intracellular region, migrating cells remodel their cytoskeleton to increase their polarity and ensure the directionality of their migration (Etienne-Manneville, 2013). Cells remodel tubulin and actin to induce their protrusion for migration, forming filopodia and lamellipodia towards the direction of cell migration. The extended filopodia and lamellipodia can adhere to the extracellular matrix by a focal complex consisting of vinculin, talin, and integrin. Using cell protrusions fixed by a focal complex, cells can move forward by contracting their rear body (Humphries et al., 2007; Mattila and Lappalainen, 2008). On the cell surface, cells secrete matrix metalloproteinases (MMPs) and digest extracellular matrix proteins such as collagens and laminin to allow them to detach and reattach to their surface as needed for migration (Friedl and Wolf, 2003). MMPs, structurally related zinc-dependent endopeptidases, degrade extracellular material. MMPs, such as MMP2 and MMP9, or membrane-anchored, such as MT1-MMP, can be secreted into the extracellular environment. MMPs can promote cell migration and invasion by cleaving and regulating extracellular molecules. For instance, MMP2 cleaves laminin-5 to promote migration of breast epithelial cells (Giannelli et al., 1997). MMPs can also promote cancer cell invasion and metastasis (Nabeshima et al., 2002), for instance by

facilitating degradation of the basement membrane (Liotta et al., 1980; Tsunezuka et al., 1996). The role of MMPs in promoting migration and invasion includes clearing away ECM occluding a cell's progression. In addition, MMPs can generate epitopes that actively promote migration (Zuo et al., 1998), and MMP activity can result in an arrangement of matrix that promotes migration (Nabeshima et al., 2002). Further, MMPs can also perform proteolysis of proteins involved in adhesion and thereby promote cancer cell invasion (Belkin et al., 2001; Kajita et al., 2001). Coordinating both intracellular and extracellular changes is required for productive movement (Bouchet and Akhmanova, 2017).

Cell Migration Regulators

Several signaling pathways have been well established as regulators of cell migration. The AKT pathway, which is a pro-survival pathway, is important for the formation of membrane protrusions like filopodia at the leading edge of a migrating cell (Montero et al., 2003; Xue and Hemmings, 2013). The inflammation-associated JNK pathway promotes cell migration by multiple mechanisms, including by phosphorylating paxillin and thereby promoting the turnover of focal adhesions needed for migration (Huang et al., 2004a; Huang et al., 2004b). ERK signaling also promotes migration (Huang et al., 2004a), and among its targets, phosphorylation of FAK and myosin light chain kinase are good candidates as mechanisms through which ERK promotes migration (Hunger-Glaser et al., 2003; Klemke et al., 1997). In addition, the three signaling pathways mentioned above can commonly regulate cell invasion through extracellular matrix digestion by controlling the transcription of MMP2 and MMP9 (Wu et al., 2015). Cells can regulate cell migration by regulating the activity of these signaling pathways in many different ways.

First, the activity of the signaling pathway can be regulated by ligands from inside or outside of the cells. Growth factors such as platelet-derived growth factor (PDGF), epidermal growth factor (EGF), fibroblast growth factor (FGF), and transforming growth factor beta (TGF-β) activate the AKT, ERK, and JNK signaling pathways (Borkham-Kamphorst and Weiskirchen, 2016; Jiang et al., 2006; Massague, 2012; Ornitz and Itoh, 2015; Ying et al., 2017). Secondly, the cell migration pathway can also be regulated by microRNAs. MicroRNAs bind to target RNAs and silence the expression of the target protein by inhibiting translation of target RNA (Ha and Kim, 2014). MicroRNAs can control cell migration by targeting ligands that activate migration-related pathways, mediators, inhibitors, or activators involved in the signaling pathway (Rajasekaran et al., 2015). Thirdly, cell migration also can be regulated by controlling the rate of extracellular matrix digestion through modulation of the activity of MMPs. MMPs are secreted in an inactive state, then converted to an active form. Once active, they can cleave proteins in the extracellular matrix. ProMMPs are maintained in an inactive state in which their catalytic domain is sequestered via thiol-Zn^{2+} interactions. When the thiol-Zn^{2+} interaction of proMMP is cleaved by proteolytic or non-proteolytic processing, the catalytic domain is exposed and proMMPs are converted to active MMPs. Proteins involved in proteolytic cleavage include Furin and MT1-MMP, while reactive oxygen species (ROS) participate in non-proteolytic cleavage (Ra and Parks, 2007). MMP activity can be suppressed by proteins containing the Kazal domain, which can prevent access of the substrate to the active site of MMPs. Reversion-inducing-cysteine-rich protein with Kazal-like motifs (RECK) is an example of a protein with Kazal-like motifs that inhibit MMPs (Takahashi et al., 1998b).

Cell Migration and Disease

A better understanding of cell migration would yield therapies for multiple different disease states, including fibrosis, atherosclerosis, and metastasis. During wounding, many of the organs of the body, such as heart (Chen and Frangogiannis, 2013), liver (Dooley and ten Dijke, 2012), and lung (Acharya et al., 2008), secrete TGFβ. Secreted TGFβ activates fibroblast proliferation and migration and induces fibroblasts to migrate to the site of injury (Acharya et al., 2008; Chen and Frangogiannis, 2013; Dooley and ten Dijke, 2012). One of the main causes of atherosclerosis is the migration of activated vascular smooth muscle cells to the site of damaged endothelial cells (Rudijanto, 2007). Furthermore, in the context of cancer, metastasizing cells remodel their extracellular environment with increased secretion of matrix metalloproteinases (MMPs) (Deryugina and Quigley, 2006), and gain increased motility through epithelial to mesenchymal transition (Kalluri and Weinberg, 2009).

RECK (Reversion-inducing cysteine-rich protein with Kazal motifs)

The RECK protein was isolated by cDNA expression cloning as a gene that induces flat morphology when expressed in a ras-transformed NIH 3T3 cell line (Takahashi et al., 1998a). RECK encodes a C-terminal GPI-membrane-anchored 110 kDa protein with multiple serine protease inhibitor motifs. RECK has been shown to inhibit cell migration by suppressing the activity of MMPs (Oh et al., 2001).

Role of RECK in Cell Migration

RECK is characterized for its role in inhibition of cell migration and invasion. RECK is an inhibitor of members of the MMP family (MMP-2, MMP-9 and MT1-MMP) and the a disintegrin and metalloproteinase family (ADAM10) (Chang et al., 2008; Hong et al., 2014; Miki et al., 2007; Oh et al., 2004; Oh et al., 2001; Takahashi et al., 1998a). Because these metalloproteinases are critical regulators of key signaling molecules that control the tissue microenvironment, including TGF-β, VEGF, and E-cadherin, RECK is expected to play an important role as a controller of the signaling and structural components of the tissue microenvironment. RECK-deficient mice die at embryonic day 10.5 as a result of reduced extracellular matrix integrity with reduced type I collagen and halted vascular development (Oh et al., 2001). Because of the absence of RECK, the rate of angiogenesis is so fast that it does not have enough time for vascular maturation (Oh et al., 2001). RECK has also been implicated in tubulin dynamics and in anterior-posterior polarity (Morioka et al., 2009). $RECK^{-/-}$ MEFs are defective in the formation of focal adhesions, have increased levels of GTP-bound Rac1 and Cdc42 activity, and lower levels of detyrosinated tubulin (Morioka et al., 2009). Thus, RECK plays a role in inhibiting cell migration by affecting both inside and outside of the cell.

Structure of RECK

The protein structure of RECK is still unclear. RECK is a heavily glycosylated protein, which makes it difficult to identify structures through X-ray crystallography. Nonetheless, the Noda group attempted to reveal the structure of RECK through transmission electron microscopy (Omura et al., 2009). According to this study, RECK forms a cowbell-shaped dimer with the two projections facing outward. However, this study has a resolution of only 25.2 **Å**, which makes it difficult to describe the detailed RECK structure.

How RECK interacts with MMPs can only be indirectly studied through the structure of the previously known Kazal-like motif. The Kazal domain, which has a central alpha-helix, a short two-stranded antiparallel beta-sheet, and several disulfide bonds, often forms a tandem array. The amino terminal segment of Kazal-like motif binds to the active site of the target protease and inhibits their function (Schlott et al., 2002; Stubbs et al., 1997; van de Locht et al., 1995)

RECK and Disease

RECK is widely expressed in normal tissue and nonneoplastic cell lines and is strongly suppressed in some tumor-derived cell lines and in cells transformed by oncogenes (Sasahara et al., 1999a; Sasahara et al., 1999b; Takahashi et al., 1998a). RECK RNA levels are downregulated in a number of tumors (Noda and Takahashi, 2007) including hepatocarcinomas (Furumoto et al., 2001), non-small cell lung cancer (Takenaka et al., 2005), prostate cancer (Rabien et al., 2007), pancreatic cancer (Masui et al., 2003), and breast cancer (Span et al., 2003). Low RECK levels have consistently been identified as an independent and significant factor predicting poor

prognosis (Furumoto et al., 2001; Noda and Takahashi, 2007; Rabien et al., 2007; Takenaka et al., 2005). Reintroduction of RECK into cancer cells reduces their ability to invade into matrigel and to metastasize to lung and lymph nodes (Takahashi et al., 1998a).

The effectiveness of some established anti-tumor treatments may reflect their effects on RECK. For example, the anti-angiogenic and anti-metastatic agents histone deacetylase inhibitors (Liu et al., 2003) and non-steroidal anti-inflammatory drugs (Liu et al., 2002) both induce RECK mRNA levels and protein levels. Manipulating RECK levels has been repeatedly proposed as a promising approach to therapy (Hsu et al., 2006; Rabien et al., 2007), but no effective strategies to manipulate RECK are currently available as therapies for cancer patients.

Alternative polyadenylation (APA)

Alterative polyadenylation events result in transcript isoforms with different 3' ends (Di Giammartino et al., 2011; Elkon et al., 2013; Tian and Manley, 2013). Because many of the recognition sites for regulators of post-transcriptional events such as microRNA recognition sites or RNA binding protein recognition sites are localized to transcript 3' UTRs, alternative polyadenylation can potentially result in altered transcript localization (Andreassi and Riccio, 2009; Michaud et al., 2014; Solomon et al., 2003), translatability (Mayr and Bartel, 2009; Pinto et al., 2011; Spies et al., 2013; Yoon et al., 2013), or stability (Allen et al., 2013; Geisberg et al., 2014; Gupta et al., 2014; Mayr and Bartel, 2009; Miyamoto et al., 1996). When alternative polyadenylation occurs among polyadenylation sites in 3' UTRs (UTR-APA), the resulting isoforms can include or exclude microRNA or RNA binding protein recognition sites. In cases in which the proximal polyadenylation site resides within the coding sequence (coding-APA), alternative polyadenylation, often coupled with alternative splicing, can result in distinct protein isoforms. These distinct protein isoforms have the potential to encode proteins that compete with each other or have different functions (Alt et al., 1980; Early et al., 1980; Lu et al., 2003; Rogers et al., 1980; Solomon et al., 2003; Vorlova et al., 2011). Computational analysis of mammalian genomes led to estimates that approximately 50% of human genes and 30% of mouse genes possess multiple polyadenylation sites (Tian et al., 2005), making alternative polyadenylation potentially a powerful mechanism of global gene regulation.

Change of APA according to the cell environment

The development of protocols to specifically map mRNA cleavage and polyadenylation

sites using high throughput sequencing (Derti et al., 2012; Jan et al., 2011; Mangone et al., 2010; Ozsolak et al., 2010; Sharon et al., 2013; Shepard et al., 2011; Sun et al., 2012) has resulted in a better appreciation of the global patterns of alternative polyadenylation in different cellular states, tissues and different species. 3' UTR lengths have been discovered to differ for a large fraction of the genome between different tissues (Hilgers et al., 2011; Lianoglou et al., 2013; Wang et al., 2008) and during development (Ji et al., 2009; Ji and Tian, 2009; Lianoglou et al., 2013; Shepard et al., 2011; Ulitsky et al., 2012). Polyadenylation site usage is more similar among samples derived from the same tissue from different species than between different tissues within a single species (Derti et al., 2012). Among tissues, neurons express particularly long 3' UTRs isoforms, while gonads express transcripts with unusually short 3' UTRs (Miura et al., 2013; Smibert et al., 2012). In general, non-dividing cells (Elkon et al., 2012) and differentiated cells (Lianoglou et al., 2013; Masamha et al., 2014; Mayr and Bartel, 2009; Sandberg et al., 2008; Ulitsky et al., 2012) predominantly use distal polyadenylation sites, while proliferating cells (Elkon et al., 2012; Lin et al., 2012; Sandberg et al., 2008), stem cells (Ji and Tian, 2009) and cancer cell lines (Masamha et al., 2014; Mayr and Bartel, 2009) generally use proximal polyadenylation sites. Alternative polyadenylation has also been implicated in a disease states in addition to cancer, such as cardiac hypertrophy (Park et al., 2011), hematologic diseases such as thalassemia (Higgs et al., 1983; Hollerer et al., 2014), and neurodegenerative disease such as fragile-X syndrome (Hollerer et al., 2014; Tassone et al., 2011).

Polyadenylation factors involved in APA

Cleavage and polyadenylation of mRNA transcripts is the result of the coordinated activity of complexes involving approximately 85 different proteins that serve as an interface between

cleavage and polyadenylation and other processes and pathways including splicing (Shi et al., 2009). The cleavage and polyadenylation specificity factor (CPSF) complex binds a hexameric sequence in a 50-nt region upstream of the cleavage site (Akman and Erson-Bensan, 2014; Elkon et al., 2012; Elkon et al., 2013). The canonical version of this poly(A) signal (PAS) is AAUAAA, but similar noncanonical sequences are also used. About 14-70 nucleotides downstream of the PAS, a U/GU-rich region provides a binding site for the CSTF2 (CstF-64) subunit of the CstF complex (Millevoi and Vagner, 2010). Cleavage and polyadenylation are then performed with the assistance of other proteins and complexes including CFI (cleavage factor I), CFII (cleavage factor II), symplekin, and poly(A) polymerase. The selection of proximal versus distal polyadenylation sites likely reflects a combination of changes in the abundance of *trans*-acting regulators such as protein members of the cleavage and polyadenylation complexes or splicing factors (Takagaki et al., 1996), and *cis*-acting elements such as RNA motifs and epigenetic changes affecting chromatin (Akman and Erson-Bensan, 2014; Di Giammartino et al., 2011; Lee and Chen, 2013; Lin et al., 2012). Increased levels of cleavage and polyadenylation factors have been reported in proliferating compared with nondividing cells (Elkon et al., 2012; Shell et al., 2005), and promoter analysis of cleavage and polyadenylation factors including CSTF2 (CstF-64), CSTF3 (CstF-77), and CPSF2 showed that these genes are responsive to the activity of E2F transcription factors (Elkon et al., 2012).

Change of protein function by APA

Coding-APA can result in proteins with divergent functions encoded by the same genomic locus. Alternative polyadenylation controls the switch from membrane-bound to secreted isoforms of the immunoglobulin M heavy chain that occurs during B lymphocyte differentiation (Alt et al., 1980;

Early et al., 1980; Rogers et al., 1980). Alternative polyadenylation can also result in the synthesis of isoforms of transmembrane proteins lacking the anchoring transmembrane domain and the intracellular kinase function (Vorlova et al., 2011). These soluble isoforms can act as decoy receptors for the signaling pathway (Vorlova et al., 2011). As another example, use of an intronic alternative polyadenylation site of TCF7L2 generates an isoform that retains the β-catenin binding domain but lacks the high mobility group box DNA-binding domain and may inhibit TCF7L2-dependent gene expression by sequestering β-catenin (Locke et al., 2011). In another study, alternative polyadenylation was discovered to result in a truncated isoform of glutamyl-prolyl tRNA synthetase, part of a complex that inhibits translation (Yao et al., 2012). The shorter protein product was found to shield transcripts from the inhibitory complex, and thereby facilitate their translation. In a final report, an isoform of the cyclin D1 gene in which the inclusion of an intron results in the use of an earlier polyadenylation site was studied (Solomon et al., 2003). This alternative isoform differs from the canonical protein in that it displays constitutive nuclear localization and exhibits transforming potential (Solomon et al., 2003).

Based on the close association between active APA and cancer cells and early development, there was a reason to believe that APA is related to cell migration, but previous studies had not demonstrated this connection. Furthermore, to understand the molecular mechanism of RECK, it is necessary to identify the protein structure of high resolution. In the following two chapters, I demonstrate an exploration of questions related to RECK, APA and cell migration.

In chapter 2, I explain how cell invasion can be controlled by APA through changes in the expression of isoforms of the RECK protein. I show that RNA and protein levels of the short form of RECK are increased in cell migratory conditions by APA. I then show that the short form of RECK functions as a dominant negative form of canonical RECK through protein-protein interactions. Short RECK can interfere with canonical RECK's ability to suppress MMP activity. In chapter 3, I demonstrate that RECK APA can also contribute to cell migration through tubulin PTM regulation in addition to invasion.

REFERENCES

Acharya, P. S., Majumdar, S., Jacob, M., Hayden, J., Mrass, P., Weninger, W., Assoian, R. K., and Pure, E. (2008). Fibroblast migration is mediated by CD44-dependent TGF beta activation. J Cell Sci *121*, 1393-1402.

Akman, H. B., and Erson-Bensan, A. E. (2014). Alternative polyadenylation and its impact on cellular processes. MicroRNA *3*, 2-9.

Allen, M., Bird, C., Feng, W., Liu, G., Li, W., Perrone-Bizzozero, N. I., and Feng, Y. (2013). HuD promotes BDNF expression in brain neurons via selective stabilization of the BDNF long 3'UTR mRNA. PloS one *8*, e55718.

Alt, F. W., Bothwell, A. L., Knapp, M., Siden, E., Mather, E., Koshland, M., and Baltimore, D. (1980). Synthesis of secreted and membrane-bound immunoglobulin mu heavy chains is directed by mRNAs that differ at their 3' ends. Cell *20*, 293-301.

Andreassi, C., and Riccio, A. (2009). To localize or not to localize: mRNA fate is in 3'UTR ends. Trends in cell biology *19*, 465-474.

Belkin, A. M., Akimov, S. S., Zaritskaya, L. S., Ratnikov, B. I., Deryugina, E. I., and Strongin, A. Y. (2001). Matrix-dependent proteolysis of surface transglutaminase by membrane-type metalloproteinase regulates cancer cell adhesion and locomotion. The Journal of biological chemistry *276*, 18415-18422.

Borkham-Kamphorst, E., and Weiskirchen, R. (2016). The PDGF system and its antagonists in liver fibrosis. Cytokine Growth F R *28*, 53-61.

Bouchet, B. P., and Akhmanova, A. (2017). Microtubules in 3D cell motility. J Cell Sci *130*, 39-50.

Chang, C. K., Hung, W. C., and Chang, H. C. (2008). The Kazal motifs of RECK protein inhibit MMP-9 secretion and activity and reduce metastasis of lung cancer cells in vitro and in vivo. Journal of cellular and molecular medicine *12*, 2781-2789.

Chen, W., and Frangogiannis, N. G. (2013). Fibroblasts in post-infarction inflammation and cardiac repair. Biochim Biophys Acta *1833*, 945-953.

Derti, A., Garrett-Engele, P., Macisaac, K. D., Stevens, R. C., Sriram, S., Chen, R., Rohl, C. A., Johnson, J. M., and Babak, T. (2012). A quantitative atlas of polyadenylation in five mammals. Genome Res *22*, 1173-1183.

Deryugina, E. I., and Quigley, J. P. (2006). Matrix metalloproteinases and tumor metastasis. Cancer Metastasis Rev *25*, 9-34.

Di Giammartino, D. C., Nishida, K., and Manley, J. L. (2011). Mechanisms and consequences of alternative polyadenylation. Molecular cell *43*, 853-866.

Dooley, S., and ten Dijke, P. (2012). TGF-beta in progression of liver disease. Cell Tissue Res *347*, 245-256.

Early, P., Rogers, J., Davis, M., Calame, K., Bond, M., Wall, R., and Hood, L. (1980). Two mRNAs can be produced from a single immunoglobulin mu gene by alternative RNA processing pathways. Cell *20*, 313-319.

Elkon, R., Drost, J., van Haaften, G., Jenal, M., Schrier, M., Vrielink, J. A., and Agami, R. (2012). E2F mediates enhanced alternative polyadenylation in proliferation. Genome biology *13*, R59.

Elkon, R., Ugalde, A. P., and Agami, R. (2013). Alternative cleavage and polyadenylation: extent, regulation and function. Nature reviews Genetics *14*, 496-506.

Etienne-Manneville, S. (2013). Microtubules in cell migration. Annu Rev Cell Dev Biol *29*, 471-499.

Friedl, P., and Wolf, K. (2003). Tumour-cell invasion and migration: diversity and escape mechanisms. Nature reviews Cancer *3*, 362-374.

Furumoto, K., Arii, S., Mori, A., Furuyama, H., Gorrin Rivas, M. J., Nakao, T., Isobe, N., Murata, T., Takahashi, C., Noda, M., and Imamura, M. (2001). RECK gene expression in hepatocellular carcinoma: correlation with invasion-related clinicopathological factors and its clinical significance. Reverse-inducing--cysteine-rich protein with Kazal motifs. Hepatology *33*, 189-195.

Geisberg, J. V., Moqtaderi, Z., Fan, X., Ozsolak, F., and Struhl, K. (2014). Global analysis of mRNA isoform half-lives reveals stabilizing and destabilizing elements in yeast. Cell *156*, 812-824.

Giannelli, G., Falk-Marzillier, J., Schiraldi, O., Stetler-Stevenson, W. G., and Quaranta, V. (1997). Induction of cell migration by matrix metalloprotease-2 cleavage of laminin-5. Science *277*, 225-228.

Gupta, I., Clauder-Munster, S., Klaus, B., Jarvelin, A. I., Aiyar, R. S., Benes, V., Wilkening, S., Huber, W., Pelechano, V., and Steinmetz, L. M. (2014). Alternative polyadenylation diversifies post-transcriptional regulation by selective RNA-protein interactions. Molecular systems biology *10*, 719.

Ha, M., and Kim, V. N. (2014). Regulation of microRNA biogenesis. Nat Rev Mol Cell Bio *15*, 509-524.

Higgs, D. R., Goodbourn, S. E., Lamb, J., Clegg, J. B., Weatherall, D. J., and Proudfoot, N. J. (1983). Alpha-thalassaemia caused by a polyadenylation signal mutation. Nature *306*, 398-400.

Hilgers, V., Perry, M. W., Hendrix, D., Stark, A., Levine, M., and Haley, B. (2011). Neural-specific elongation of 3' UTRs during Drosophila development. Proceedings of the National Academy of Sciences of the United States of America *108*, 15864-15869.

Hollerer, I., Grund, K., Hentze, M. W., and Kulozik, A. E. (2014). mRNA 3'end processing: A tale of the tail reaches the clinic. EMBO molecular medicine *6*, 16-26.

Hong, K. J., Wu, D. C., Cheng, K. H., Chen, L. T., and Hung, W. C. (2014). RECK inhibits stemness gene expression and tumorigenicity of gastric cancer cells by suppressing ADAM-mediated Notch1 activation. J Cell Physiol *229*, 191-201.

Hsu, M. C., Chang, H. C., and Hung, W. C. (2006). HER-2/neu represses the metastasis suppressor RECK via ERK and Sp transcription factors to promote cell invasion. The Journal of biological chemistry *281*, 4718-4725.

Huang, C., Jacobson, K., and Schaller, M. D. (2004a). MAP kinases and cell migration. Journal of cell science *117*, 4619-4628.

Huang, C., Jacobson, K., and Schaller, M. D. (2004b). A role for JNK-paxillin signaling in cell migration. Cell Cycle *3*, 4-6.

Humphries, J. D., Wang, P., Streuli, C., Geiger, B., Humphries, M. J., and Ballestrem, C. (2007). Vinculin controls focal adhesion formation by direct interactions with talin and actin. J Cell Biol *179*, 1043-1057.

Hunger-Glaser, I., Salazar, E. P., Sinnett-Smith, J., and Rozengurt, E. (2003). Bombesin, lysophosphatidic acid, and epidermal growth factor rapidly stimulate focal adhesion kinase phosphorylation at Ser-910: requirement for ERK activation. The Journal of biological chemistry *278*, 22631-22643.

Jan, C. H., Friedman, R. C., Ruby, J. G., and Bartel, D. P. (2011). Formation, regulation and evolution of Caenorhabditis elegans 3'UTRs. Nature *469*, 97-101.

Ji, Z., Lee, J. Y., Pan, Z., Jiang, B., and Tian, B. (2009). Progressive lengthening of 3' untranslated regions of mRNAs by alternative polyadenylation during mouse embryonic development. Proceedings of the National Academy of Sciences of the United States of America *106*, 7028-7033.

Ji, Z., and Tian, B. (2009). Reprogramming of 3' untranslated regions of mRNAs by alternative polyadenylation in generation of pluripotent stem cells from different cell types. PloS one *4*, e8419.

Jiang, Q., Zhou, C. L., Bi, Z. G., and Wan, Y. S. (2006). EGF-induced cell migration is mediated by ERK and PI3K/AKT pathways in cultured human lens epithelial cells. J Ocul Pharmacol Th *22*, 93-102.

Kajita, M., Itoh, Y., Chiba, T., Mori, H., Okada, A., Kinoh, H., and Seiki, M. (2001). Membrane-type 1 matrix metalloproteinase cleaves CD44 and promotes cell migration. The Journal of cell biology *153*, 893-904.

Kalluri, R., and Weinberg, R. A. (2009). The basics of epithelial-mesenchymal transition. J Clin Invest *119*, 1420-1428.

Klemke, R. L., Cai, S., Giannini, A. L., Gallagher, P. J., de Lanerolle, P., and Cheresh, D. A. (1997). Regulation of cell motility by mitogen-activated protein kinase. The Journal of cell biology *137*, 481-492.

Lake, J. I., and Heuckeroth, R. O. (2013). Enteric nervous system development: migration, differentiation, and disease. Am J Physiol Gastrointest Liver Physiol *305*, G1-24.

Lee, C. Y., and Chen, L. (2013). Alternative polyadenylation sites reveal distinct chromatin accessibility and histone modification in human cell lines. Bioinformatics *29*, 1713-1717.

Lianoglou, S., Garg, V., Yang, J. L., Leslie, C. S., and Mayr, C. (2013). Ubiquitously transcribed genes use alternative polyadenylation to achieve tissue-specific expression. Genes & development *27*, 2380-2396.

Lin, Y., Li, Z., Ozsolak, F., Kim, S. W., Arango-Argoty, G., Liu, T. T., Tenenbaum, S. A., Bailey, T., Monaghan, A. P., Milos, P. M., and John, B. (2012). An in-depth map of polyadenylation sites in cancer. Nucleic acids research *40*, 8460-8471.

Liotta, L. A., Tryggvason, K., Garbisa, S., Hart, I., Foltz, C. M., and Shafie, S. (1980). Metastatic potential correlates with enzymatic degradation of basement membrane collagen. Nature *284*, 67-68.

Liu, L. T., Chang, H. C., Chiang, L. C., and Hung, W. C. (2002). Induction of RECK by nonsteroidal anti-inflammatory drugs in lung cancer cells. Oncogene *21*, 8347-8350.

Liu, L. T., Chang, H. C., Chiang, L. C., and Hung, W. C. (2003). Histone deacetylase inhibitor up-regulates RECK to inhibit MMP-2 activation and cancer cell invasion. Cancer research *63*, 3069-3072.

Locke, J. M., Da Silva Xavier, G., Rutter, G. A., and Harries, L. W. (2011). An alternative polyadenylation signal in TCF7L2 generates isoforms that inhibit T cell factor/lymphoid-enhancer factor (TCF/LEF)-dependent target genes. Diabetologia *54*, 3078-3082.

Lu, F., Gladden, A. B., and Diehl, J. A. (2003). An alternatively spliced cyclin D1 isoform, cyclin D1b, is a nuclear oncogene. Cancer research *63*, 7056-7061.

Mangone, M., Manoharan, A. P., Thierry-Mieg, D., Thierry-Mieg, J., Han, T., Mackowiak, S. D., Mis, E., Zegar, C., Gutwein, M. R., Khivansara, V., *et al.* (2010). The landscape of C. elegans 3'UTRs. Science *329*, 432-435.

Masamha, C. P., Xia, Z., Yang, J., Albrecht, T. R., Li, M., Shyu, A. B., Li, W., and Wagner, E. J. (2014). CFIm25 links alternative polyadenylation to glioblastoma tumour suppression. Nature. Massague, J. (2012). TGF beta signalling in context. Nat Rev Mol Cell Bio *13*, 616-630.

Masui, T., Doi, R., Koshiba, T., Fujimoto, K., Tsuji, S., Nakajima, S., Koizumi, M., Toyoda, E., Tulachan, S., Ito, D., *et al.* (2003). RECK expression in pancreatic cancer: its correlation with lower invasiveness and better prognosis. Clinical cancer research : an official journal of the American Association for Cancer Research *9*, 1779-1784.

Mattila, P. K., and Lappalainen, P. (2008). Filopodia: molecular architecture and cellular functions. Nat Rev Mol Cell Biol *9*, 446-454.

Mayor, R., and Etienne-Manneville, S. (2016). The front and rear of collective cell migration. Nat Rev Mol Cell Biol *17*, 97-109.

Mayr, C., and Bartel, D. P. (2009). Widespread shortening of 3'UTRs by alternative cleavage and polyadenylation activates oncogenes in cancer cells. Cell *138*, 673-684.

Michaud, M., Ubrig, E., Filleur, S., Erhardt, M., Ephritikhine, G., Marechal-Drouard, L., and Duchene, A. M. (2014). Differential targeting of VDAC3 mRNA isoforms influences mitochondria morphology. Proceedings of the National Academy of Sciences of the United States of America *111*, 8991-8996.

Miki, T., Takegami, Y., Okawa, K., Muraguchi, T., Noda, M., and Takahashi, C. (2007). The reversion-inducing cysteine-rich protein with Kazal motifs (RECK) interacts with membrane type 1 matrix metalloproteinase and CD13/aminopeptidase N and modulates their endocytic pathways. The Journal of biological chemistry *282*, 12341-12352.

Millevoi, S., and Vagner, S. (2010). Molecular mechanisms of eukaryotic pre-mRNA 3' end processing regulation. Nucleic acids research *38*, 2757-2774.

Miura, P., Shenker, S., Andreu-Agullo, C., Westholm, J. O., and Lai, E. C. (2013). Widespread and extensive lengthening of 3' UTRs in the mammalian brain. Genome Res *23*, 812-825.

Miyamoto, S., Chiorini, J. A., Urcelay, E., and Safer, B. (1996). Regulation of gene expression for translation initiation factor eIF-2 alpha: importance of the 3' untranslated region. The Biochemical journal *315 (Pt 3)*, 791-798.

Montero, J. A., Kilian, B., Chan, J., Bayliss, P. E., and Heisenberg, C. P. (2003). Phosphoinositide 3-kinase is required for process outgrowth and cell polarization of gastrulating mesendodermal cells. Current biology : CB *13*, 1279-1289.

Morioka, Y., Monypenny, J., Matsuzaki, T., Shi, S., Alexander, D. B., Kitayama, H., and Noda, M. (2009). The membrane-anchored metalloproteinase regulator RECK stabilizes focal adhesions and anterior-posterior polarity in fibroblasts. Oncogene *28*, 1454-1464.

Nabeshima, K., Inoue, T., Shimao, Y., and Sameshima, T. (2002). Matrix metalloproteinases in tumor invasion: role for cell migration. Pathology international *52*, 255-264.

Noda, M., and Takahashi, C. (2007). Recklessness as a hallmark of aggressive cancer. Cancer science *98*, 1659-1665.

Oh, J., Seo, D. W., Diaz, T., Wei, B., Ward, Y., Ray, J. M., Morioka, Y., Shi, S., Kitayama, H., Takahashi, C., *et al.* (2004). Tissue inhibitors of metalloproteinase 2 inhibits endothelial cell migration through increased expression of RECK. Cancer research *64*, 9062-9069.

Oh, J., Takahashi, R., Kondo, S., Mizoguchi, A., Adachi, E., Sasahara, R. M., Nishimura, S., Imamura, Y., Kitayama, H., Alexander, D. B., *et al.* (2001). The membrane-anchored MMP inhibitor RECK is a key regulator of extracellular matrix integrity and angiogenesis. Cell *107*, 789-800.

Omura, A., Matsuzaki, T., Mio, K., Ogura, T., Yamamoto, M., Fujita, A., Okawa, K., Kitayama, H., Takahashi, C., Sato, C., and Noda, M. (2009). RECK forms cowbell-shaped dimers and inhibits matrix metalloproteinase-catalyzed cleavage of fibronectin. J Biol Chem *284*, 3461-3469.

Ornitz, D. M., and Itoh, N. (2015). The Fibroblast Growth Factor signaling pathway. Wires Dev Biol *4*, 215-266.

Ozsolak, F., Kapranov, P., Foissac, S., Kim, S. W., Fishilevich, E., Monaghan, A. P., John, B., and Milos, P. M. (2010). Comprehensive polyadenylation site maps in yeast and human reveal pervasive alternative polyadenylation. Cell *143*, 1018-1029.

Park, J. Y., Li, W., Zheng, D., Zhai, P., Zhao, Y., Matsuda, T., Vatner, S. F., Sadoshima, J., and Tian, B. (2011). Comparative analysis of mRNA isoform expression in cardiac hypertrophy and development reveals multiple post-transcriptional regulatory modules. PloS one *6*, e22391.

Pinto, P. A., Henriques, T., Freitas, M. O., Martins, T., Domingues, R. G., Wyrzykowska, P. S., Coelho, P. A., Carmo, A. M., Sunkel, C. E., Proudfoot, N. J., and Moreira, A. (2011). RNA polymerase II kinetics in polo polyadenylation signal selection. The EMBO journal *30*, 2431-2444.

Ra, H. J., and Parks, W. C. (2007). Control of matrix metalloproteinase catalytic activity. Matrix Biology *26*, 587-596.

Rabien, A., Burkhardt, M., Jung, M., Fritzsche, F., Ringsdorf, M., Schicktanz, H., Loening, S. A., Kristiansen, G., and Jung, K. (2007). Decreased RECK expression indicating proteolytic

imbalance in prostate cancer is associated with higher tumor aggressiveness and risk of prostate-specific antigen relapse after radical prostatectomy. European urology *51*, 1259-1266.

Rajasekaran, S., Rajaguru, P., and Gandhi, P. S. S. (2015). MicroRNAs as potential targets for progressive pulmonary fibrosis. Front Pharmacol *6*.

Rogers, J., Early, P., Carter, C., Calame, K., Bond, M., Hood, L., and Wall, R. (1980). Two mRNAs with different 3' ends encode membrane-bound and secreted forms of immunoglobulin mu chain. Cell *20*, 303-312.

Rudijanto, A. (2007). The role of vascular smooth muscle cells on the pathogenesis of atherosclerosis. Acta Med Indones *39*, 86-93.

Sandberg, R., Neilson, J. R., Sarma, A., Sharp, P. A., and Burge, C. B. (2008). Proliferating cells express mRNAs with shortened 3' untranslated regions and fewer microRNA target sites. Science *320*, 1643-1647.

Sasahara, R. M., Takahashi, C., and Noda, M. (1999a). Involvement of the Sp1 site in ras-mediated downregulation of the RECK metastasis suppressor gene. Biochemical and biophysical research communications *264*, 668-675.

Sasahara, R. M., Takahashi, C., Sogayar, M. C., and Noda, M. (1999b). Oncogene-mediated downregulation of RECK, a novel transformation suppressor gene. Brazilian journal of medical and biological research = Revista brasileira de pesquisas medicas e biologicas / Sociedade Brasileira de Biofisica [et al] *32*, 891-895.

Schlott, B., Wohnert, J., Icke, C., Hartmann, M., Ramachandran, R., Guhrs, K. H., Glusa, E., Flemming, J., Gorlach, M., Grosse, F., and Ohlenschlager, O. (2002). Interaction of Kazal-type inhibitor domains with serine proteinases: biochemical and structural studies. J Mol Biol *318*, 533-546.

Sharon, D., Tilgner, H., Grubert, F., and Snyder, M. (2013). A single-molecule long-read survey of the human transcriptome. Nat Biotechnol *31*, 1009-1014.

Shell, S. A., Hesse, C., Morris, S. M., Jr., and Milcarek, C. (2005). Elevated levels of the 64-kDa cleavage stimulatory factor (CstF-64) in lipopolysaccharide-stimulated macrophages influence gene expression and induce alternative poly(A) site selection. J Biol Chem *280*, 39950-39961.

Shepard, P. J., Choi, E. A., Lu, J., Flanagan, L. A., Hertel, K. J., and Shi, Y. (2011). Complex and dynamic landscape of RNA polyadenylation revealed by PAS-Seq. Rna *17*, 761-772.

Shi, Y., Di Giammartino, D. C., Taylor, D., Sarkeshik, A., Rice, W. J., Yates, J. R., 3rd, Frank, J., and Manley, J. L. (2009). Molecular architecture of the human pre-mRNA 3' processing complex. Molecular cell *33*, 365-376.

Smibert, P., Miura, P., Westholm, J. O., Shenker, S., May, G., Duff, M. O., Zhang, D., Eads, B. D., Carlson, J., Brown, J. B., *et al.* (2012). Global patterns of tissue-specific alternative polyadenylation in Drosophila. Cell reports *1*, 277-289.

Solomon, D. A., Wang, Y., Fox, S. R., Lambeck, T. C., Giesting, S., Lan, Z., Senderowicz, A. M., Conti, C. J., and Knudsen, E. S. (2003). Cyclin D1 splice variants. Differential effects on localization, RB phosphorylation, and cellular transformation. J Biol Chem *278*, 30339-30347.

Span, P. N., Sweep, C. G., Manders, P., Beex, L. V., Leppert, D., and Lindberg, R. L. (2003). Matrix metalloproteinase inhibitor reversion-inducing cysteine-rich protein with Kazal motifs: a prognostic marker for good clinical outcome in human breast carcinoma. Cancer *97*, 2710-2715.

Spies, N., Burge, C. B., and Bartel, D. P. (2013). 3' UTR-isoform choice has limited influence on the stability and translational efficiency of most mRNAs in mouse fibroblasts. Genome Res *23*, 2078-2090.

Stubbs, M. T., Morenweiser, R., Sturzebecher, J., Bauer, M., Bode, W., Huber, R., Piechottka, G. P., Matschiner, G., Sommerhoff, C. P., Fritz, H., and Auerswald, E. A. (1997). The three-dimensional structure of recombinant leech-derived tryptase inhibitor in complex with trypsin. Implications for the structure of human mast cell tryptase and its inhibition. J Biol Chem *272*, 19931-19937.

Sun, Y., Fu, Y., Li, Y., and Xu, A. (2012). Genome-wide alternative polyadenylation in animals: insights from high-throughput technologies. Journal of molecular cell biology *4*, 352-361.

Takagaki, Y., Seipelt, R. L., Peterson, M. L., and Manley, J. L. (1996). The polyadenylation factor CstF-64 regulates alternative processing of IgM heavy chain pre-mRNA during B cell differentiation. Cell *87*, 941-952.

Takahashi, C., Sheng, Z., Horan, T. P., Kitayama, H., Maki, M., Hitomi, K., Kitaura, Y., Takai, S., Sasahara, R. M., Horimoto, A., *et al.* (1998a). Regulation of matrix metalloproteinase-9 and inhibition of tumor invasion by the membrane-anchored glycoprotein RECK. Proceedings of the National Academy of Sciences of the United States of America *95*, 13221-13226.

Takahashi, C., Sheng, Z. Q., Horan, T. P., Kitayama, H., Maki, M., Hitomi, K., Kitaura, Y., Takai, S., Sasahara, R. M., Horimoto, A., *et al.* (1998b). Regulation of matrix metalloproteinase-9 and inhibition of tumor invasion by the membrane-anchored glycoprotein RECK. Proc Natl Acad Sci U S A *95*, 13221-13226.

Takenaka, K., Ishikawa, S., Yanagihara, K., Miyahara, R., Hasegawa, S., Otake, Y., Morioka, Y., Takahashi, C., Noda, M., Ito, H., *et al.* (2005). Prognostic significance of reversion-inducing cysteine-rich protein with Kazal motifs expression in resected pathologic stage IIIA N2 non-small-cell lung cancer. Annals of surgical oncology *12*, 817-824.

Tassone, F., De Rubeis, S., Carosi, C., La Fata, G., Serpa, G., Raske, C., Willemsen, R., Hagerman, P. J., and Bagni, C. (2011). Differential usage of transcriptional start sites and polyadenylation sites in FMR1 premutation alleles. Nucleic acids research *39*, 6172-6185.

Tian, B., Hu, J., Zhang, H., and Lutz, C. S. (2005). A large-scale analysis of mRNA polyadenylation of human and mouse genes. Nucleic acids research *33*, 201-212.

Tian, B., and Manley, J. L. (2013). Alternative cleavage and polyadenylation: the long and short of it. Trends in biochemical sciences *38*, 312-320.

Tsunezuka, Y., Kinoh, H., Takino, T., Watanabe, Y., Okada, Y., Shinagawa, A., Sato, H., and Seiki, M. (1996). Expression of membrane-type matrix metalloproteinase 1 (MT1-MMP) in tumor cells enhances pulmonary metastasis in an experimental metastasis assay. Cancer research *56*, 5678-5683.

Ulitsky, I., Shkumatava, A., Jan, C. H., Subtelny, A. O., Koppstein, D., Bell, G. W., Sive, H., and Bartel, D. P. (2012). Extensive alternative polyadenylation during zebrafish development. Genome Res *22*, 2054-2066.

van de Locht, A., Lamba, D., Bauer, M., Huber, R., Friedrich, T., Kroger, B., Hoffken, W., and Bode, W. (1995). Two heads are better than one: crystal structure of the insect derived double domain Kazal inhibitor rhodniin in complex with thrombin. Embo J *14*, 5149-5157.

Verollet, C., Charriere, G. M., Labrousse, A., Cougoule, C., Le Cabec, V., and Maridonneau-Parini, I. (2011). Extracellular proteolysis in macrophage migration: losing grip for a breakthrough. Eur J Immunol *41*, 2805-2813.

Vorlova, S., Rocco, G., Lefave, C. V., Jodelka, F. M., Hess, K., Hastings, M. L., Henke, E., and Cartegni, L. (2011). Induction of antagonistic soluble decoy receptor tyrosine kinases by intronic polyA activation. Molecular cell *43*, 927-939.

Wang, E. T., Sandberg, R., Luo, S., Khrebtukova, I., Zhang, L., Mayr, C., Kingsmore, S. F., Schroth, G. P., and Burge, C. B. (2008). Alternative isoform regulation in human tissue transcriptomes. Nature *456*, 470-476.

Wu, Y. J., Neoh, C. A., Tsao, C. Y., Su, J. H., and Li, H. H. (2015). Sinulariolide Suppresses Human Hepatocellular Carcinoma Cell Migration and Invasion by Inhibiting Matrix Metalloproteinase-2/-9 through MAPKs and PI3K/Akt Signaling Pathways. Int J Mol Sci *16*, 16469-16482.

Xue, G., and Hemmings, B. A. (2013). PKB/Akt-dependent regulation of cell motility. Journal of the National Cancer Institute *105*, 393-404.

Yao, P., Potdar, A. A., Arif, A., Ray, P. S., Mukhopadhyay, R., Willard, B., Xu, Y., Yan, J., Saidel, G. M., and Fox, P. L. (2012). Coding region polyadenylation generates a truncated tRNA synthetase that counters translation repression. Cell *149*, 88-100.

Ying, H. Z., Chen, Q., Zhang, W. Y., Zhang, H. H., Ma, Y., Zhang, S. Z., Fang, J., and Yu, C. H. (2017). PDGF signaling pathway in hepatic fibrosis pathogenesis and therapeutics. Mol Med Rep *16*, 7879-7889.

Yoon, Y., McKenna, M. C., Rollins, D. A., Song, M., Nuriel, T., Gross, S. S., Xu, G., and Glatt, C. E. (2013). Anxiety-associated alternative polyadenylation of the serotonin transporter mRNA confers translational regulation by hnRNPK. Proceedings of the National Academy of Sciences of the United States of America *110*, 11624-11629.

Zuo, J., Ferguson, T. A., Hernandez, Y. J., Stetler-Stevenson, W. G., and Muir, D. (1998). Neuronal matrix metalloproteinase-2 degrades and inactivates a neurite-inhibiting chondroitin sulfate proteoglycan. The Journal of neuroscience : the official journal of the Society for Neuroscience *18*, 5203-5211.

CHAPTER 2:

RECK isoforms have opposing effects on cell migration

RECK isoforms have opposing effects on cell migration

Ha Neul Lee[a], Mithun Mitra[b,c], Oye Bosompra[b], David C. Corney[b,c,d], Elizabeth L. Johnson[d], Nadine Rashed[e], Linda D. Ho[b], and Hilary A. Coller[a,b,c,*]

[a]Molecular Biology Institute, [b]Department of Molecular, Cell and Developmental Biology, [c]Department of Biological Chemistry, David Geffen School of Medicine, and [e]Department of Microbiology, Immunology, and Molecular Genetics, University of California, Los Angeles, Los Angeles, CA 90095; [d]Department of Molecular Biology, Princeton University, Princeton, NJ 08544

ABSTRACT **Cell migration is a highly conserved process involving cytoskeletal reorganization and restructuring of the surrounding extracellular matrix. Although there are many studies describing mechanisms underlying cell motility, little has been reported about the contribution of alternative isoform use toward cell migration. Here, we investigated whether alternative isoform use can affect cell migration focusing on reversion-inducing-cysteine-rich protein with Kazal motifs (RECK), an established inhibitor of cell migration. We found that a shorter isoform of RECK is more highly expressed in proliferating fibroblasts, in TGF-β–treated fibroblasts, and in tumors compared with differentiated tissue. Knockdown of this short RECK isoform reduces fibroblast migration through Matrigel. Thus, this short isoform of RECK generated by a combination of alternative splicing and alternative polyadenylation plays an opposing role to the canonical RECK isoform, as knockdown of canonical RECK results in faster cell migration through Matrigel. We show that the short RECK protein competes with matrix metalloprotease 9 (MMP9) for binding to the Kazal motifs of canonical RECK, thus liberating MMP9 from an inactivating interaction with canonical RECK. Our studies provide a new paradigm and a detailed mechanism for how alternative isoform use can regulate cell migration by producing two proteins with opposing effects from the same genetic locus.**

Monitoring Editor
A. Gregory Matera
University of North Carolina

Received: Dec 11, 2017
Revised: Apr 26, 2018
Accepted: Jun 1, 2018

INTRODUCTION

Alternative splicing is the incorporation of different exons from the same gene into the final transcript in different contexts (Kornblihtt *et al.*, 2013). Alternative polyadenylation (APA) occurs when the same genetic locus produces multiple transcripts ending at different polyadenylation sites (Tian and Manley, 2013). Combinations of alternative splicing and alternative polyadenylation in the coding

This article was published online ahead of print in MBoC in Press (http://www.molbiolcell.org/cgi/doi/10.1091/mbc.E17-12-0708) on June 6, 2018.

The authors declare no competing financial interest.

H.N.L., M.M., D.C.C., E.L.J., and H.A.C. designed the study and analyzed the data. H.N.L., M.M., O.B., D.C.C., E.L.J., N.R., and L.D.H performed experiments. H.N.L. wrote the manuscript with help from O.B., N.R., and H.A.C. All authors participated in editing the manuscript.

*Address correspondence to: Hilary A. Coller (hcoller@ucla.edu).

Abbreviations used: 7dCI, 7 d contact inhibited; 7dSS, 7 d serum starved; ADAM, a disintegrin and metalloproteinase; ADAM10, A Disintegrin and MetalloProteinase family; ANOVA, analysis of variance; APA, alternative polyadenylation; ATCC, American Type Culture Collection; BCA, bicinchoninic acid; BiFC, bimolecular fluorescence complementation; BSA, bovine serum albumin; CRISPR, clustered regularly interspaced short palindromic repeats; DSB, double-strand break; ELISA, enzyme-linked immunosorbent assay; ER, endoplasmic reticulum; ERK, extracellular signal-regulated kinase; FBS, fetal bovine serum; GPI, glycosylphosphatidylinositol; GST, glutathione-*S*-transferase; GTP, guanosine triphosphate; HA, hemagglutinin; HEK293, human embryonic kidney; HER2, human epidermal growth factor receptor 2; IACUC, Institutional Animal Care and Use Committee; IRB, institutional review board; JNK, c-Jun N-terminal kinase; KLH, keyhole limpet hemocyanin; long RECK, long RECK isoform; MCF, Michigan Cancer Foundation; MEF, mouse embryonic fibroblast; MMP, matrix metalloproteinase; MMP2, matrix metalloproteinase 2; MMP9, matrix metalloproteinase 9; MT1-MMP, membrane type I matrix metalloproteinase; P, proliferating; PAM, protospacer adjacent motif; PAS, polyadenylation site; PBS, phosphate-buffered saline; PBS-T, phosphate-buffered saline-Tween; PI-PLC, phosphatidylinositol-specific phospholipase C; RECK, reversion-inducing-cysteine-rich protein with Kazal motifs; RIPA, radioimmunoprecipitation assay; RNA-Seq, RNA sequencing; RTK, receptor tyrosine kinase; RTK1, receptor tyrosine kinase 1; RT-PCR, reverse transcriptase-PCR; RU, relative units; RUD, relative use of the distal polyadenylation site; shRNA, short hairpin RNA; short RECK, short RECK isoform; TCGA, The Cancer Genome Atlas; TGF-β, transforming growth factor β; UBC, ubiquitin c; WCL, whole cell lysate; WST-1, water soluble tetrazolium salt-1.

© 2018 Lee *et al*. This article is distributed by The American Society for Cell Biology under license from the author(s). Two months after publication it is available to the public under an Attribution–Noncommercial–Share Alike 3.0 Unported Creative Commons License (http://creativecommons.org/licenses/by-nc-sa/3.0).

"ASCB®," "The American Society for Cell Biology®," and "Molecular Biology of the Cell®" are registered trademarks of The American Society for Cell Biology.

sequence of genes can result in the expression of distinct proteins from the same genetic locus (Li *et al.*, 2017). Alternative terminal exon use can convert IgM heavy chain from its membrane-bound to its secreted form (Alt *et al.*, 1980; Takagaki *et al.*, 1996; Peterson, 2011), and receptor tyrosine kinases (RTKs) can be converted to soluble decoy RTKs (Vorlova *et al.*, 2011). Proliferating cells, cancer cells, stem cells in the early stages of mouse development, and tumors tend to use proximal polyadenylation sites (Mayr and Bartel, 2009; Elkon *et al.*, 2012; Morris *et al.*, 2012; Masamha *et al.*, 2014; Rehfeld *et al.*, 2014), possibly due to higher levels of cleavage and polyadenylation factors (Morris *et al.*, 2012).

Matrix metalloproteinases (MMPs) are important contributors to cell migration (Nabeshima *et al.*, 2002). MMPs, structurally related zinc-dependent endopeptidases, degrade extracellular material. Some MMPs, such as MMP2 and MMP9, can be secreted into the extracellular environment, while others like MT1-MMP are membrane-anchored. The role of MMPs in promoting migration and invasion includes clearing away extracellular matrix that may occlude a cell's advancement (Wolf *et al.*, 2013). In addition, MMPs can generate epitopes that actively promote migration (Zuo *et al.*, 1998). Further, MMPs can also digest proteins involved in adhesion and thereby promote cancer cell invasion (Belkin *et al.*, 2001; Kajita *et al.*, 2001).

Reversion-inducing-cysteine-rich protein with Kazal motifs (RECK), a glycosylphosphatidylinositol (GPI)-anchored MMP inhibitor, has been shown to inhibit cell migration (Oh *et al.*, 2001; Morioka *et al.*, 2009). RECK was originally isolated as a gene that reverts the morphology of transformed cells (Takahashi *et al.*, 1998). RECK was later discovered to inhibit members of the MMP family (MMP-2, MMP-9, and MT1-MMP) and the A Disintegrin And Metalloproteinase (ADAM) family (ADAM10) (Takahashi *et al.*, 1998; Oh *et al.*, 2001, 2004; Miki *et al.*, 2007; Chang *et al.*, 2008; Hong *et al.*, 2014). RECK's ability to inhibit matrix metalloproteinases is important for its role in suppressing cell migration (Takahashi *et al.*, 1998). RECK$^{-/-}$ mouse embryonic fibroblasts (MEFs) exhibit a lack of anterior-posterior polarity, faster migration, more rapid changes in direction as they migrate, and fewer focal adhesions and actin stress fibers compared with controls (Morioka *et al.*, 2009). RECK$^{-/-}$ MEFs also contained increased levels of GTP-bound Rac1 and Cdc42 (Morioka *et al.*, 2009).

We hypothesized that changes in the expression of different gene isoforms might be related to the migratory capacity of cells. We report here on our studies investigating the role of RECK isoforms in fibroblast migration. We propose a novel model in which changes in the capacity for migration are mediated through the expression of different isoforms of RECK.

RESULTS

The ratio of a short RECK isoform to canonical, long RECK is higher in proliferative and TGF-β–treated cells

Our laboratory applied a targeted methodology, polyadenylation site–enriched RNA-Seq, to monitor the extent to which transcripts terminate at different possible polyadenylation sites in order to identify genes that undergo APA when primary human dermal fibroblasts exit the proliferative cell cycle and enter quiescence (unpublished data). The Gnomegen RNA-Seq Library Preparation Kit was used to create cDNA libraries containing fragments enriched for 3′ UTR ends. To generate these libraries, mRNA was fragmented; transcripts were incubated with poly(T) sequences attached to biotin; polyadenylated transcripts were captured with streptavidin beads; and polyadenylation sites were sequenced on an Illumina sequencer. Our data show that RECK can be expressed in dermal fibroblasts as either a long, canonical isoform (long RECK) or shorter isoforms generated by a combination of alternative splicing and APA (short RECK; Figure 1A). The transcript encoding the longer RECK isoform was more highly expressed in fibroblasts induced into quiescence by contact inhibition of proliferation or serum starvation, while the transcript encoding the shorter RECK isoform was expressed more highly in proliferating fibroblasts (Figure 1B). In three independent poly(A)-enriched RNA-Seq experiments, the full-length RECK isoform (long RECK) exhibited a statistically significant shift toward increased use of the distal polyadenylation site in fibroblasts induced into quiescence via contact inhibition of proliferation or serum starvation, compared with proliferating fibroblasts ($p < 0.001$, Student's *t* test; Figure 1C). Because the short RECK transcript includes a 3′ UTR that is eliminated via splicing from the long RECK transcript, we could design real-time reverse transcriptase-PCR (RT-PCR) primers specific for the long or short RECK isoforms, in addition to primers that recognize both isoforms (Figure 1D). Real-time RT-PCR with isoform-specific primers confirmed increased expression of the long RECK isoform and decreased expression of the short RECK isoform in fibroblasts induced into quiescence by 7 d of contact inhibition (7dCI) compared with proliferating fibroblasts (P; Figure 1E). The short RECK isoform encodes a shorter protein (NM_001316348.1, 25 kDa), distinct from the protein encoded by the longer, canonical RECK (NM_021111.2, 110 kDa; Figure 1A). The final, 13-amino-acid exon of short RECK and the 3′ UTR of short RECK are not present in the mRNA encoding long RECK. These distinctions between the amino acid sequences of the proteins encoded by the short and long RECK isoforms allowed us to design short RECK-specific antibodies that recognize short RECK's unique final exon (Supplemental Figure S1). Immunoblotting with this short RECK-specific polyclonal antibody confirmed that short RECK protein levels are lower in fibroblasts induced into quiescence by 7 d of contact inhibition than proliferating fibroblasts (Figure 1E).

Treating fibroblasts with TGF-β, a strong inducer of fibroblast migration (Cordeiro *et al.*, 2000; Acharya *et al.*, 2008), resulted in increased expression of short RECK isoform transcripts (Figure 1F) and short RECK protein (Figure 1F). We analyzed a published data set on the use of polyadenylation sites in tissues and cancer cell lines (Lianoglou *et al.*, 2013). We counted the number of polyadenylation site–enriched RNA-Seq reads for each sample that mapped either to the final exon of the short RECK isoform or the final exon of the long RECK isoform. We found that differentiated tissues such as ovary, muscle, breast, and brain contained more RNA-Seq reads mapping to the final exon of the long RECK isoform and fewer reads mapping to the last exon of the short RECK isoform (Figure 1G). In contrast, the tumorigenic cancer cell lines (HeLa and MCF7) and the nontumorigenic MCF10a cell line contained more reads mapping to the last exon of the short RECK isoform and fewer reads mapping to the final exon of the long RECK isoform (Figure 1G). We also investigated RNA-Seq data from The Cancer Genome Atlas (TCGA). RNA-Seq read counts for each exon were obtained from tumor tissues and paired normal tissues through the public data portal. RNA-Seq read counts assigned to the unique short RECK isoform final exon and the long RECK final exon were used to infer expression of short and long RECK isoforms, respectively. This analysis revealed that the ratio of short RECK to long RECK increased in all 13 tumors analyzed compared with normal tissue from the same site (Figure 1H). Levels of long RECK decreased in eight types of cancer compared with normal tissue, while levels of short RECK increased in seven types of cancer compared with normal tissue (Supplemental Figure S2). When we investigated breast cancer in more depth, we discovered that the ratio of short to long

RECK was particularly high in the basal-like breast cancer subtype, which largely overlaps with the highly metastatic triple negative breast cancer subtype (Figure 1I; Lin *et al.*, 2008; Tseng *et al.*, 2013). Altogether, the short isoform is induced in proliferating versus quiescent fibroblasts, TGF-β–treated versus control fibroblasts, and cancer cells versus differentiated cells.

Knockdown of short RECK reduces fibroblast migration

To understand the role of RECK isoforms in cell migration, we generated lentiviral vectors expressing short hairpin RNAs (shRNAs) that specifically target either short or long RECK and introduced them into HEK293T cells (Figure 2A). These isoform-specific shRNAs did not affect protein levels of the other isoform (Figure 2A). We used a real-time imaging instrument to monitor cell migration in fibroblasts expressing shRNAs that target RECK isoforms or fibroblasts expressing control shRNAs (Figure 2B). To specifically test the effects of RECK on the ability of cells to migrate through the extracellular matrix, we denuded an area on a tissue culture well, and coated the well with Matrigel (Figure 2B). By monitoring cell migration into Matrigel, we observed that knockdown of long RECK resulted in increased fibroblast migration (Figure 2, C and D, and Supplemental Movie S1), consistent with previous reports (Mahl *et al.*, 2016). Strikingly, knockdown of short RECK resulted in the opposite result, decreased migration (Figure 2, C and D, and Supplemental Movie S1). To clarify whether these differences in cell migration could reflect effects of RECK isoforms on cell proliferation rather than a difference in the cells' migration, we monitored cell proliferation rates using a WST-1 assay. No significant differences in proliferation rates were discovered over a 48 h time course after either short RECK or long RECK knockdown (Supplemental Figure S3A). Overexpression of the short RECK isoform, the long RECK isoform, or both together did not affect fibroblast migration rates through Matrigel (Supplemental Figure S3B). Taken together, our findings show that cell migration can be regulated through changes in RECK isoform expression. Our results further demonstrate that reducing the levels of the long RECK isoform promotes cell migration while reducing the levels of the short RECK isoform results in slower cell migration.

RECK isoforms do not change the activity of the AKT, ERK, or JNK signaling pathways

We then tested whether knockdown of a RECK isoform would affect the activity of signaling pathways established as regulators of cell migration (Klemke *et al.*, 1997; Hunger-Glaser *et al.*, 2003; Montero *et al.*, 2003; Huang *et al.*, 2004; Xue and Hemmings, 2013). We tested the activity of the AKT, ERK, and JNK signaling pathways using total and phosphospecific antibodies. We did not detect significant changes in the levels of total or phosphorylated AKT, ERK, or JNK in short or long RECK knockdown fibroblasts (Supplemental Figure S4). Any minor changes observed in the levels of the phosphorylated forms of these proteins did not support a role for any of these pathways in the changes in cell migration induced by RECK isoforms. These observations suggest that fibroblast cell migration can be regulated independently of these established cell migration signaling pathways.

Short RECK and long RECK interact with each other

Alternative terminal exon use can result in the production of shorter, truncated protein isoforms that interfere with and inhibit the full-length protein's activity (Yao *et al.*, 2012). Previous studies have shown that long RECK proteins dimerize (Omura *et al.*, 2009). With this in mind, we hypothesized that short RECK may inhibit the anti-migratory function of long RECK through protein–protein interactions. We introduced Flag-tagged-short RECK and S-tagged-long RECK into 293T cells and observed an interaction when we immunoprecipitated for either short RECK or long RECK (Figure 3A). Using coimmunoprecipitation, we also confirmed previous studies that the long RECK isoform can interact with itself (Omura *et al.*, 2009) (Supplemental Figure S5A). In addition, we observed that the short RECK isoform can interact with itself as well (Supplemental Figure S5B).

Coimmunoprecipitation of endogenous short and long RECK with a commercially available long RECK-specific antibody and the antibody we generated against short RECK revealed short RECK and long RECK interact in human fibroblasts (Figure 3B). In sum, our data show that short RECK generated via a combination of alternative splicing and alternative polyadenylation can bind to canonical long RECK in human fibroblasts.

Short and long RECK associate with each other in the secretory pathway and on the cell surface

To understand how and where short RECK might affect the role of the long, canonical RECK protein as a binding partner, we visualized the interaction between short and long RECK using a bimolecular fluorescence complementation assay (BiFC; Figure 4A). Introduction of the N-terminus of Venus and the C-terminus of Venus with neither conjugated to RECK resulted in diffuse green fluorescence throughout the cell (Supplemental Figure 6A). Fibroblasts that were transduced with a lentiviral vector expressing the N-terminus of Venus (Supplemental Figure 6B), the C-terminus of Venus (Supplemental Figure 6B), long RECK fused to the N-terminus of Venus 1-172 (Supplemental Figure 6B), or short RECK fused to the C-terminus of Venus 155-238 (Supplemental Figure 6B) exhibited no fluorescent signal. Fibroblasts expressing the N-terminus of Venus and the C-terminus of Venus exhibited fluorescence throughout the cell (Supplemental Figure 6B). Fibroblasts expressing the long isoform of RECK fused to the N-terminus of Venus and the unlabeled C-terminus of Venus, or the short isoform of RECK fused to the C-terminus of Venus and the unlabeled N-terminus of Venus exhibited no fluorescence (Figure 4A, top and middle). Fibroblasts expressing both short RECK fused to the C-terminus of Venus and long RECK fused to the N-terminus of Venus (short RECK–Long RECK BiFC fibroblasts) exhibited fluorescent signals in the perinuclear region of the cell and on the cell surface (Figure 4A, bottom). To further investigate the subcellular location of the interaction between short and long RECK, we stained short RECK–Long RECK BiFC fibroblasts with GM130, a Golgi marker, or calnexin, an ER marker. We observed that ~50% of the short RECK–long RECK interaction overlaps with calnexin (Figure 4B), and ~70% of the signal from the Golgi marker overlaps with the short RECK–long RECK interaction signal (Figure 4C). The overlap between the localization of short RECK and long RECK was also observed on the cell surface using immunofluorescence staining without permeabilization (Supplemental Figure S6C).

To further explore how long and short RECK interact with each other, we used CRISPR/Cas9 technology to specifically mutate and inactivate the gene encoding RECK in 293T cells. Sequencing revealed inactivating frameshifts in both RECK alleles (Figure 4D, top) and immunoblotting revealed a lack of expression of RECK (Figure 4D, bottom). Using RECK$^{-/-}$ 293T cells, we tested more specifically for short RECK–long RECK interaction on the cell surface. We overexpressed S-tagged long RECK and Flag-tagged short RECK and treated with phosphatidylinositol-specific phospholipase C (PI-PLC) to cleave the long RECK GPI anchor (Figure 4E, left). Immunoblotting of conditioned medium revealed increased levels

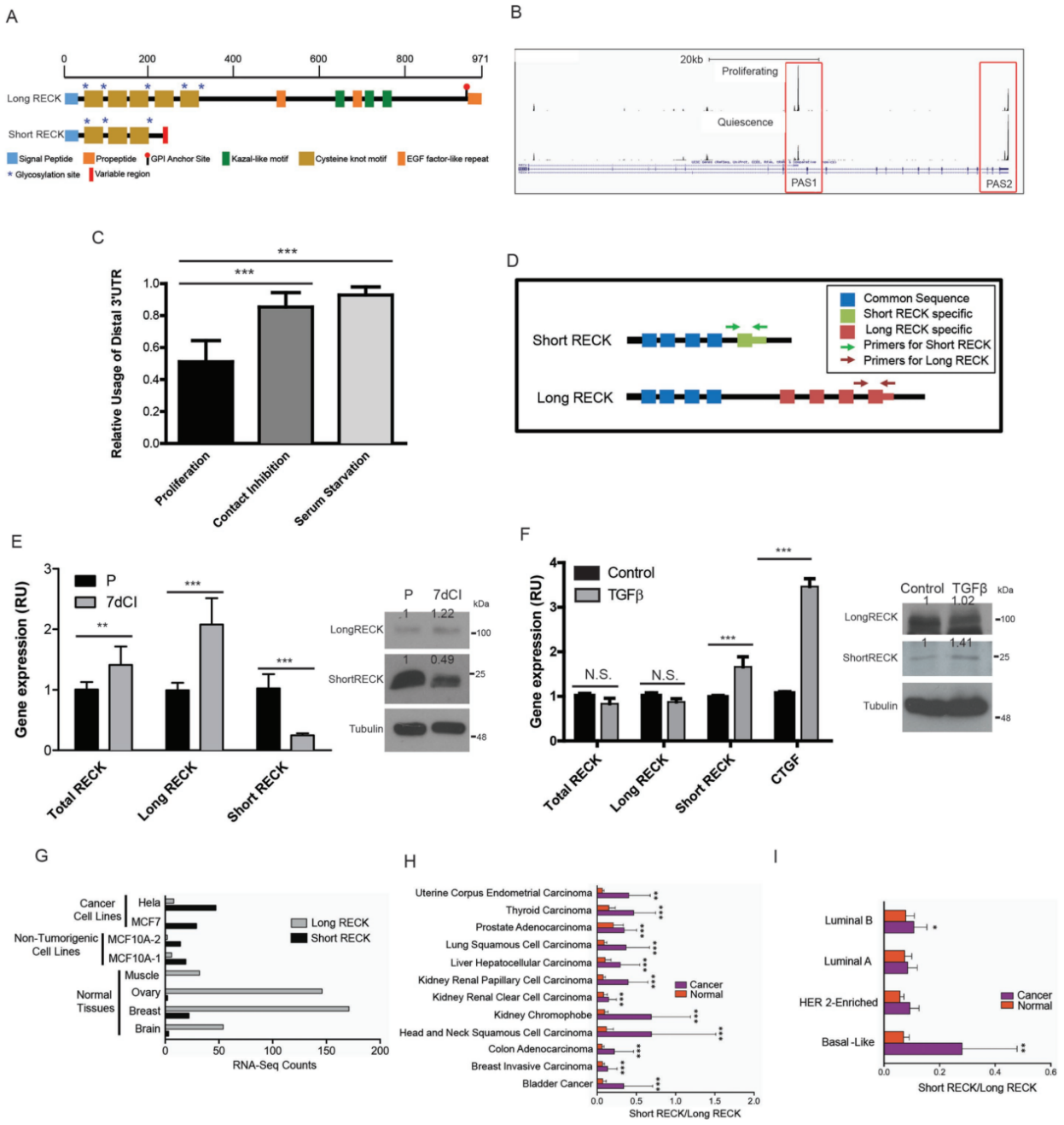


FIGURE 1: Short RECK isoform levels are elevated in proliferating and TGF-β–treated fibroblasts and cancer cells. (A) Schematic showing the short RECK isoform (NM_001316348.1) and the long RECK isoform (NM_021111.2). The short RECK isoform (molecular weight = 25 kDa) shares 212 amino acids with the long RECK isoform (molecular weight = 110 kDa) and contains a 13 amino acid–long sequence specific for the short RECK isoform at its C-terminus. (B) Poly(A) site–enriched RNA-Seq data from proliferating and serum-starved fibroblasts for RECK. PAS1 indicates the proximal polyadenylation site that produces the short RECK isoform, and PAS2 indicates the distal polyadenylation site that produces the long RECK isoform. (C) Average relative usage of the distal isoform (RUD) plotted for RECK in proliferating, 7-d contact inhibition of proliferation, and 7-d serum starvation fibroblasts with poly(A) site–enriched RNA-Seq. Data were generated in three independent biological replicates and error bars reflect SD. RECK RUD values for contact inhibition ($p < 0.001$, unpaired two-sided t test) and serum starvation ($p < 0.001$, unpaired two-sided t test) conditions are significantly higher than RUD values for proliferating cells. Averages and SD are shown. (D) Diagram illustrating primers targeting specific RECK isoforms. (E) RECK isoform expression in proliferating and contact-inhibited fibroblasts. Real-time RT-PCR analysis of total RECK, long RECK, and short RECK mRNA expression under proliferating

of both short and long RECK upon PI-PLC treatment (Figure 4E, middle). Coimmunoprecipitation of conditioned media from PI-PLC–treated cells revealed the interaction between short and long RECK, further supporting our finding that short RECK can bind to long RECK on the cell surface (Figure 4E, right). Taken together, our data support a model in which there is an interaction between short and long RECK, that this interaction is initiated within the ER, and that a complex containing both protein isoforms follows the protein secretion pathway via the Golgi apparatus to finally localize on the cell surface (Figure 4F).

Short RECK interacts with long RECK at the Kazal motif region

To dissect the region within long RECK that mediates interaction with short RECK, we engineered a series of deletion mutants of long RECK (Figure 5A). All of the engineered RECK proteins were expressed (Figure 5B, input). As the deleted regions shifted closer to the GPI anchor, the efficiency with which they localized on the cell surface and were released by PI-PLCase treatment decreased (Supplemental Figure 7A). We introduced Flag-tagged short RECK and one of the deletion mutants of S-tagged long RECK into RECK$^{-/-}$ 293T cells and tested their interaction with coimmunoprecipitation. Immunoprecipitation of Flag-tagged–short RECK showed dramatically reduced binding for the long RECK Δ635–773 mutant, indicating that the region between amino acids 635 and 773 of long RECK is important for short RECK binding (Figure 5B). GST–pull down assays also showed similar results (Supplemental Figure S7B). Amino acids 635–773 of RECK include the Kazal motif region shown to be important for suppressing MMP activity through protein–protein interactions (Miki *et al.*, 2007; Chang *et al.*, 2008). We performed a similar experiment to compare the binding sites for short RECK–long RECK interaction with the region(s) important for long RECK–long RECK interaction. We cointroduced long RECK with a Myc tag and one of a series of deletion mutants of long RECK with an S-tag. Coimmunoprecipitation revealed that the C-terminal region of the long RECK isoform, amino acids 774–941, were important for long-RECK–long RECK interaction (Supplemental Figure S7C). This mutant was missing multiple C-terminal amino acids but retained the GPI anchor. The localization of long RECK–long RECK interaction to the C-terminus is consistent with an earlier report that came to a similar conclusion based on single-particle reconstruction (Omura *et al.*, 2009). Taken together, our findings about the interaction among RECK isoforms support the importance of the Kazal motif region for long RECK–short RECK interaction.

Short RECK competes with MMP9 for binding to long RECK

Because short RECK interacts with long RECK in a region that includes the Kazal motifs, we hypothesized that short RECK competes with MMPs for binding to long RECK. To test this model, we introduced long RECK, MMP2, or MMP9, and increasing concentrations of short RECK into RECK$^{-/-}$ 293T cells for competitive coimmunoprecipitation. Increasing short RECK expression reduced coimmunoprecipitation between MMP9 and long RECK by as much as 88% of the binding level observed without short RECK (Figure 6A). Binding to MMP2 was unaffected (Figure 6B). We also tested whether

(P) or 7-d contact inhibition (7dCI) conditions was performed. Data are shown as relative units (RUs) compared with the baseline state, total RECK in proliferating conditions, which is represented as 1 and indicates the target transcript divided by the internal control. Total RECK mRNA increases with quiescence induced by contact inhibition of proliferation ($p < 0.01$, unpaired two-sided Student's *t* test). Long RECK mRNA expression increases in 7-d contact inhibition conditions ($p < 0.001$, unpaired two-sided Student's *t* test), whereas short RECK mRNA expression decreases in the same condition ($p < 0.001$, unpaired two-sided Student's *t* test). RECK was amplified with real-time primers and normalized to UBC control primers (*Materials and Methods*). Averages and SD are shown. On the right, immunoblotting of proliferating and 7-d contact-inhibited fibroblast protein lysates with an antibody against the long RECK isoform and a polyclonal antibody against the short RECK isoform is shown. Tubulin served as a loading control. (F) RECK isoform expression with TGF-β treatment. Real-time RT-PCR data for RECK isoform expression in fibroblasts treated with TGF-β. CTGF served as a positive control for TGF-β response. mRNA levels of total RECK or long RECK do not change with TGF-β treatment. mRNA expression of the short RECK isoform increases with TGF-β treatment ($p < 0.001$, unpaired two-sided Student's *t* test). Data are shown as relative units compared with the control condition. There was no significant difference in long RECK mRNA expression levels when fibroblasts were treated with TGF-β ($p = 0.18$, Student's *t* test). Averages and SD are shown. Immunoblotting for the long RECK isoform, the short RECK isoform, and tubulin are shown on the right for control fibroblasts and fibroblasts treated with TGF-β. Short RECK protein levels increase in response to TGF-β treatment. (G) Cancer cell lines have higher short-to-long RECK isoform ratios compared with differentiated tissues such as brain, breast, ovary, and muscle. Published data on the frequency of genome-wide polyadenylation site usage in multiple tissues and cancer cell lines (Lianoglou *et al.*, 2013) was analyzed for the number of reads mapping to the last exon of the long or short RECK isoform. (H) A higher ratio of short to long RECK isoforms is consistently observed in tumors. Per-exon RNA-Seq read counts for tumor tissues and paired normal tissues along with any available clinical data were obtained from the TCGA public data portal. For comparison of RECK expression between tumor and paired normal tissue, read counts were normalized to the total number of reads per sample. RNA-Seq read counts assigned to the unique short RECK isoform exon and the final long RECK exon were used to infer expression of short and long RECK isoforms, respectively. Short-to-long RECK isoform ratios, as well as normalized short and long RECK read counts, were determined for tumor and paired normal samples. Two-tailed paired *t* tests were performed separately for each tumor type using GraphPad Prism 6.04. (I) To determine RECK isoform expression in breast cancers with different clinical characteristics, the relative use of the distal isoform (RUD) was calculated and the $\log_2$-fold change between tumor and paired normal was determined and plotted based on breast cancer subtype. Breast cancer subtypes (basal-like, HER2-enriched, Luminal A, or Luminal B) were determined based on the PAM50 subtype, a 50-gene breast cancer subtype predictor (Parker *et al.*, 2009). The basal-like gene expression pattern overlaps most significantly with triple-negative breast cancers. Statistical significance was determined by one-way ANOVA followed by Tukey post-hoc test for two-way comparisons to control for multiple hypothesis testing. For all figures, *, $p < 0.05$; **, $p < 0.01$; ***, $p < 0.001$.

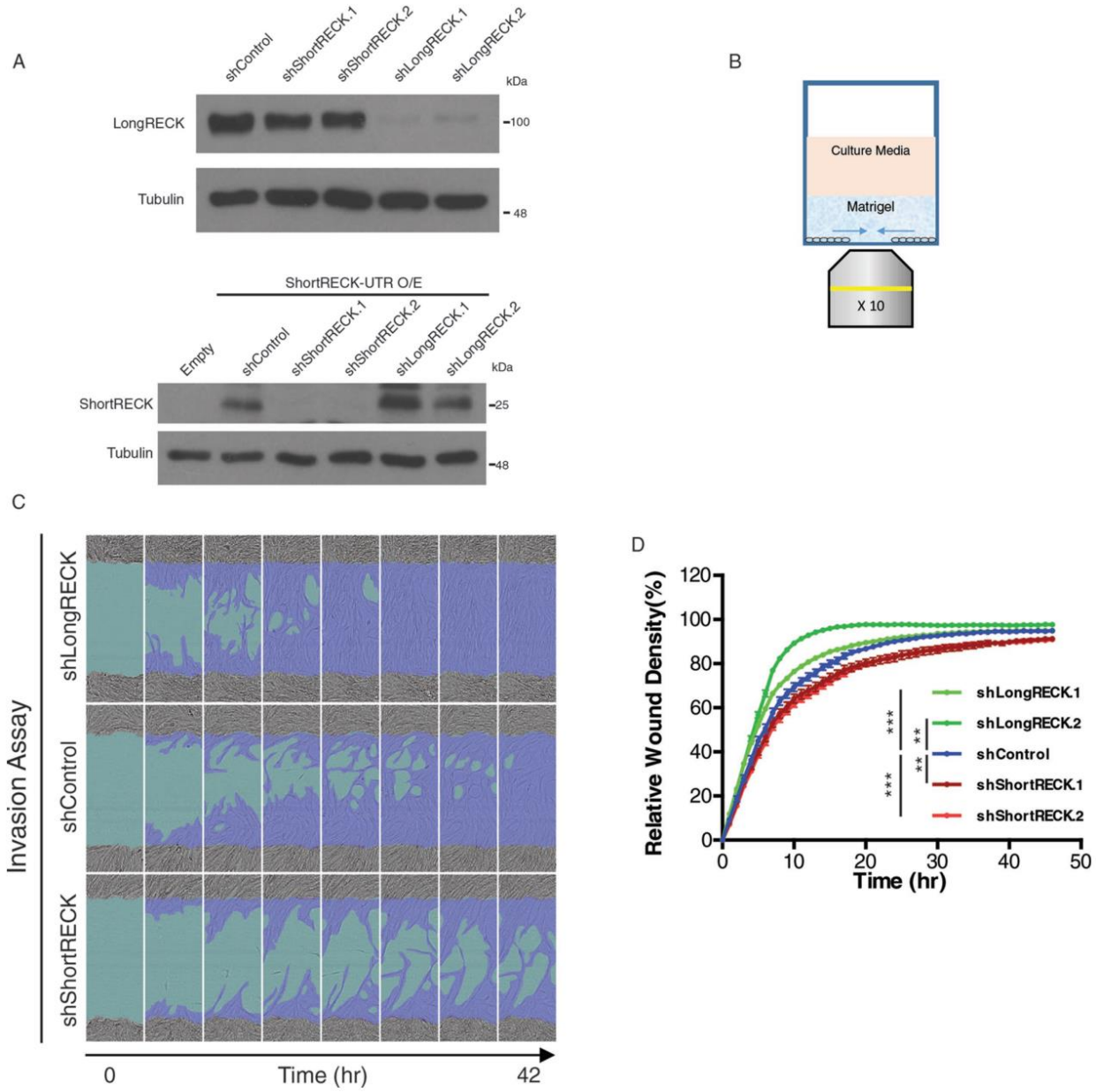


FIGURE 2: The short RECK isoform is essential for cell migration. (A) Western blot results showing the effects of shRNAs that target RECK isoforms on RECK expression levels. On top, shRNAs that target the long RECK isoform expressed in HEK293T cells reduce levels of the long RECK isoform, while shRNAs that target the short RECK isoform have little effect on levels of the long RECK isoform. On the bottom, HEK293T cells overexpressing short RECK with its 3′ UTR were used to monitor the effects of knockdown of short and long RECK on the short RECK isoform. shRNAs that target the short RECK isoform resulted in down-regulation of the short RECK isoform, whereas shRNAs that target the long RECK isoform had little effect on levels of the short RECK isoform. (B) Schematic depicting the methodology for testing cell invasion. (C, D) Isoform-specific RECK knockdown affects fibroblast migration. Fibroblasts expressing shRNAs that target the long RECK isoform migrate more rapidly than fibroblasts expressing a control shRNA. (C) Still images taken from movies of migrating cells. (D) Quantifications of relative wound density (100 * density in wound/density outside wound) over time. shControl vs. shLongRECK.1 ($p < 0.001$, repeated measures two-way ANOVA with Dunnett's multiple comparison test [simplified as ANOVA]), shControl vs. shLongRECK.2 ($p < 0.01$, ANOVA). Fibroblasts expressing shRNAs that target the short RECK isoform migrate more slowly than fibroblasts expressing a control shRNA. shControl vs. shShortRECK.1 ($p < 0.01$, ANOVA), shControl vs. shShortRECK.2 ($p < 0.001$, ANOVA). Averages and SEM are shown.

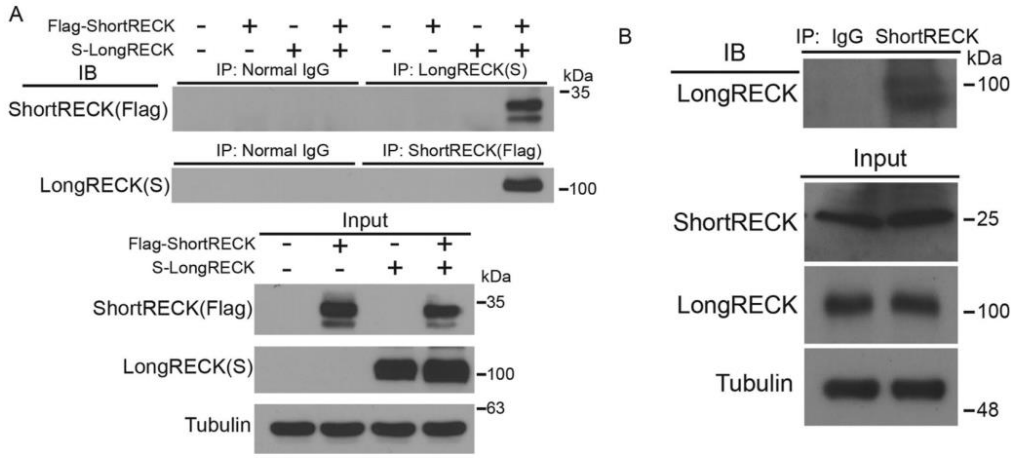


FIGURE 3: The short RECK isoform interacts with the long RECK isoform. (A) Coimmunoprecipitation revealed an interaction between the short and long RECK isoforms. Both Flag-tagged short RECK and S-tagged long RECK isoforms were overexpressed in 293T cells. Protein lysates were analyzed with coimmunoprecipitation, and an association was observed between short and long RECK isoforms. The association was observed when either the short RECK or long RECK isoform was used for immunoprecipitation. Expression levels of input proteins are shown at the bottom. (B) Coimmunoprecipitation with endogenous short RECK and long RECK isoforms. Cell lysates were collected from primary cultured human fibroblasts, proteins were pulled down using a short RECK-specific antibody, and immunoblotting was performed with a long RECK-specific antibody.

short RECK can disrupt dimerization of long RECK (Chang *et al.*, 2008; Omura *et al.*, 2009). Using coimmunoprecipitation, we found that introducing increasing amounts of short RECK did not affect the ability of long RECK to dimerize (Supplemental Figure S8). These results show that short RECK can compete with MMP9 for binding at the Kazal motif region of long RECK, and does not interfere with long RECK dimerization.

DISCUSSION

Our studies support a model in which alternative isoform use can regulate cell migration through its effects on the protein RECK. Several previous studies have provided evidence for a correlation between isoform length and cell migration. For example, during early stages of mouse development, transcripts tend to undergo polyadenylation at proximal polyadenylation sites, resulting in shorter 3′ UTRs (Ji *et al.*, 2009). Similarly, widespread shortening of the 3′ UTR region of oncogenic mRNA transcripts is also observed in cancer cells (Mayr and Bartel, 2009). Considering that enhanced cell migration is a characteristic of cells during early developmental stages and proliferative cancer cell conditions (Friedl and Gilmour, 2009; Aman and Piotrowski, 2010), these findings would support a correlation between isoform length and cell migration.

We discovered that the short isoform of RECK is expressed more highly during proliferation and after treatment with TGF-β. Moreover, when we analyzed tissue samples from cancer patients, we observed more short RECK expression in cancer tissue than normal tissue biopsies from the same site. The most aggressive breast cancer type, the basal type, had the highest ratio of short RECK to long RECK (Figure 1). We then demonstrated based on shRNA-mediated knockdown that short RECK reduces cell migration (Figure 2). This was especially surprising given that previous studies have reported that canonical RECK is a migration inhibitor. We considered two models for the effects of short RECK on cell migration: 1) short RECK could activate cell migration–related signaling pathways, or 2) short RECK could suppress the role of long RECK in cell migration. We examined three representative signaling pathways (AKT, ERK, and JNK) that have established roles in cell migration (Klemke *et al.*, 1997; Hunger-Glaser *et al.*, 2003; Montero *et al.*, 2003; Huang *et al.*, 2004; Xue and Hemmings, 2013), but did not observe any significant changes following short RECK knockdown (Supplemental Figure S4). Although it is possible that short RECK has the potential to activate other signaling pathways that we have not studied, we turned our attention toward the effects of short RECK on long RECK. We discovered that short and long RECK can interact with each other via protein–protein interactions (Figures 3 and 4). Using bimolecular fluorescence, we visualized this interaction as a complex that appeared in the ER, the Golgi apparatus, and the cell surface (Figure 4). We also demonstrated that short RECK binds to long RECK at the Kazal motif region using domain-specific deletion mutants of long RECK. Deletion of the Kazal motif region resulted in a reduced ability for the two isoforms to interact with each other (Figure 5). Finally, we demonstrate that short RECK competes with MMP9 for binding to the Kazal motif of long RECK (Figure 6). Through the generation of short versus long RECK in proliferative and migratory cells, alternative isoform use can affect MMP activity, the quality of the extracellular matrix, and the ability of cells to migrate.

A previous study has shown that receptor tyrosine kinase 1 (RTK1) can undergo APA and the short isoform of RTK1 can act as a dominant negative and as a decoy for active RTK1 (Vorlova *et al.*, 2011). This situation is similar to the model we propose for RECK in that a shorter isoform can inhibit the activity of the full-length isoform, but in the case of RECK, we do not have evidence that short RECK is displacing one of the versions of long RECK in a dimer. In fact, our competition assays showed no effects on canonical RECK dimerization as short RECK was introduced (Supplemental Figure S8).

Previous studies have shown that the activity of MMP2 or MMP9 is reduced by interaction with long RECK (Oh *et al.*, 2001; Chang *et al.*, 2008). In our study, interactions among RECK, MMP9, and MMP2 were confirmed. One interesting finding in our study was that, while the short RECK isoform outcompetes MMP9 in binding

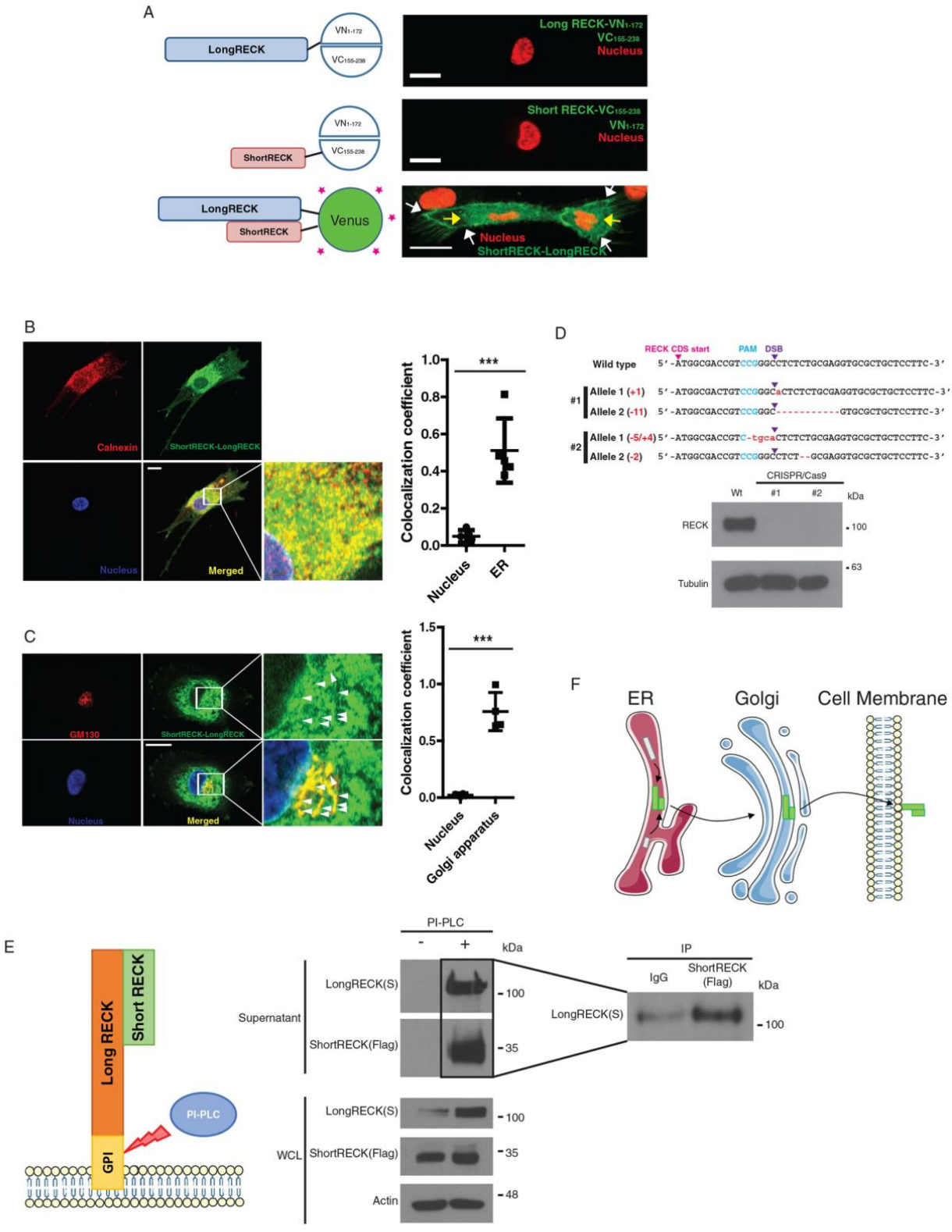


FIGURE 4: A short RECK–long RECK complex is localized in the perinuclear region and on the cell surface. (A) The N-terminal half of Venus (1–172) was conjugated to the long RECK isoform, and the C-terminal half of Venus (155–238) was conjugated to the short RECK isoform for bimolecular fluorescence complementary (BiFC) assays. When either long RECK-VN and free VC or short RECK-VC and free VN were overexpressed, no green signal was observed (top and

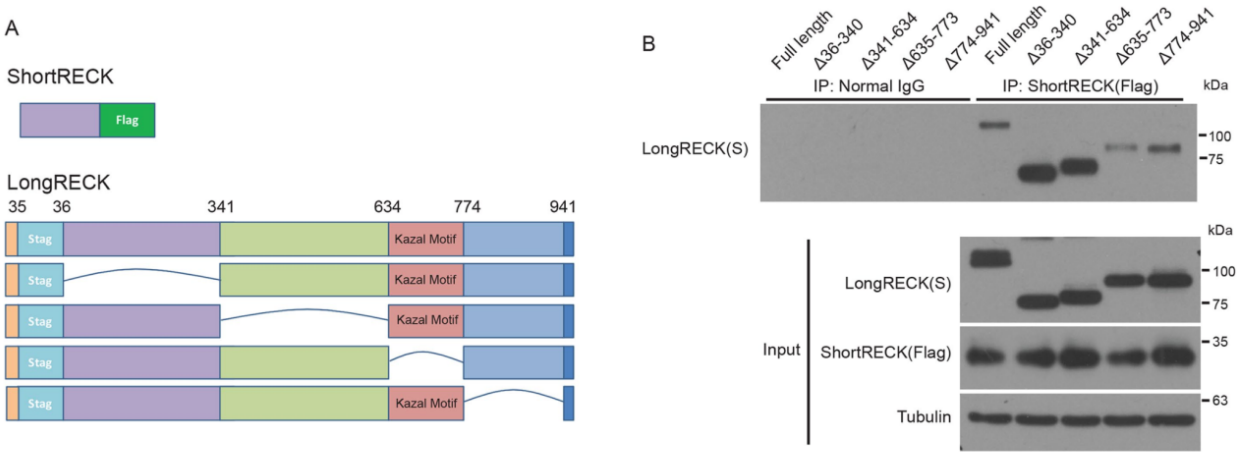


FIGURE 5: The Kazal-like motif domain is important for short RECK binding to long RECK. (A) Schematic depiction of the structure of the short RECK isoform conjugated to Flag and versions of the long RECK isoform with domain-specific deletions constructed for coimmunoprecipitation. (B) Results from a coimmunoprecipitation experiment with the constructs shown in A. Input samples are shown at the bottom. Short RECK–long RECK interaction was reduced when the domain containing the Kazal-like motif was deleted (Δ635-773).

to long RECK, short RECK cannot effectively compete with MMP2 for binding to the long RECK isoform. This might be attributed to the fact that among all secreted MMPs, only MMP9 forms a homodimer (Dufour *et al.*, 2010), which could affect its interaction with other binding partners. Further studies on the structure of these complexes will be required to assess this possibility.

The short RECK isoform that we have been studying is not the only shorter isoform of the RECK gene. In a recent publication, the authors reported on two short isoforms of RECK, RECK-B, and RECK-I (Trombetta-Lima *et al.*, 2015). Neither of these is the same as the isoform we have been studying. The study did not observe any significant effects of overexpressing either of these two short RECK isoforms in cultured glioblastoma cell lines for their role in cell migration or invasion, but did discover that overexpressing RECK-B promoted anchorage-independent growth. In our studies, our polyadenylation site–enriched RNA-Seq methodology would detect all three short isoforms. The real-time PCR we performed was specific for the short RECK isoform that we have been investigating. The polyclonal antibodies we developed are also specific for the isoform we are studying. One of the shRNAs directed against the short RECK isoform we have been investigating would target the isoform we are studying and RECK-B. The other shRNA would target the isoform we have been studying, RECK-B and RECK-I.

Our findings raise the possibility that short RECK is an important and previously unrecognized contributor to cancer cell invasion. Although long RECK is considered a tumor suppressor (Takemoto *et al.*, 2007; Chang *et al.*, 2008; Kim *et al.*, 2008), long RECK is infrequently mutated in tumors (cBioportal; Cerami *et al.*, 2012), raising the possibility that other isoforms generated from the same locus promote cancer. The increased levels of the short RECK to long RECK ratio observed in multiple tumors are consistent with a possible role for RECK alternative isoform expression in tumor progression. Our studies also raise the possibility that when fibroblasts are activated to proliferate, for instance, in a wound, that the short RECK isoform is induced and contributes to fibroblast migration.

middle). When both long RECK-VN and short RECK-VC were overexpressed in the same cell, a green signal was observed on the cell surface (white arrows) and in the perinuclear region (yellow arrows; bottom). The scale bar indicates 20 μm. (B) Immunofluorescence staining of short RECK-long RECK BiFC cells (green) with calnexin, an ER marker (red). About 50% of the short RECK–long RECK interaction signal overlaps with calnexin. The scale bar indicates 20 μm. Averages and SD are shown. $p < 0.001$, unpaired two-sided Student's *t* test. (C) Immunofluorescence staining of short RECK–long RECK BiFC cells with GM130, a Golgi apparatus marker. The green signal indicating tubule structures around the nucleus (white arrowheads) overlapped with the red GM130 signal to produce a merged yellow signal. About 70% of GM130 overlaps with the short RECK–long RECK interaction signal. The scale bar indicates 20 μm. Averages and SD are shown. $p < 0.001$, unpaired two-sided Student's *t* test. (D) Characterization of a RECK knockout HEK293T cell line established by CRISPR/Cas9. Top panel, sequencing results from two different RECK knockout cell lines. Frameshift mutations were introduced into the RECK sequence by introducing Cas9 endonuclease and a guide RNA targeting RECK (PAM, protospacer adjacent motif; DSB, double-strand break). Bottom panel, Western blot results showing knockout of RECK in CRISPR/Cas9-engineered 293Ts. (E) Left panel, strategy to detect short RECK–long RECK complex on the cell surface. PI-PLC cleaves the GPI anchor attaching long RECK to the cell surface, releasing the complex into the supernatant. Middle panel, Western blot results showing the release of short RECK on the cell surface by PI-PLC treatment. The short RECK isoform, which does not have a GPI anchor, is liberated from the cell surface when long RECK is cleaved from the cell surface by PI-PLC. Right panel, liberated short RECK and long RECK isoforms in the supernatant interact based on coimmunoprecipitation. WCL, whole cell lysate. (F) Hypothesized model for the trafficking of a short RECK–long RECK complex. According to the model, short RECK–long RECK complexes are formed in the ER and then transported to the cell surface via the Golgi apparatus.

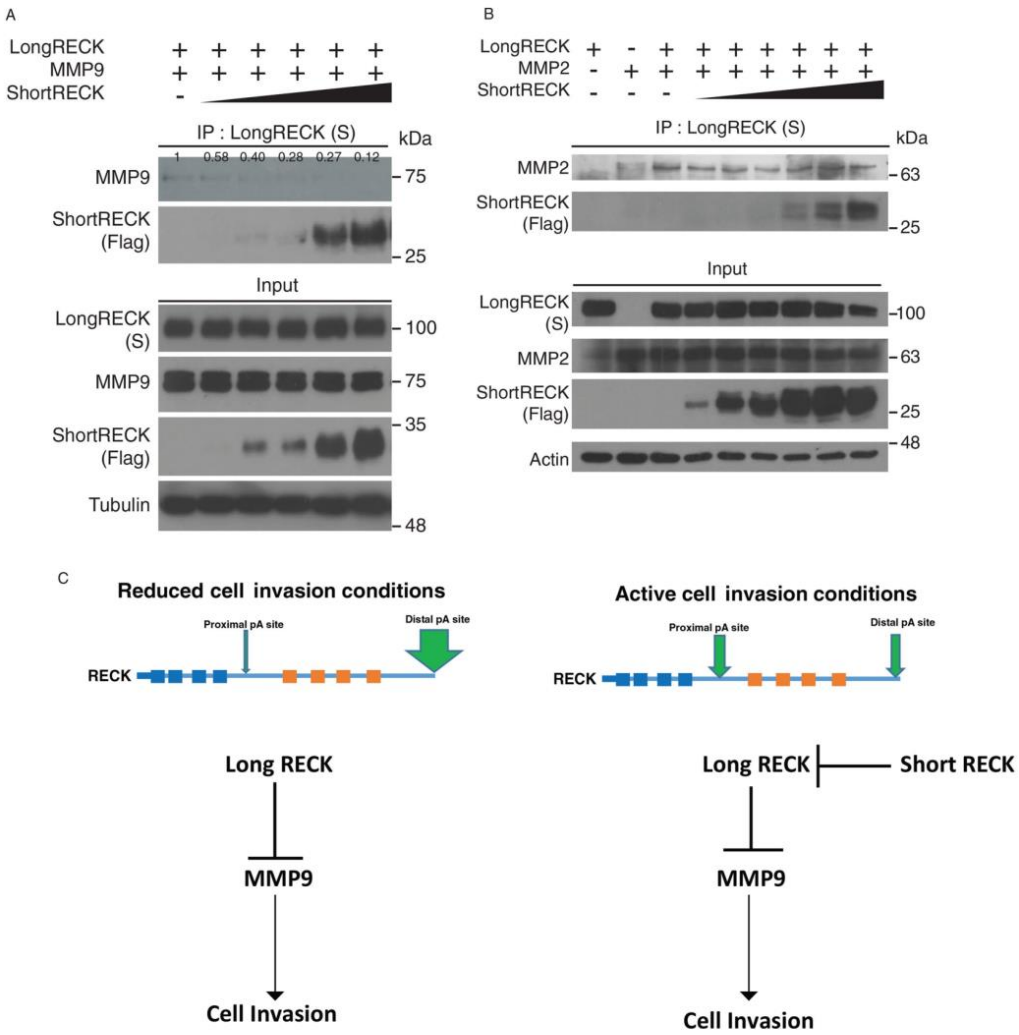


FIGURE 6: The short RECK isoform competes with MMP9 for binding to the long RECK isoform. (A) We generated RECK-null 293T cells that overexpress the long RECK isoform and MMP9. Increasing amounts of the short RECK isoform was transfected into cells as shown on the top of each lane. Western blots of input for immunoprecipitation are shown at the bottom. Samples were immunoprecipitated for the long RECK isoform with an antibody against S-tag and immunoblotted for the short RECK isoform with an anti-Flag antibody or an antibody against MMP9. The interaction between MMP9 and the long RECK isoform decreased with increasing levels of the short RECK isoform. The number above each band indicates relative expression level quantified with ImageJ. (B) RECK-null 293T cells overexpressing the long RECK isoform, MMP2, and increasing levels of the short RECK isoform were analyzed by coimmunoprecipitation. Western blots of input are shown at the bottom. Samples were immunoprecipitated with an antibody to S protein and analyzed with immunoblotting for the short RECK isoform and MMP2. The interaction between MMP2 and the long RECK isoform was not affected by increasing levels of the short RECK isoform. (C) Working model. In reduced cell migration conditions, the long RECK isoform tends to be expressed, resulting in a low short RECK:long RECK ratio. Under these conditions, the long RECK isoform suppresses MMP9 activity to inhibit cell migration. In contrast, under conditions of active cell migration, polyadenylation factors target proximal polyadenylation sites, resulting in a high short RECK:long RECK ratio. Short RECK inhibits the functions of long RECK through protein–protein interaction, leading to increased free MMP9, which can contribute to increased cell invasion.

MATERIALS AND METHODS

Cell culture and treatments

Human foreskin samples for establishing primary fibroblast cell lines were obtained by the National Disease Research Interchange. All protocols were approved by the Princeton University IRB (protocol number 3134) and the University of California, Los Angeles, IRB (protocol number 14-000145). BJ5ta (immortalized fibroblasts), 293T cells, and HT1080 were purchased from the America Type Culture Collection (ATCC). These cells were maintained in 10% fetal bovine serum (FBS) in DMEM in a 37°C humid incubator under 5% CO_2. 7dCI fibroblasts were collected 7 d after plating, or at an equivalent density, while 7dSS fibroblasts were seeded in full serum medium (10% FBS in

DMEM), changed to reduced serum medium (0.1% FBS in DMEM), and collected 7 d after adding the reduced serum medium.

Polyadenylation site–enriched RNA-Seq

cDNA libraries containing fragments enriched for 3′ UTR ends were created with the Gnomegen RNA-Seq Library Preparation Kit for RNA profiling (Gnomegen, San Diego, CA). In short, mRNA was fragmented to a size range of 100–2000 base pairs using metal cations. Transcripts were incubated with a poly(T) sequence attached to biotin and polyadenylated transcripts were captured with streptavidin beads. RNA adapters were ligated to the 5′ end of the fragmented RNA and incubated at 37°C for 2 h. Agencourt Ampure XP beads (Beckman Coulter, Indianapolis, IN) were used to remove ligation reaction products. First-strand cDNA was synthesized by incubation with Superscript III reverse transcriptase (Life Technologies, Grand Island, NY) at 42°C for 40 min. Amgen Ampure XP beads were used to remove reverse transcription products from first-strand cDNA. Second-strand cDNA synthesis and Illumina sequencing adapter ligations were achieved through PCR amplification of first-strand cDNA product. Common forward primers were used for all samples; reverse primers with a unique barcode sequence were specific for each sample. The size distribution of the cDNA library was confirmed using a High Sensitivity DNA chip (Agilent Technologies) on a Bioanalyzer 2100 Instrument (Agilent Technologies). Libraries with a uniform size distribution between 200 and 1000 base pairs were subjected to gel size selection to enrich for 200–300 base pair–sized fragments. Single-end 140 base pair reads were generated on an Illumina HiSeq 2000 Instrument. The sequencing reaction was run for 147 cycles. Reads from polyadenylation site–enriched cDNA libraries were aligned to the human genome (hg19) using the STAR algorithm, which is designed to align untemplated adenosines (Dobin *et al.*, 2013).

TCGA analysis

Data were obtained from The Cancer Genome Atlas (Cancer Genome Atlas, 2012a,b; Cancer Genome Atlas Research, 2012, 2013, 2014a,b; Cancer Genome Atlas Research *et al.*, 2013). Per-exon RNA-Seq read counts for tumor tissues and paired normal tissues along with any available clinical data were obtained from the TCGA public data portal. For comparison of RECK expression between tumor and paired normal tissue, read counts were normalized to the total number of reads per sample. RNA-Seq read counts assigned to the unique short RECK exon and the final long RECK exon were used to infer expression of short and long RECK isoforms, respectively. Short-to-long RECK isoform ratios, as well as normalized short and long RECK read counts, were determined for tumor and paired normal samples. Two-tailed paired *t* tests were performed separately for each tumor type using GraphPad Prism 6.04. To determine RECK isoform expression in breast cancers with different clinical characteristics, the relative use of the distal isoform (RUD) was calculated and the $\log_2$-fold change between tumor and paired normal was determined and plotted based on PAM50 subtype. Statistical significance was determined by one-way analysis of variance (ANOVA) followed by Tukey post-hoc test for two-way comparisons to control for multiple hypothesis testing.

Real-time RT-PCR

Cells were harvested in TRIzol reagent (Invitrogen). Chloroform was added and the lysate was centrifuged. The aqueous supernatant containing RNA was collected. Isopropanol was added to precipitate the RNA. The precipitated RNA pellet was washed with 70% ethanol, then dissolved in water and quantified by NanoDrop 2000C (Thermo Scientific). RNA (50 ng) was used for one reaction of reverse transcription and amplified using a SuperScript III Platinum SYBR Green One-Step qRT-PCR Kit (Invitrogen). A reaction of 25 µl was amplified in 96-well plates (USA Scientific) in triplicate for each gene. Real-time RT-PCR was performed in a CFX96 real-time system (Bio-Rad) and all results were normalized to the expression level of UBC in the same sample. Gene expression levels were calculated using the $2^{-\Delta\Delta Ct}$ method. We removed outliers, which were defined as values that were ±100% of the average of the other values. Primer sequences are as follows: short RECK isoform, 5′-TTGCGCCTCTATTAGTCCACAA-3′ and 5′-AGTAATAATTGCTCATTGGCAAAA-3′; long RECK isoform 5′-CAGAAATTGTGATCCTGATCATTCC-3′ and 5′-AAAGTCGGGCTGTCAGAGTTGATA-3′; total RECK 5′-AAATGTGCCGTGATGTATGTGAAC-3′ and 5′-TTAAACACACCTGGCAAAGATGAA-3′; UBC 5′-TCTTGTTTGTGGATCGCTGTGA-3′ and 5′-CAGGAGGGATGCCTTCCTTATC-3′; CTGF 5′-CTGCAGGCTAGAGAAGCAGAGC-3′ and 5′-GCTCAAACTTGATAGGCTTGGAGA-3′.

Antibodies

A monoclonal antibody against RECK (long isoform) and an antibody against tubulin were obtained from Thermo Fisher Scientific. For detection of FLAG, S-tag, GST, and HA, antibodies were purchased from Sigma-Aldrich, Cell Signaling Technology, Santa Cruz Biotechnology, and One World Lab, respectively. Antibodies against phospho-AKT, total AKT, phospho-ERK, total ERK, phospho-JNK, and total JNK were obtained from Cell Signaling Technology. To detect MMP2 and MMP9, antibodies were obtained from Abcam and Thermo Fisher Scientific. Antibodies against tubulin and actin used for loading controls were purchased from Sigma-Aldrich and Cell Signal Technology, respectively. Custom rabbit anti-human short RECK polyclonal antibody was generated twice. The first polyclonal was generated by GenScript (Piscataway, NJ) with experiments approved by the GenScript IACUC. The peptide CTDMFEFFANEQL was conjugated to KLH at the N-terminus. This peptide sequence was chosen to maximize antigenicity while maintaining predicted specificity to the short isoform of RECK. The peptide-KLH conjugate was used as an immunogen for New Zealand rabbits. Lyophilized antigen, preimmune serum, and affinity-purified antibody dissolved in phosphate-buffered saline (PBS; pH 7.4) with 0.02% sodium azide were provided by GenScript. Indirect enzyme-linked immunosorbent assays (ELISAs) were performed to validate the antibody. Free peptide (4 µg/ml) was plated at 100 µl/well in PBS, pH 7.4. A goat-raised anti-rabbit immunoglobulin G (H&L) secondary antibody conjugated to peroxidase was used as a secondary antibody. When the purified antibody was used as the primary antibody in these ELISAs, a clear signal above background, defined as either blank or preimmune serum, was observed at a 1:512,000 dilution. The titer (defined as the highest dilution with signal/blank ≥ 2.1) was determined as 1:512,000. For purification, Flag-tagged short RECK protein from 293T lysate was covalently immobilized onto beads conjugated with an anti-Flag antibody (Sigma-Aldrich). After mixing polyclonal short RECK antibody with the beads, the bound antibody was eluted using glycine (pH 2.5).

The second polyclonal antibody was generated by New England Peptide. The procedures were approved by the IACUC for SDIX LLC. The immunizing antigen was Ac-KKKC(dPEG4)DMFEFFANEQLLLL-OH. The peptide was conjugated to KLH and used to immunize rabbits multiple times. Serum from the rabbits was confirmed to react against the immunizing peptide conjugated to bovine serum albumin (BSA) by ELISA and to react more strongly to the immunizing peptide than to an irrelevant peptide conjugated to BSA.

Immunoblotting

Harvested cells were lysed in RIPA buffer (10 mM Tris-Cl, pH 8.0, 0.1% sodium deoxycholate, 0.5 mM EGTA, 1 mM EDTA, 0.1% SDS, 1% Triton X-100, 140 mM NaCl) containing protease inhibitor (Roche Applied Science) for 15 min on ice. After centrifugation, the supernatant was collected and the concentration was measured using a Thermo Scientific Pierce BCA Protein Assay kit (Thermo Fisher Scientific). Samples of 20 µg per well were loaded on SDS–PAGE gels and electrophoresed for 1 h and 25 min. The electrophoresed samples were transferred to 0.45 µm polyvinylidene difluoride membrane (Millipore) and blocked in 5% skim milk in 0.1% PBS-Tween (PBST) for 30 min. The primary and secondary antibody incubation steps were performed under conditions recommended by the antibody provider. Immunoblot data were quantified using ImageJ.

Coimmunoprecipitation and GST–pull down assay

Plasmids engineered to express the short RECK isoform or the long RECK isoform (4 µg) were introduced into 293T cells using Lipofectamine 2000 according to the manufacturer's instructions. After transfection (48 h), cells were harvested and lysed in NETN buffer (100 mM NaCl, 0.5 mM EDTA, 20 mM Tris-Cl, pH 8.0, and 0.5% NP-40) containing protease inhibitor (Roche). Protein concentrations were measured by a BCA protein assay kit. Cell lysates (1 mg) were incubated overnight at 4°C with 2 µg of antibody. The next day, washed Sepharose A and G mixture (Sigma-Aldrich) was added and incubated for 1 h at 4°C. The protein mixture precipitated with the antibody and the precipitate was analyzed by Western blot using SDS–PAGE gels. For GST–pull down assays, short RECK conjugated to a GST tag and long RECK isoforms with domain-specific deletions were introduced into cells. Protein lysates were collected and GST-containing proteins were precipitated with GST•Bind Resin (EMD Millipore).

Plasmids and vectors

For short and long RECK isoforms, the short RECK isoform was synthesized by Genewiz (South Plainfield, NJ), and a cDNA encoding the long RECK isoform was purchased from Thermo Scientific. 3X Flag-tagged short RECK and long RECK isoforms were subcloned into pRRL-CMV-MCS-IRES-Hygro (UCLA Virus Core Laboratory) for mammalian cell overexpression. A vector expressing the long RECK isoform was obtained from Dharmacon. Plasmids containing MMP2 or MMP9 were purchased from DNASU, Arizona State University, and subcloned into a pRRL-CMV-MCS-IRES-Hygro vector for overexpression in mammalian cells. pBiFC-VC155 and pBiFC-VN173 were obtained from Addgene and subcloned into pRRL-CMV-MCS-IRES-Hygro for overexpression or lentivirus production.

RECK isoform-specific shRNAs were designed using the Broad Institute TRC design pipeline (https://www.broadinstitute.org/rnai/public/seq/search) and BLOCK-iT RNAi Designer (https://rnaidesigner.thermofisher.com/rnaiexpress). Knockdown shRNAs were cloned into the *Bam*HI and *Eco*RI sites of the lentiviral plasmid pGreenPuro (Systems Biosciences) and expressed under control of the H1 promoter. Sequences are provided: shControl.1, 5′-GATCCCCTAAGGTTAAGTCGCCCTCGTTCAAGAGACGAGGGCGACTTAACCTTAGGTTTTTG-3′ and 5′-AATTCAAAAACCTAAGGTTAAGTCGCCCTCGTCTCTTGAACGAGGGCGACTTAACCTTAGGG-3′; shControl.2 5′-GATCCCAACAAGATGAAGAGCACCAACTTCCTGTCAGATTGGTGCTCTTCATCTTGTTGTTTTTG-3′ and 5′-AATTCAAAAACAACAAGATGAAGAGCACCAATCTGACAGGAAGTTGGTGCTCTTCATCTTGTTGG-3′; shShortRECK.1 5′-GATCCGCTTTGTACATCCTGGAATCCCTTCCTGTCAGAGGATTCCAGGATGTACAAAGCTTTTTG-3′ and 5′-AATTCAAAAAGCTTTGTACATCCTGGAATCCTCTGACAGGAAGGGATTCCAGGATGTACAAAGCG-3′; shShortRECK.2 5′-GATCCGATCTGTGCTCTCTGACATTTCTTCCTGTCAGAAAATGTCAGAGAGCACAGATCTTTTTG-3′ and 5′-AATTCAAAAAGATCTGTGCTCTCTGACATTTTCTGACAGGAAGAAATGTCAGAGAGCACAGATCG-3′; shLongRECK.1 5′-GATCCGCGTGGCAGTCGATTACTATGTTCAAGAGACATAGTAATCGACTGCCACGCTTTTTG-3′ and 5′-AATTCAAAAAGCGTGGCAGTCGATTACTATGTCTCTTGAACATAGTAATCGACTGCCACGCG-3′; shLongRECK.2 5′-GATCCGCATCAAAGCATCTTGCATTACTTCCTGTCAGATAATGCAAGATGCTTTGATGCTTTTTG-3′ and 5′-AATTCAAAAAGCATCAAAGCATCTTGCATTATCTGACAGGAAGTAATGCAAGATGCTTTGATGCG-3′; lentiviral plasmids were cotransfected with pLP1, pLP2, and pLP/VSV.G packaging plasmids (Systems Biosciences) into 293T cells using Lipofectamine2000 (Life Technologies). Supernatants containing lentivirus were collected 48 and 72 h posttransfection and used to infect human fibroblasts. Stable lines were generated by adding selectable markers puromycin (for 5 d at 500 µg/ml) or hygromycin (for 3 d at 2 µg/ml).

Cell migration assays

Cells were plated in IncuCyte ImageLock 96-well microplates (Essen Bioscience) at a concentration of 25,000 cells/well the day before the experiment. Plates were coated with Matrigel (Corning) at 100 µg/ml before cell seeding. The next day, a scratch wound of 700–800 µm width was generated in the center of the well using the IncuCyte WoundMaker (Essen Bioscience). After the wounds were generated, they were filled with 50 µl of 0.5 mg/ml Matrigel on ice. Matrigel was allowed to solidify at 37°C for 30 min. Complete medium (100 ml) was poured on top of the Matrigel, and wound recovery was monitored with live imaging for up to 96 h. The results were analyzed with Incucyte Zoom software.

WST-1 assay

Cells (20,000) were plated in 24-well plates. After cell plating (48 h), cell proliferation was compared using the Premixed WST-1 cell proliferation assay system (Clonetech) as described in the manufacturer's protocol. The WST-1 solution was added to complete media and incubated at 37°C for 2 h. The plate was analyzed for absorbance at 440 nm.

Immunofluorescence staining

Cells grown on coverslips were rinsed with PBS and then fixed with 4% paraformaldehyde in PBS, pH 7.4 for 15 min. For permeabilization, cells were incubated for 10 min in 0.25% Triton X-100 in PBS. After blocking for 30 min using 1% BSA in PBST, cells were incubated with primary antibody (diluted 1:100) in 1% BSA in PBST overnight at 4°C. Cells were stained with secondary antibody (diluted 1:200) for 1 h at room temperature and counterstained with 4′,6-diamidino-2-phenylindole to visualize nuclei. When observing the cell surface, the permeabilization step was omitted.

RECK knockout by CRISPR/Cas9

By participating in Horizon's free CRISPR Guide RNA program, we were able to test five different guide RNAs for their efficiency in knocking out RECK. The double-strand-break efficiency was tested using the GeneArt Genomic Cleavage Detection Kit (Life Technologies). A plasmid containing Cas9 and 5′-GCGCACCTCGCAGAGAGGCC-3′ showed the highest efficiency and was introduced into 293T cells to introduce DNA breaks via nonhomologous end joining. Individual cells were plated at limiting dilution and clones were grown.

Cell lines derived from a single cell were monitored with immunoblotting for RECK levels. Individual clones with reduced levels of the long RECK isoform were selected for further analysis. The DNA sequence near the region targeted by the RECK guide RNA was amplified by PCR (5′-AACAAAGAGCCCTGGTACGG-3′ and 5′-CATCTAAACCTCGCGACGAT-3′) and the PCR product was cloned into pCR4Blunt-TOPO plasmid using Zero Blunt TOPO PCR Cloning Kits (Invitrogen). Sequencing was performed by Genewiz using primers targeting the T3 priming site 5′-ATTAACCCTCACTAAAGGGA-3′.

PI-PLC treatment to cleave the GPI anchor

On the day before the transfection, RECK knockout 293T cells were seeded with 4,400,000 cells per 10 cm dish. For transfection, 4 µg of short RECK and long RECK overexpression vectors were introduced into the RECK knockout 293T cell line using Lipofectamine 2000 (Invitrogen). After transfection (24 h), cells were rinsed twice with PBS and then incubated in 5 ml of PI-PLC (Sigma-Aldrich) in DMEM at 100 mU/ml or DMEM without PI-PLC for the control. After 24 h of PI-PLC treatment, the supernatant and cells were separately harvested for analysis. The supernatant was filtered through a 0.45 µm syringe filter and used for Western blotting.

Cytokines

Recombinant human TGF-β (BioLegend) was prepared in PBS at 5 µg/ml for a final concentration of 5 ng/ml.

Data availability

The full alternative polyadenylation data set described in this study is available through the Gene Express Omnibus database as accession number GSE117337 deposited on July 18, 2018.

ACKNOWLEDGMENTS

We thank the Eli and Edythe Broad Center for Regenerative Medicine and Stem Cell Research for Core Facilities that house a confocal microscope and IncuCyte instrument. We acknowledge Jeff Long (University of California, Los Angeles [UCLA]) for sharing equipment for cloning and a confocal microscope. H.A.C. was the Milton E. Cassel scholar of the Rita Allen Foundation (http://www.ritaallenfoundation.org). H.N.L. acknowledges a Whitcome Fellowship from the UCLA Molecular Biology Institute. E.L.J. was supported in part by National Science Foundation Graduate Research Fellowship DGE-0646086. This work was funded by grants to H.A.C. from National Institute of General Medical Sciences Center of Excellence Grant no. P50 GM071508, PhRMA Foundation Grant no. 2007RSGl9572, National Institute of General Medical Sciences R01 GM081686, National Institute of General Medical Sciences R01 GM0866465, the Eli and Edythe Broad Center for Regenerative Medicine and Stem Cell Research, the Iris Cantor Women's Health Center/UCLA, National Cancer Institute P50 CA092131, the UCLA Life Science Innovation Fund, UCLA Clinical and Translational Science Institute Grant no. UL1TR000124, the Leukemia Lymphoma Society, and funds from Rockefeller University. H.A.C. is a member of the Eli and Edythe Broad Center of Regenerative Medicine and Stem Cell Research, the Jonsson Comprehensive Cancer Center, the UCLA Molecular Biology Institute, and the UCLA Bioinformatics Interdepartmental Program. We thank Luisa Iruela-Arispe, Tracy Johnson, William Lowry, Jorge Torres, and Jose Rodriguez for helpful input, Barry Coller for suggestions on the choice of peptides for immunization to prepare the antibody to the short form of RECK, and Hina Zafar for assistance with RECK ELISA. The funders had no role in study design, data collection and analysis, decision to publish, or preparation of the manuscript. Some images in this paper were modified from Servier Medical Art (http://smart.servier.com/).

REFERENCES

Acharya PS, Majumdar S, Jacob M, Hayden J, Mrass P, Weninger W, Assoian RK, Pure E (2008). Fibroblast migration is mediated by CD44-dependent TGFβ activation. J Cell Sci 121, 1393–1402.

Alt FW, Bothwell AL, Knapp M, Siden E, Mather E, Koshland M, Baltimore D (1980). Synthesis of secreted and membrane-bound immunoglobulin mu heavy chains is directed by mRNAs that differ at their 3′ ends. Cell 20, 293–301.

Aman A, Piotrowski T (2010). Cell migration during morphogenesis. Dev Biol 341, 20–33.

Belkin AM, Akimov SS, Zaritskaya LS, Ratnikov BI, Deryugina EI, Strongin AY (2001). Matrix-dependent proteolysis of surface transglutaminase by membrane-type metalloproteinase regulates cancer cell adhesion and locomotion. J Biol Chem 276, 18415–18422.

Cancer Genome Atlas N (2012a). Comprehensive molecular characterization of human colon and rectal cancer. Nature 487, 330–337.

Cancer Genome Atlas N (2012b). Comprehensive molecular portraits of human breast tumours. Nature 490, 61–70.

Cancer Genome Atlas Research N (2012). Comprehensive genomic characterization of squamous cell lung cancers. Nature 489, 519–525.

Cancer Genome Atlas Research N (2013). Comprehensive molecular characterization of clear cell renal cell carcinoma. Nature 499, 43–49.

Cancer Genome Atlas Research N, Weinstein JN, Collisson EA, Mills GB, Shaw KR, Ozenberger BA, Ellrott K, Shmulevich I, Sander C, Stuart JM (2013). The Cancer Genome Atlas Pan-Cancer analysis project. Nat Genet 45, 1113–1120.

Cancer Genome Atlas Research N (2014a). Comprehensive molecular characterization of urothelial bladder carcinoma. Nature 507, 315–322.

Cancer Genome Atlas Research N (2014b). Comprehensive molecular profiling of lung adenocarcinoma. Nature 511, 543–550.

Cerami E, Gao J, Dogrusoz U, Gross BE, Sumer SO, Aksoy BA, Jacobsen A, Byrne CJ, Heuer ML, Larsson E, *et al*. (2012). The cBio cancer genomics portal: an open platform for exploring multidimensional cancer genomics data. Cancer Discov 2, 401–404.

Chang CK, Hung WC, Chang HC (2008). The Kazal motifs of RECK protein inhibit MMP-9 secretion and activity and reduce metastasis of lung cancer cells in vitro and in vivo. J Cell Mol Med 12, 2781–2789.

Cordeiro MF, Bhattacharya SS, Schultz GS, Khaw PT (2000). TGF-β1, -β2, and -β3 in vitro: biphasic effects on Tenon's fibroblast contraction, proliferation, and migration. Invest Ophthalmol Vis Sci 41, 756–763.

Dobin A, Davis CA, Schlesinger F, Drenkow J, Zaleski C, Jha S, Batut P, Chaisson M, Gingeras TR (2013). STAR: ultrafast universal RNA-seq aligner. Bioinformatics 29, 15–21.

Dufour A, Zucker S, Sampson NS, Kuscu C, Cao J (2010). Role of matrix metalloproteinase-9 dimers in cell migration: design of inhibitory peptides. J Biol Chem 285, 35944–35956.

Elkon R, Drost J, van Haaften G, Jenal M, Schrier M, Vrielink JA, Agami R (2012). E2F mediates enhanced alternative polyadenylation in proliferation. Genome Biol 13, R59.

Friedl P, Gilmour D (2009). Collective cell migration in morphogenesis, regeneration and cancer. Nat Rev Mol Cell Biol 10, 445–457.

Hong KJ, Wu DC, Cheng KH, Chen LT, Hung WC (2014). RECK inhibits stemness gene expression and tumorigenicity of gastric cancer cells by suppressing ADAM-mediated Notch1 activation. J Cell Physiol 229, 191–201.

Huang C, Jacobson K, Schaller MD (2004). MAP kinases and cell migration. J Cell Sci 117, 4619–4628.

Hunger-Glaser I, Salazar EP, Sinnett-Smith J, Rozengurt E (2003). Bombesin, lysophosphatidic acid, and epidermal growth factor rapidly stimulate focal adhesion kinase phosphorylation at Ser-910: requirement for ERK activation. J Biol Chem 278, 22631–22643.

Ji Z, Lee JY, Pan Z, Jiang B, Tian B (2009). Progressive lengthening of 3′ untranslated regions of mRNAs by alternative polyadenylation during mouse embryonic development. Proc Natl Acad Sci USA 106, 7028–7033.

Kajita M, Itoh Y, Chiba T, Mori H, Okada A, Kinoh H, Seiki M (2001). Membrane-type 1 matrix metalloproteinase cleaves CD44 and promotes cell migration. J Cell Biol 153, 893–904.

Kim NY, Lee JE, Chang HJ, Lim CS, Nam DH, Min BH, Park GH, Oh JS (2008). Gamma-irradiation enhances RECK protein levels in Panc-1 pancreatic cancer cells. Mol Cells 25, 105–111.
Klemke RL, Cai S, Giannini AL, Gallagher PJ, de Lanerolle P, Cheresh DA (1997). Regulation of cell motility by mitogen-activated protein kinase. J Cell Biol 137, 481–492.
Kornblihtt AR, Schor IE, Allo M, Dujardin G, Petrillo E, Munoz MJ (2013). Alternative splicing: a pivotal step between eukaryotic transcription and translation. Nat Rev Mol Cell Biol 14, 153–165.
Li QQ, Liu Z, Lu W, Liu M (2017). Interplay between alternative splicing and alternative polyadenylation defines the expression outcome of the plant unique OXIDATIVE TOLERANT-6 gene. Sci Rep 7, 2052.
Lianoglou S, Garg V, Yang JL, Leslie CS, Mayr C (2013). Ubiquitously transcribed genes use alternative polyadenylation to achieve tissue-specific expression. Genes Dev 27, 2380–2396.
Lin NU, Claus E, Sohl J, Razzak AR, Arnaout A, Winer EP (2008). Sites of distant recurrence and clinical outcomes in patients with metastatic triple-negative breast cancer: high incidence of central nervous system metastases. Cancer 113, 2638–2645.
Mahl C, Egea V, Megens RT, Pitsch T, Santovito D, Weber C, Ries C (2016). RECK (reversion-inducing cysteine-rich protein with Kazal motifs) regulates migration, differentiation and Wnt/β-catenin signaling in human mesenchymal stem cells. Cell Mol Life Sci 73, 1489–1501.
Masamha CP, Xia Z, Yang J, Albrecht TR, Li M, Shyu AB, Li W, Wagner EJ (2014). CFIm25 links alternative polyadenylation to glioblastoma tumour suppression. Nature 510, 412–416.
Mayr C, Bartel DP (2009). Widespread shortening of 3'UTRs by alternative cleavage and polyadenylation activates oncogenes in cancer cells. Cell 138, 673–684.
Miki T, Takegami Y, Okawa K, Muraguchi T, Noda M, Takahashi C (2007). The reversion-inducing cysteine-rich protein with Kazal motifs (RECK) interacts with membrane type 1 matrix metalloproteinase and CD13/aminopeptidase N and modulates their endocytic pathways. J Biol Chem 282, 12341–12352.
Montero JA, Kilian B, Chan J, Bayliss PE, Heisenberg CP (2003). Phosphoinositide 3-kinase is required for process outgrowth and cell polarization of gastrulating mesendodermal cells. Curr Biol 13, 1279–1289.
Morioka Y, Monypenny J, Matsuzaki T, Shi S, Alexander DB, Kitayama H, Noda M (2009). The membrane-anchored metalloproteinase regulator RECK stabilizes focal adhesions and anterior-posterior polarity in fibroblasts. Oncogene 28, 1454–1464.
Morris AR, Bos A, Diosdado B, Rooijers K, Elkon R, Bolijn AS, Carvalho B, Meijer GA, Agami R (2012). Alternative cleavage and polyadenylation during colorectal cancer development. Clin Cancer Res 18, 5256–5266.
Nabeshima K, Inoue T, Shimao Y, Sameshima T (2002). Matrix metalloproteinases in tumor invasion: role for cell migration. Pathol Int 52, 255–264.
Oh J, Seo DW, Diaz T, Wei B, Ward Y, Ray JM, Morioka Y, Shi S, Kitayama H, Takahashi C, *et al.* (2004). Tissue inhibitors of metalloproteinase 2 inhibits endothelial cell migration through increased expression of RECK. Cancer Res 64, 9062–9069.
Oh J, Takahashi R, Kondo S, Mizoguchi A, Adachi E, Sasahara RM, Nishimura S, Imamura Y, Kitayama H, Alexander DB, *et al.* (2001). The membrane-anchored MMP inhibitor RECK is a key regulator of extracellular matrix integrity and angiogenesis. Cell 107, 789–800.
Omura A, Matsuzaki T, Mio K, Ogura T, Yamamoto M, Fujita A, Okawa K, Kitayama H, Takahashi C, Sato C, Noda M (2009). RECK forms cowbell-shaped dimers and inhibits matrix metalloproteinase-catalyzed cleavage of fibronectin. J Biol Chem 284, 3461–3469.
Parker JS, Mullins M, Cheang MC, Leung S, Voduc D, Vickery T, Davies S, Fauron C, He X, Hu Z, *et al.* (2009). Supervised risk predictor of breast cancer based on intrinsic subtypes. J Clin Oncol 27, 1160–1167.
Peterson ML (2011). Immunoglobulin heavy chain gene regulation through polyadenylation and splicing competition. Wiley Interdiscip Rev RNA 2, 92–105.
Rehfeld A, Plass M, Dossing K, Knigge U, Kjaer A, Krogh A, Friis-Hansen L (2014). Alternative polyadenylation of tumor suppressor genes in small intestinal neuroendocrine tumors. Front Endocrinol (Lausanne) 5, 46.
Takagaki Y, Seipelt RL, Peterson ML, Manley JL (1996). The polyadenylation factor CstF-64 regulates alternative processing of IgM heavy chain pre-mRNA during B cell differentiation. Cell 87, 941–952.
Takahashi C, Sheng Z, Horan TP, Kitayama H, Maki M, Hitomi K, Kitaura Y, Takai S, Sasahara RM, Horimoto A, *et al.* (1998). Regulation of matrix metalloproteinase-9 and inhibition of tumor invasion by the membrane-anchored glycoprotein RECK. Proc Natl Acad Sci USA 95, 13221–13226.
Takemoto N, Tada M, Hida Y, Asano T, Cheng S, Kuramae T, Hamada J, Miyamoto M, Kondo S, Moriuchi T (2007). Low expression of reversion-inducing cysteine-rich protein with Kazal motifs (RECK) indicates a shorter survival after resection in patients with adenocarcinoma of the lung. Lung Cancer 58, 376–383.
Tian B, Manley JL (2013). Alternative cleavage and polyadenylation: the long and short of it. Trends Biochem Sci 38, 312–320.
Trombetta-Lima M, Winnischofer SM, Demasi MA, Astorino Filho R, Carreira AC, Wei B, de Assis-Ribas T, Konig MS, Bowman-Colin C, Oba-Shinjo SM, *et al.* (2015). Isolation and characterization of novel RECK tumor suppressor gene splice variants. Oncotarget 6, 33120–33133.
Tseng LM, Hsu NC, Chen SC, Lu YS, Lin CH, Chang DY, Li H, Lin YC, Chang HK, Chao TC, *et al.* (2013). Distant metastasis in triple-negative breast cancer. Neoplasma 60, 290–294.
Vorlova S, Rocco G, Lefave CV, Jodelka FM, Hess K, Hastings ML, Henke E, Cartegni L (2011). Induction of antagonistic soluble decoy receptor tyrosine kinases by intronic polyA activation. Mol Cell 43, 927–939.
Wolf K, Te Lindert M, Krause M, Alexander S, Te Riet J, Willis AL, Hoffman RM, Figdor CG, Weiss SJ, Friedl P (2013). Physical limits of cell migration: control by ECM space and nuclear deformation and tuning by proteolysis and traction force. J Cell Biol 201, 1069–1084.
Xue G, Hemmings BA (2013). PKB/Akt-dependent regulation of cell motility. J Natl Cancer Inst 105, 393–404.
Yao P, Potdar AA, Arif A, Ray PS, Mukhopadhyay R, Willard B, Xu Y, Yan J, Saidel GM, Fox PL (2012). Coding region polyadenylation generates a truncated tRNA synthetase that counters translation repression. Cell 149, 88–100.
Zuo J, Ferguson TA, Hernandez YJ, Stetler-Stevenson WG, Muir D (1998). Neuronal matrix metalloproteinase-2 degrades and inactivates a neurite-inhibiting chondroitin sulfate proteoglycan. J Neurosci 18, 5203–5211.

Supplemental Materials

Molecular Biology of the Cell

Lee et al.

Supplemental Figure 1: Validation of the short RECK-specific antibody.(A) We introduced Flag-tagged short RECK or Flag-tagged long RECK into 293T cells and collected protein lysates. We performed immunoblotting with an antibody to Flag, a commercially-available antibody to the C-terminus of the long RECK isoform, or the polyclonal antibody we generated that targets the amino acids present in the short RECK isoform, but not the long RECK isoform. The antibody that we generated against the short RECK isoform recognized short RECK protein and not long RECK protein. The arrowhead indicates the protein expressed by the short RECK isoform. (B) Validation of the second short RECK-specific antibody.The second polyclonal short RECK-specific antibody also recognizes the short RECK protein and not the long RECK protein.

Supplemental Figure 2: RNA-Seq read counts from The Cancer Genome Atlas were compiled for different types of cancer for the short and long isoforms of RECK. Read counts for the long (A) and short (B) RECK isoforms are plotted for different tumor types and control tissue.

Supplemental Figure 3: RECK isoforms do not affect cell proliferation and RECK isoform overexpression does not affect migration through Matrigel. (A) The WST-1 assay was performed 48 hours after cell plating to monitor the number of viable cells. There was no significant difference in cell proliferation among samples expressing control shRNAs, an shRNA against the long RECK isoform or an shRNA against the short RECK isoform. shControl versus shLong RECK.1, shLongRECK.2 (p=0.81, p=0.64;unpaired two-sided Student's t-test), shControl versus shShortRECK.1, shShortRECK.2 (p=0.78, p=0.07;unpaired two-sided Student's t-test). Abbreviation: N.S.: not significant(B) Fibroblasts were transduced with lentiviral vectors that overexpress the short RECK isoform, the long RECK isoform or both. Immunoblotting

confirmed overexpression of the indicated proteins (left). Fibroblast migration through Matrigel was similar in controls and fibroblasts overexpressing a RECK isoform (right).

Supplemental Figure 4: RECK isoforms do not activate AKT, ERK, orJNK pathways. AKT, ERK,and JNK pathways were not regulated by RECK isoforms. Western blot results showing phosphorylated and total AKT, ERK, and JNK levels in fibroblasts expressing shRNAs that target either short or long RECK.

Supplemental Figure 5: Long RECK interacts with itself and short RECK interacts with itself.(A) HEK293T cells were co-transfected with S-tagged long RECK and Myc-tagged long RECK. Immunoprecipitation with antibodies against Myc and immunoblotting with an antibody against the S tagrevealed an interaction between long RECK isoforms. A similar result was observed when immunoprecipitation was performed with an antibody against the S tagand immunoblotting was performed with an antibody against Myc. (B) Short RECK isoforms interact with each other.Short RECK isoforms fused to Flag or S tags were introduced into HEK293T cells. Immunoprecipitated with antibodies against Flagfollowed by immunoblotting with antibodies against S tag, revealed co-immunoprecipitation. Similar results were observed from immunoprecipitation with antibodies against S and immunoblotting with antibodies against Flag.

Supplemental Figure 6: Further validation of the interaction between the short and long RECK isoforms at the cell surface.(A) ControlBiFCassays. Fibroblasts expressing the N-terminal portion of Venus of the C-terminal portion of Venus alone exhibited no fluorescent signal. Fibroblasts expressing the N-terminal portion of Venus and the C-terminal portion of Venus contained a diffuse green signal throughout the cell. In contrast, when BiFCwas performed with short RECK fused to the C terminal half of

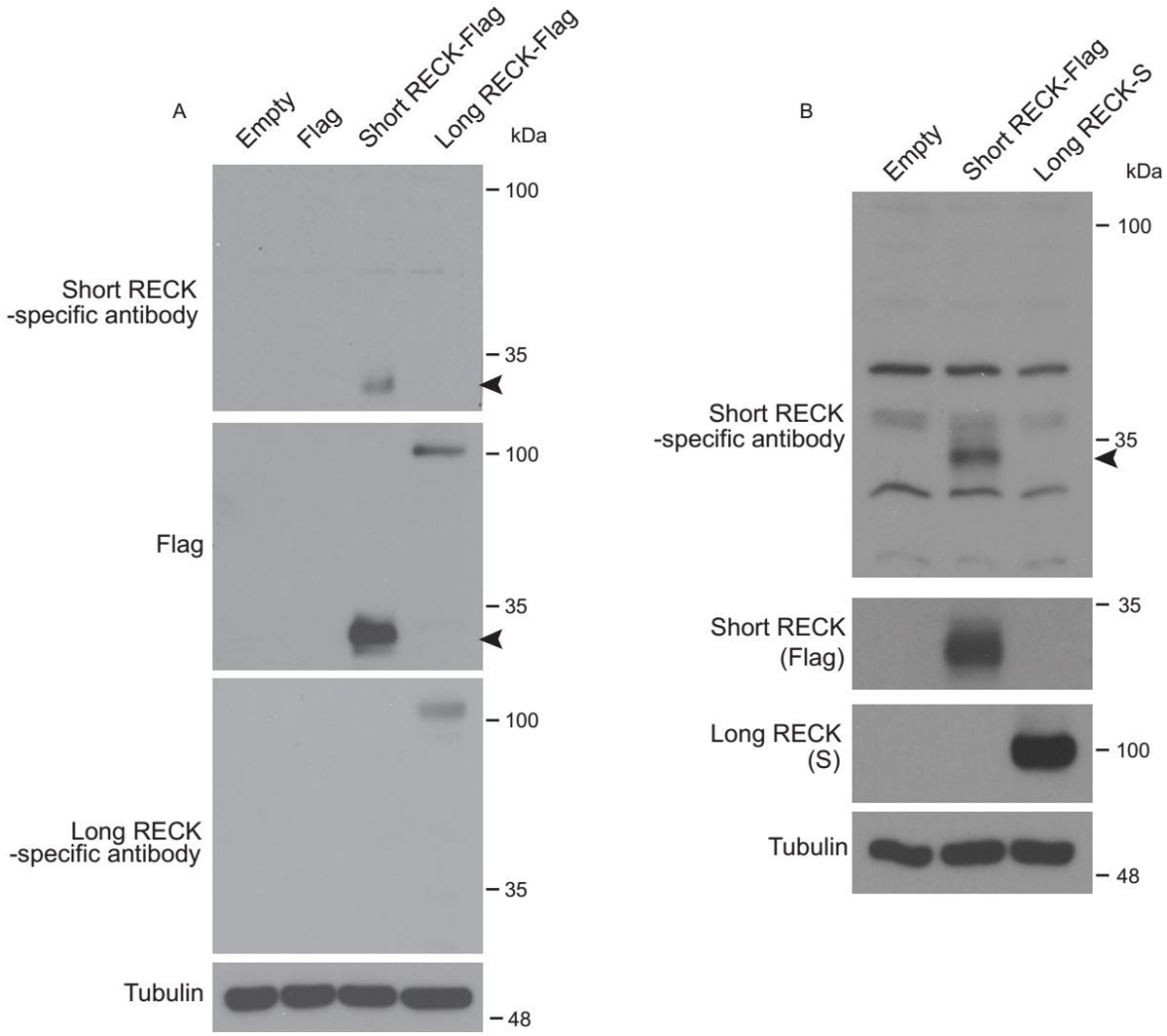
Venus and long RECK fused to the N terminal half of Venus, a signal is observed in the ER, Golgi and cell surface (Figure 4B). (B) Control BiFC assay with RECK isoforms. No signal was observed when the C-terminal half of Venus conjugated to short RECK or the N-terminal half of Venus conjugated to long RECK was introduced into fibroblasts. (C) Immunofluorescence staining consistent with short RECK-long RECK interaction on the cell surface. To observe an interaction between the short and long RECK isoforms on the fibroblast cell surface, staining was performed without cell permeabilization. Quantification of the data shows that approximately 30% of the signal from the shortRECK isoform on the cell surface overlaps with the signal from the long RECK isoform.Averages and S.D. are shown.$p<0.01$, unpaired two-sided Student's t-test. Two asterisks indicate$p< 0.01$.

Supplemental Figure 7: The portion of long RECK residing between amino acids 635 and 773 is important for binding to short RECK, while the C terminus of long RECK is important for long RECK dimerization.(A)Liberation of the long RECK isoform with domain-specific deletionsby PI-PLC treatment. Full length, Δ36-340, and Δ341-634 RECK proteins were released to the supernatant by PI-PLC and observed with short film exposure. RECK with Δ635-773 and Δ774-941 deletions were observed in the supernatant after PI-PLC treatment after longer exposure. (B) Results from a GST-pull down assay.Similar to the results with co-immunoprecipitation (Figure 6), short RECK-long RECK interaction is dramatically reduced when the domain containing the Kazal-like motif was deleted (Δ635-773). (C) The long RECK isoform interacts with itself through its C-terminal region. Myc-tagged long RECK and S-tagged deletion mutants of long RECK were co-introduced into 293T cells. Co-immunoprecipitation immunoblots are shown below. Immunoprecipitation against S-tagged long RECK and

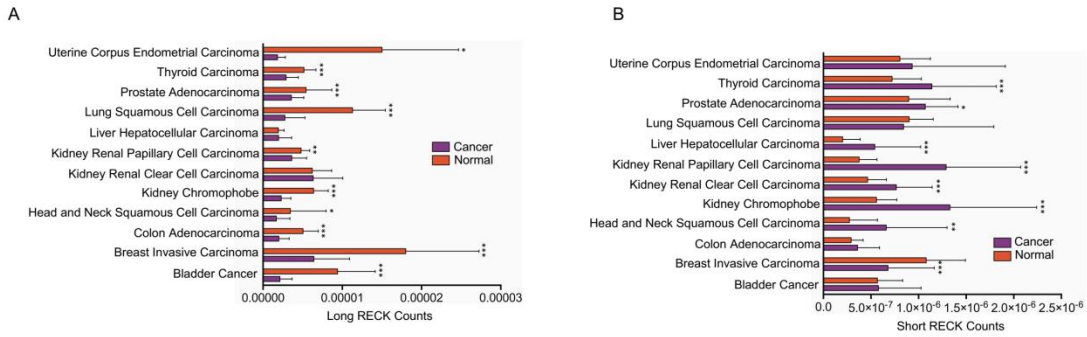
immunoblotting for Myc-tagged long RECK revealed reduced binding for a mutated form of long RECK missing amino acids 774 to 941.

Supplemental Figure 8 The short RECK isoform does not affect dimerization of the long RECK isoform.293T cells were transfected with two different versions of the long RECK isoform (Myc or S tagged), and increasing levels of the short RECK isoform. Samples were immunoprecipitated with an antibody to Myc and analyzed with an antibody to S tag to test whether the short RECK isoform affects long RECK dimerization.

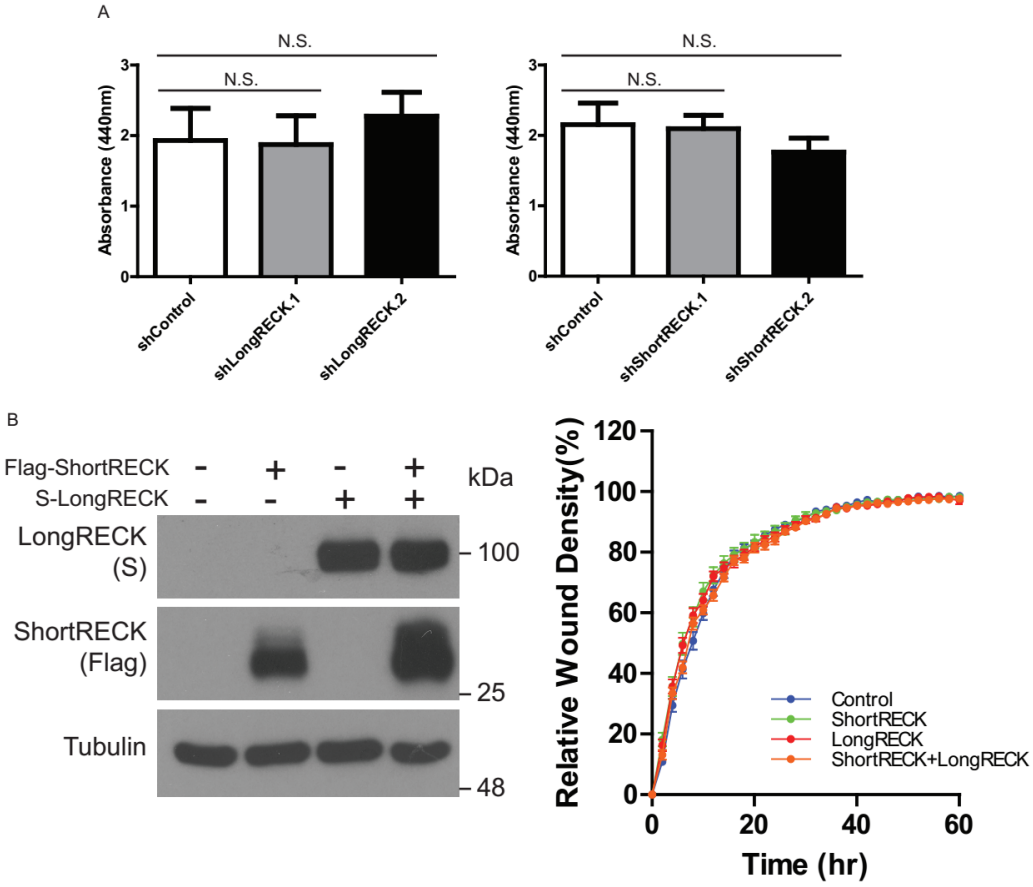
Supplemental Figure S1



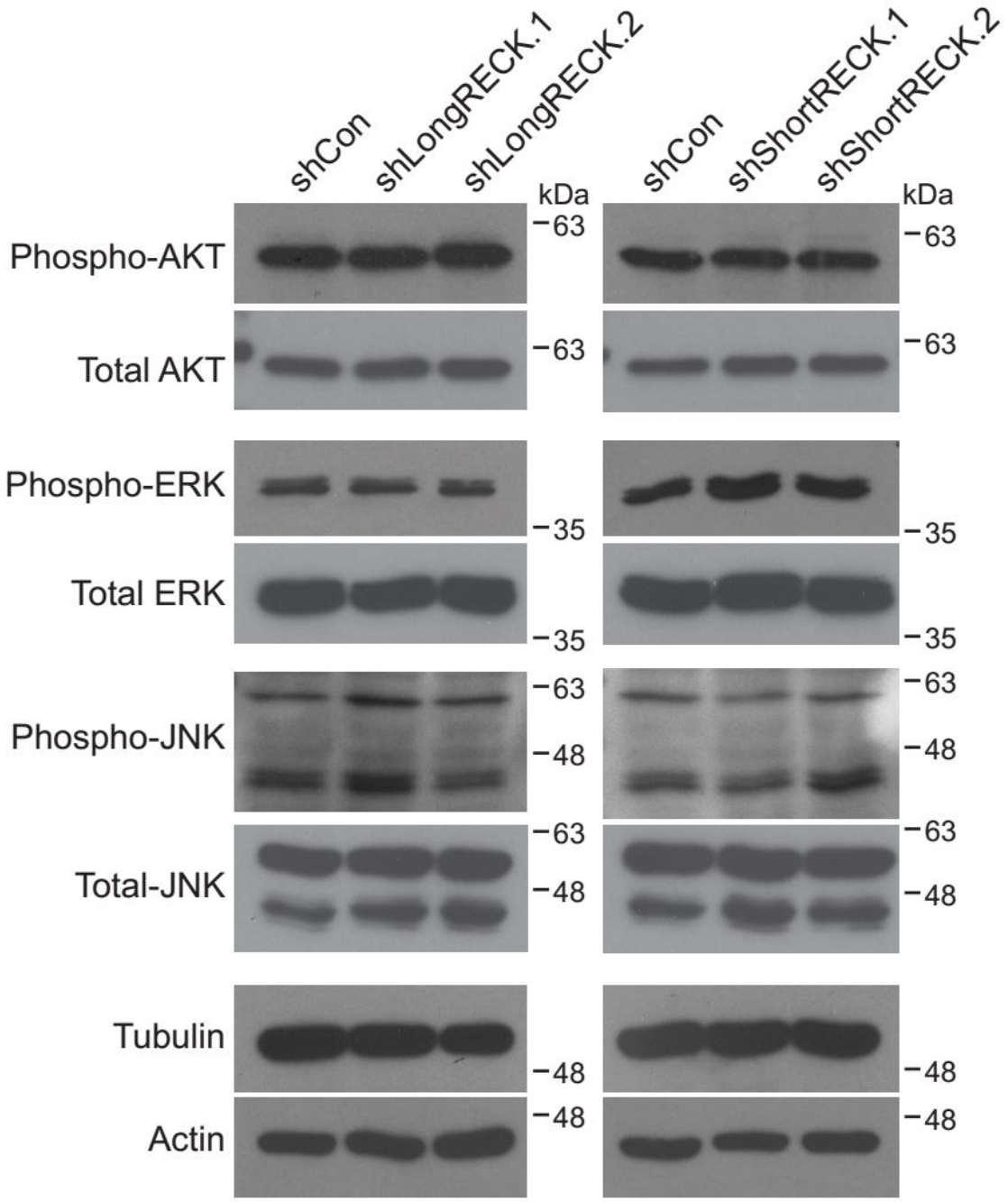
Supplemental Figure S2



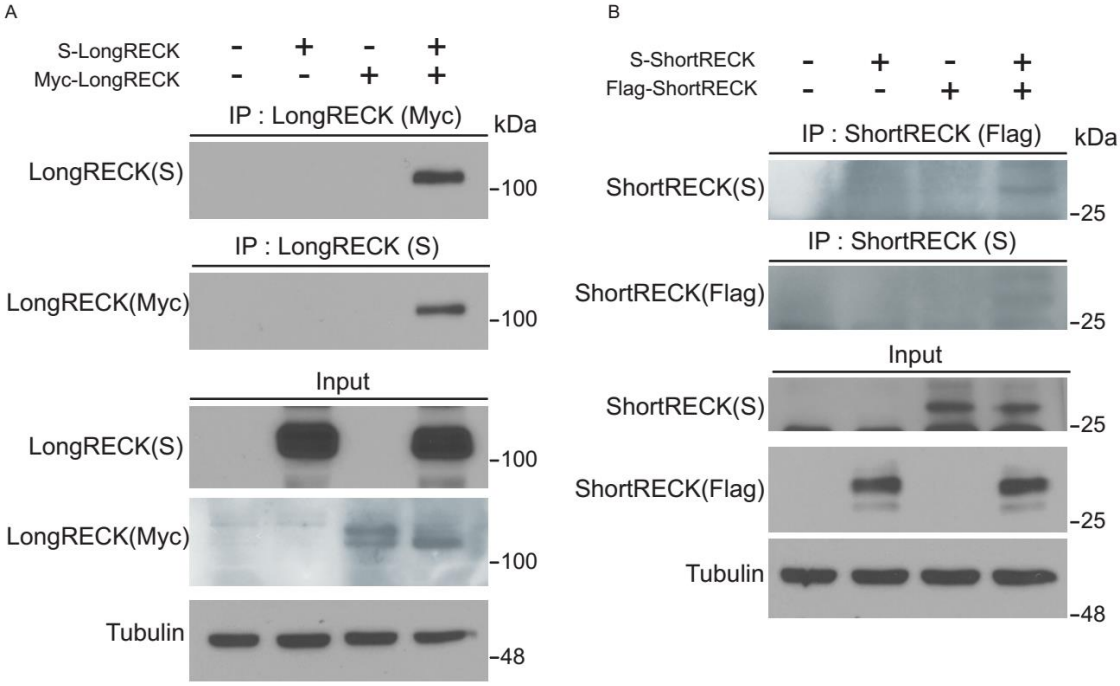
Supplemental Figure S3



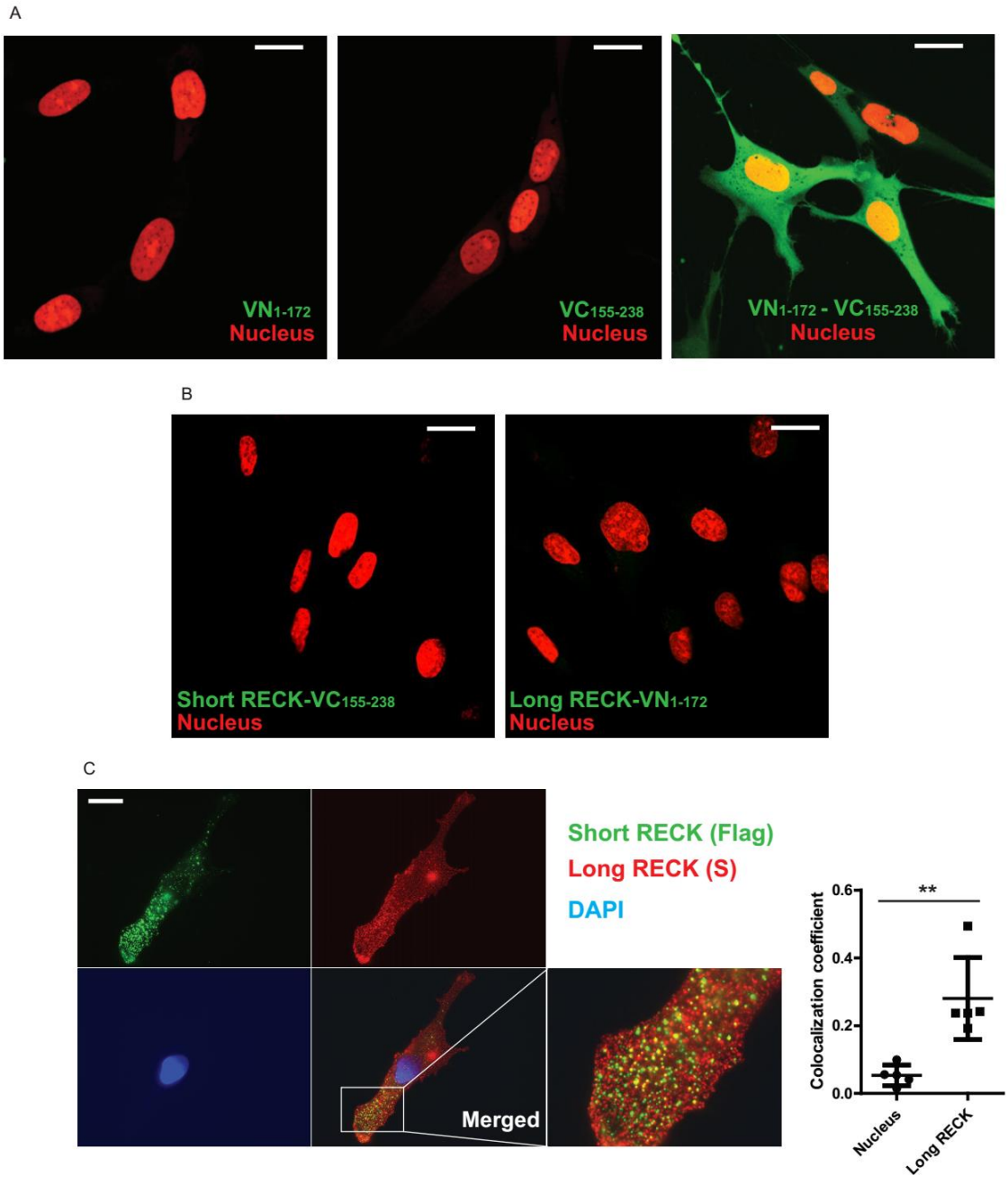
Supplemental Figure S4



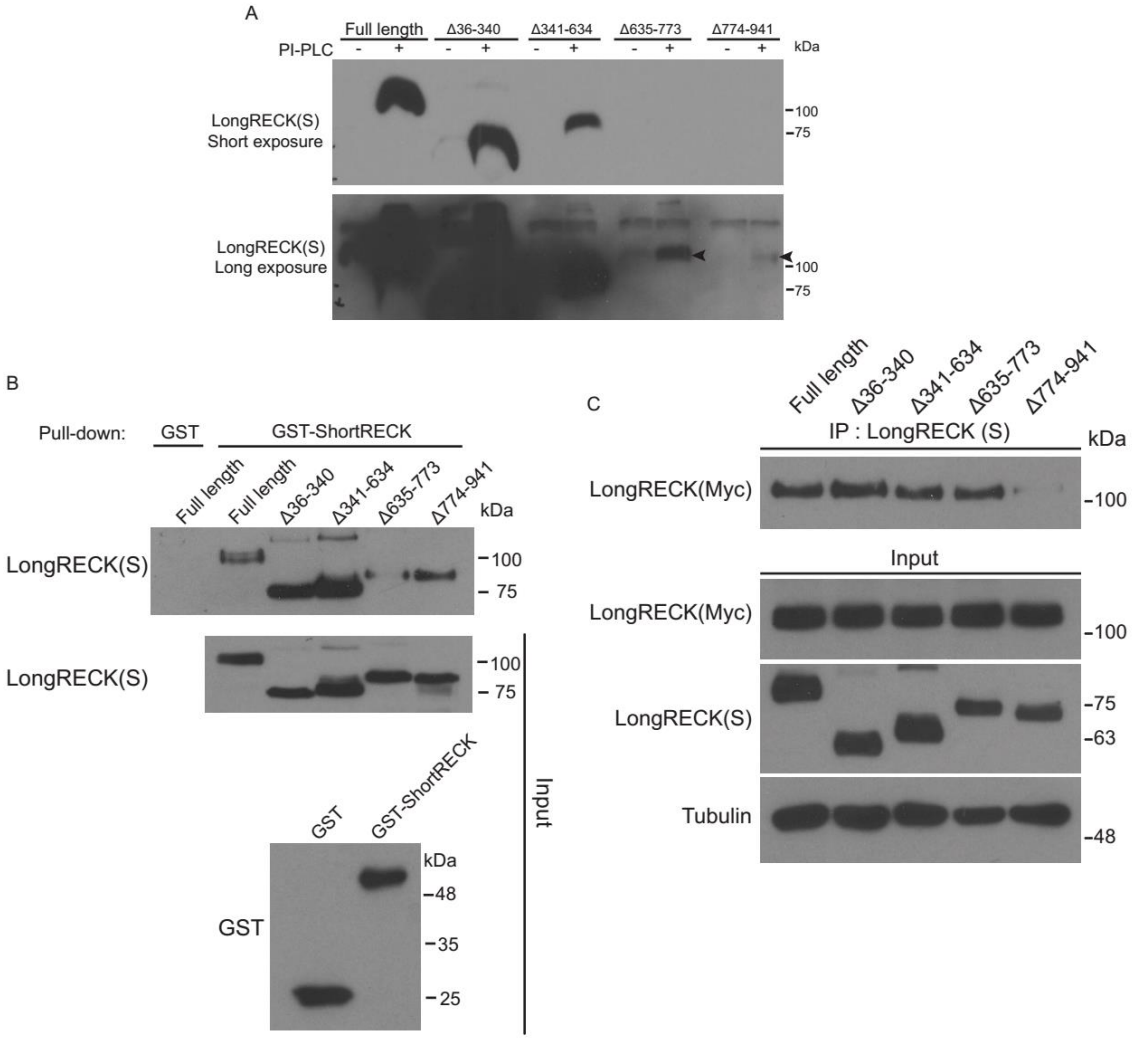
Supplemental Figure S5



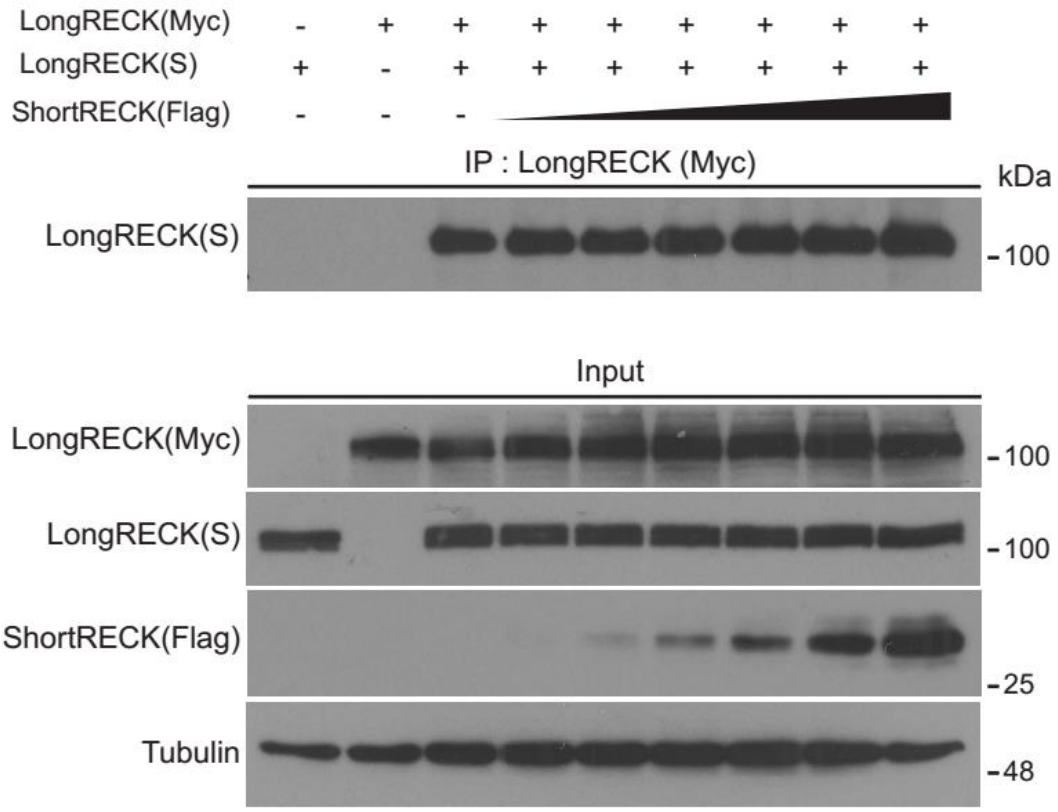
Supplemental Figure S6



Supplemental Figure S7



Supplemental Figure S8



CHAPTER 3:

RECK isoforms differentially regulate fibroblast migration by modulating tubulin post-translational modifications

Biochemical and Biophysical Research Communications xxx (xxxx) xxx

Contents lists available at ScienceDirect

Biochemical and Biophysical Research Communications

journal homepage: www.elsevier.com/locate/ybbrc

RECK isoforms differentially regulate fibroblast migration by modulating tubulin post-translational modifications

Ha Neul Lee [a, 1], Oye A. Bosompra [b, 1], Hilary A. Coller [a, b, c, *]

[a] Molecular Biology Institute, University of California, Los Angeles, Los Angeles, CA, 90095, USA
[b] Department of Molecular, Cell and Developmental Biology, University of California, Los Angeles, Los Angeles, CA, 90095, USA
[c] Department of Biological Chemistry, David Geffen School of Medicine, Los Angeles, Los Angeles, CA, 90095, USA

ARTICLE INFO

Article history:
Received 4 January 2019
Accepted 12 January 2019
Available online xxx

Keywords:
RECK isoforms
Fibroblast migration
Tubulin PTM
MMP9
Integrin

ABSTRACT

Cell migration is essential for proper development and the defense against pathogens. Our previous work detailed a pathway of REversion-inducing-Cysteine-rich protein with Kazal motifs (RECK) isoform-mediated invasion in which a shorter RECK protein competes with MMP9 for interaction with the canonical RECK protein on the cell surface. Here we demonstrate that the mechanism through which RECK isoforms affect cell migration is mediated through changes in the levels of post-translational modifications (PTM) of α-tubulin. We show that both the canonical and short RECK isoforms modulate levels of tubulin acetylation and detyrosination. We demonstrate that these changes are sufficient to modulate the rate of fibroblast migration. If these tubulin PTMs are not altered, the effects of the canonical RECK isoform on cell migration are reversed. In defining the molecular pathway linking RECK and tubulin PTMs, we found that MMP9 and integrin activity both act as upstream regulators of tubulin acetylation and detyrosination. Overall, we propose a mechanism in which RECK isoforms on the cell surface have opposing effects on cell migration through MMP9-modulated changes to integrin-extracellular matrix (ECM) interactions that, in turn, affect microtubule PTMs.

© 2019 Elsevier Inc. All rights reserved.

1. Introduction

The process of cell migration is multifaceted and driven through an array of both intracellular and extracellular rearrangements. Cytoskeletal components are important for the formation of protrusions emanating from the leading edges of migrating cells [1]. In addition to microfilaments, microtubules also affect cell migration. Stabilization of microtubule plus ends is essential for proper fibroblast migration [2]. In response to the generation of a wound in monolayer cultures of fibroblasts or treatment with lysophosphatidic acid (LPA), cells generate an asymmetric microtubule array with stable microtubules mostly oriented toward the wound or LPA treatment [3–6]. Stable microtubules can accumulate PTMs of α-tubulin including detyrosination (removal of the C-terminal tyrosine to reveal a glutamine) or acetylation on lysine 40, which faces the lumen [7]. Tyrosination is catalyzed by tubulin-tyrosine ligase (TTL), while detyrosination [8] was recently discovered to be performed by vasohibins [9]. Acetylation is performed by αTAT1 [10] and is removed by histone deacetylase 6 (HDAC6) [11] or sirtuin 2 [12].

RECK is a membrane-bound, GPI-anchored glycoprotein that has been extensively studied as a direct regulator of matrix metalloproteinases (MMPs) that control cell migration [13]. RECK can directly bind MMPs to reduce MMP activity, change levels of ECM proteins, and alter cell motility. Morioka and colleagues found that RECK-null mouse embryonic fibroblasts (MEFs) have lower levels of detyrosinated tubulin [14]; however, this finding has not been pursued further.

In our previous study, we showed that RECK isoforms can have opposing roles in fibroblast invasion, with the longer RECK isoform (long RECK) inhibiting cell invasion and the shorter RECK isoform (short RECK) enhancing cell invasion [15]. We discovered that short RECK interacts with long RECK on the cell surface and interferes with MMP9–long RECK interaction, thus liberating MMP9. In our previous study, invasion was modeled by coating cells with Matrigel to simulate the complex ECM found *in vivo*. Here we address how RECK isoforms modulate cell migration and report our

* Corresponding author. Terasaki Life Science Building 5145, 610 Charles E. Young Drive E., Los Angeles, CA, 90095, USA.
E-mail address: hcoller@ucla.edu (H.A. Coller).
[1] These authors contributed equally to this work.

https://doi.org/10.1016/j.bbrc.2019.01.063
0006-291X/© 2019 Elsevier Inc. All rights reserved.

findings that RECK mediates these effects through tubulin PTMs.

2. Materials and methods

2.1. Cell culture

Primary human fibroblast cell lines were established using samples of human foreskin from the National Disease Research Interchange as previously described [16]. BJ5ta (immortalized fibroblasts) and 293T cells were purchased from America Type Culture Collection (ATCC). All cell lines were stored in a 5% CO_2-controlled humid incubator at 37 °C and were cultured on tissue culture plates in 10% FBS in DMEM. The above protocols were subject to approval by the University of California, Los Angeles IRB (protocol number 14-000145).

2.2. Migration assay

Eighteen hours prior to experimentation, cells were seeded into individual wells of an IncuCyte® ImageLock 96-well microplate (Essen Bioscience) at a concentration of 25,000 cells/well and were stored in a 37 °C incubator. The following day, the IncuCyte® WoundMaker™ (Essen Bioscience) was used to generate a 700−800 μm scratch in the center of each well. The wells were then filled with 100 μL of complete medium. Repopulation of the denuded area was tracked in 2 h intervals for up to 96 h using the IncuCyte ZOOM® live imaging software. Relative wound density was calculated as cell density in the wound area relative to cell density outside of the wound area over time. More details can be found on the manufacturer's website (https://www.essenbioscience.com/en/applications/live-cell-assays/scratch-wound-cell-migration-invasion/).

2.3. Real-time RT-PCR

Fifty nanograms of RNA were reverse transcribed and amplified in a total volume of 25 μl per reaction using SuperScript® III Platinum® SYBR® Green One-Step qRT-PCR Kit (Invitrogen). The CFX96 Real-time system (Bio-Rad) was used for real-time RT PCR, and ubiquitin-C (UBC) levels were referenced for normalization of gene expression. We calculated gene expression using the $2^{-\Delta\Delta Ct}$ method. Primer sequences are as follows: αTAT1, 5′-AACTCGACACTCTCGTGCTG-3′ and 5′-CTGTTTAGGGGCCAAGGAGG-3'; TTL 5′-GGAGAGGGCAACGTTTGGAT-3′ and 5′-CAAGACCCAGCTTCGGATGT-3'.

2.4. Western blot

Prior to the western blot, proteins were extracted from harvested fibroblasts using radioimmunoprecipitation assay (RIPA) lysis buffer (10 mM Tris-Cl pH8.0, 0.1% sodium deoxycholate, 0.5 mM EGTA, 1 mM EDTA, 0.1% SDS, 1% Triton X-100, 140 mM NaCl) that also contained a single tablet of protease inhibitor (Roche Applied Science). Cell lysates containing all proteins were analyzed using Thermo Scientific™ Pierce™ BCA™ Protein Assay kit (ThermoFischer). Twenty μgs of protein was loaded per lane for western blots. Each western blot was repeated two or three times.

2.5. Antibodies

To detect alpha-tubulin and Flag, antibodies were purchased from Sigma-Aldrich. For detection of MMP9 and long RECK, antibodies were obtained from Thermo Fisher Scientific. Antibodies against acetyl-tubulin and Glu-tubulin were purchased from Cell Signaling Technology and Millipore, respectively. All primary antibodies were diluted in 5% skim milk in 0.1% Tween-TBS and the dilution rates were as follows. Alpha-tubulin: 1:5000; Flag: 1:2500; MMP9: 1:1000; long RECK: 1:1000; acetyl-tubulin: 1:1000; Glu-tubulin: 1:1000.

2.6. shRNA cell line engineering

shRNAs were designed through https://rnaidesigner.thermofisher.com/rnaiexpress. Knockdown shRNAs were cloned into the lentiviral plasmid pGreenPuro (Systems Biosciences) at BamHI and EcoRI sites, and the following sequences were expressed under the control of the H1 promoter. Sequences are provided as below:

shControl.1: 5'-GATCCCCTAAGGTTAAGTCGCCCTCGTTCAAGAGACGAGGGCGACTTAACCTTAGGTTTTTG-3′ and 5′-AATTCAAAAACCTAAGGTTAAGTCGCCCTCGTCTCTTGAACGAGGGCGACTTAACCTTAGGG-3';

shControl.2: 5'-GATCCCAACAAGATGAAGAGCACCAACTTCCTGTCAGATTGGTGCTCTTCATCTTGTTGTTTTTG-3′ and 5′-AATTCAAAAACAACAAGATGAAGAGCACCAATCTGACAGGAAGTTGGTGCTCTTCATCTTGTTGG-3';

shShortRECK.1: 5'-GATCCGCTTTGTACATCCTGGAATCCCTTCCTGTCAGAGGATTCCAGGATGTACAAAGCTTTTTG-3′ and 5′-AATTCAAAAAGCTTTGTACATCCTGGAATCCTCTGACAGGAAGGGATTCCAGGATGTACAAAGCG-3';

shShortRECK.2: 5'-GATCCGATCTGTGCTCTCTGACATTTCTTCCTGTCAGAAAATGTCAGAGAGCACAGATCTTTTTG-3′ and 5′-AATTCAAAAAGATCTGTGCTCTCTGACATTTTCTGACAGGAAGAAATGTCAGAGAGCACAGATCG-3';

shLongRECK.1: 5′-GATCCGCGTGGCAGTCGATTACTATGTTCAAGAGACATAGTAATCGACTGCCACGCTTTTTG - 3′ and 5′-AATTCAAAAAGCGTGGCAGTCGATTACTATGTCTCTTGAACATAGTAATCGACTGCCACGCG-3'; shLongRECK.2: 5′- GATCCGCATCAAAGCATCTTGCATTACTTCCTGTCAGATAATGCAAGATGCTTTGATGCTTTTTG- 3′ and 5′-AATTCAAAAAGCATCAAAGCATCTTGCATTATCTGACAGGAAGTAATGCAAGATGCTTTGATGCG-3';

shαTAT1.1: 5'-GATCCGGATGATCGTGAGGCTCATAACTTCCTGTCAGATTATGAGCCTCACGATCATCCTTTTTG-3′ and 5′-AATTCAAAAAGGATGATCGTGAGGCTCATAATCTGACAGGAAGTTATGAGCCTCACGATCATCCG-3';

shαTAT1.2: 5'-GATCCGCGAGAACTCTTCCAGTATATCTTCCTGTCAGAATATACTGGAAGAGTTCTCGCTTTTTG −3′ and 5′-AATTCAAAAAGCGAGAACTCTTCCAGTATATTCTGACAGGAAGATATACTGGAAGAGTTCTCGCG-3'; shTTL: 5′- GATCCGCTTCAGAGCTTCTCGATTTCCTTCCTGTCAGAGAAATCGAGAAGCTCTGAAGCTTTTTG-3′ and 5′-AATTCAAAAAGCTTCAGAGCTTCTCGATTTCTCTGACAGGAAGGAAATCGAGAAGCTCTGAAGCG-3'. Lentivirus concentrations were tested by flow cytometry analysis using 293T cells. Virus titrated to a multiplicity of infection (M.O.I.) of 1 was used to treat fibroblasts with polybrene (final concentration: 10 μg/ml) and infected cells were selected using 2 μg/ml puromycin (Invivogen) in 10% FBS DMEM for 3 days.

2.7. Inhibitor treatment

All inhibitors were incubated with cultured cells at 37 °C for 24 h. The manufacturers and final concentrations are as follows: SB-3CT (iMMP2/iMMP9) (Santa Cruz Biotechnology) 13.9 nM; MMP-9 Inhibitor I (iMMP9) (Santa Cruz Biotechnology) 5 nM; Cilengitide (ApexBio) 37 nM; RGD (Arg-Gly-Asp) peptides (ApexBio) 30 μM; Cyclo(-RGDfK) (ApexBio) 50 μM; Firategrast (ApexBio) 50 μl.

2.8. Statistical and image analysis

Excel 2013 and GraphPad Prism 5 were used to analyze all

results. Data are shown as mean ± S.D. or S.E.

Significance was determined by repeated measures two-way ANOVA with Dunnett's multiple comparison test or unpaired two-sided *t*-test. $P < 0.05$ was considered significant. Image J was used to quantify western blots.

3. Results & discussion

3.1. Long RECK & short RECK isoforms modulate fibroblast migration

We wondered whether short RECK could regulate cell migration beyond ECM digestion. To test this idea, we monitored the dynamics of fibroblast migration using the IncuCyte® WoundMaker™ in the absence of Matrigel (Fig. 1A). We investigated fibroblasts stably expressing shRNAs that target either long RECK or short RECK. Isoform-specific knockdown of either short or long RECK in these fibroblasts was demonstrated in our previous report [15]. Long RECK knockdown increased cell migration, while short RECK knockdown decreased cell migration (Fig. 1B and C). These results were similar to those observed with the invasion assay [15]. Taken together, we have found that long RECK promotes both fibroblast invasion and migration, while short RECK inhibits both invasion and migration. Without Matrigel, the fibroblasts in all states migrated more quickly than when Matrigel was present (compare Fig. 1A and B with Lee et al., 2018, Fig. 2C and D), consistent with reduced ECM without Matrigel treatment. Because we found that RECK can affect cell migration even without Matrigel present, the results suggested to us that RECK may have additional effects on cell migration besides ECM degradation.

3.2. RECK isoforms influence levels of tubulin PTMs

We sought to determine whether RECK affects intracellular factors that mediate cell migration. Previous studies showed that RECK knockout cell lines have lower levels of detyrosinated (Glu) tubulin [14]. In addition, metastatic and aggressive breast cancers contain high levels of acetylated α-tubulin [17]. We thus sought to

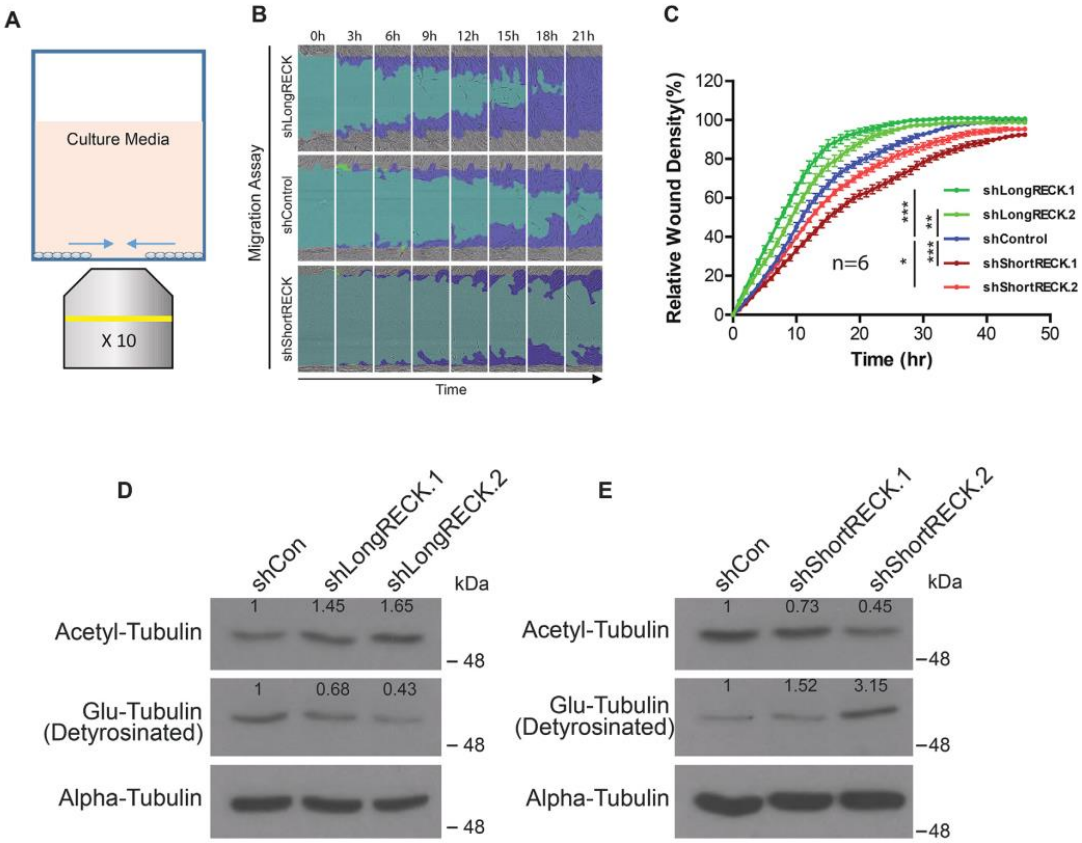


Fig. 1. RECK isoforms differentially regulate cell migration and tubulin PTM levels. (A) Schematic representing *in vitro* cell migration assay. (B) Representative time-lapse images of fibroblast migration as a result of RECK isoform-specific shRNA knockdown. The light blue region depicts the initial wound created by IncuCyte WoundMaker, while the dark blue region depicts cell movement over a span of 24 h. shLongRECK-expressing cells migrated more rapidly, while fibroblasts expressing shShortRECK migrated more slowly. (C) Quantification of the migration assay as relative wound density (100 * density in wound/density outside wound) over time. Data is shown as mean ± S.E. with 6 replicates. Significance was calculated using a repeated measures two-way ANOVA with Dunnett's multiple comparison test (simplified as ANOVA). One asterisk indicates $p < 0.05$, two asterisks indicate $p < 0.01$, three asterisks indicates $p < 0.001$. Three independent experiments were performed with similar results, and data from one experiment is presented. (D and E) RECK isoforms can modulate levels of tubulin PTMs. Western blotting reveals long RECK knockdown increases acetyl-tubulin levels and decreases Glu-tubulin levels; conversely, short RECK knockdown decreases levels of acetylated tubulin and increases tubulin detyrosination. Two independent experiments showed similar results, and data from one experiment is shown. Two types of shRNAs that target different regions of the same RECK isoform showed similar trends. The stable fibroblast cell lines with RECK isoform knockdown used here are the same as those that we characterized in our previous report [15]. Numbers on the western blots indicate relative protein expression level compared to control. (For interpretation of the references to colour in this figure legend, the reader is referred to the Web version of this article.)

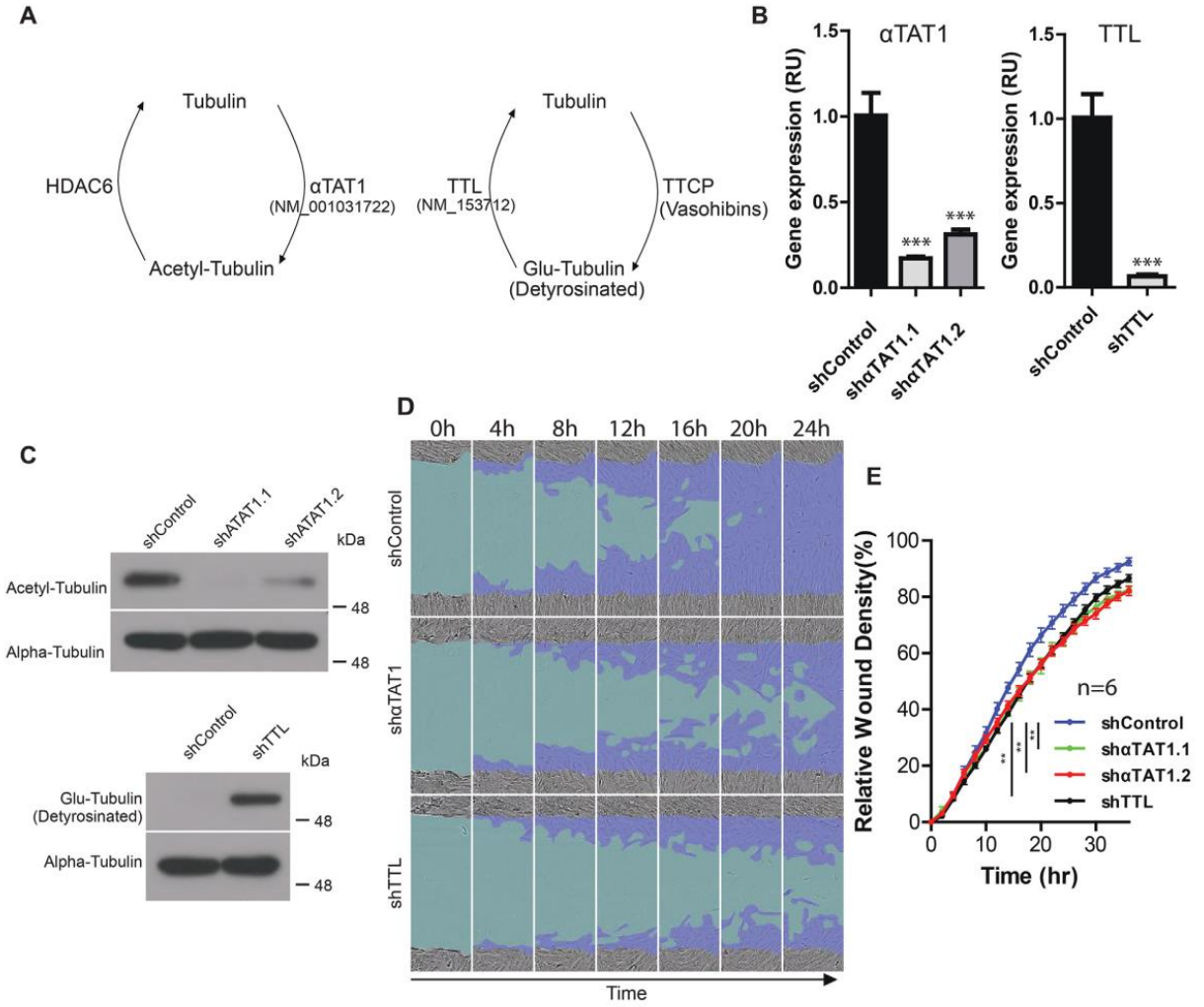


Fig. 2. Tubulin PTMs can regulate cell migration. (A) Diagram depicting cycles of tubulin PTMs. (B) Gene expression following αTAT1 and TTL shRNA knockdown in immortalized fibroblasts measured with real-time RT-PCR. Gene expression was normalized to UBC and then the relative fold change compared to the control shRNA was calculated. Data shown as mean ± S.D. Three asterisks indicates $p < 0.001$ (unpaired two-sided *t*-test). (C) Levels of acetylated tubulin and Glu-tubulin as a result of αTAT1 and TTL knockdown, respectively. (D) Representative images of decreased fibroblast migration over a timespan of 24 h as a result of reduction in tubulin acetylation and increased Glu-tubulin. Light blue region depicts the initial wound created by IncuCyte WoundMaker, while dark blue region depicts cell movement over a span of 24 h. (E) Quantification of migration assay. Data are shown as mean ± S.E. with 6 replicates. Two asterisks indicate $p < 0.01$ based on ANOVA analysis. Three independent experiments showed similar results. Data from one experiment is shown. (For interpretation of the references to colour in this figure legend, the reader is referred to the Web version of this article.)

elucidate the role of RECK isoforms in regulating tubulin PTMs as a possible mechanism for RECK's effects on cell migration. To begin our analysis, we knocked down either long RECK or short RECK with shRNAs and monitored the levels of acetylated tubulin or Glu-tubulin. Knockdown of long RECK resulted in increased levels of acetyl-tubulin and decreased levels of Glu-tubulin, while knocking down short RECK resulted in decreased levels of acetyl-tubulin and increased levels of Glu-tubulin (Fig. 1D and E). These results show that short and long RECK isoforms have opposing effects on tubulin PTMs that could potentially contribute to cytoskeletal organization through tubulin flexibility and stability. The findings are also somewhat surprising because in previous studies, both acetylated tubulin and Glu-tubulin were associated with stable microtubules [9,18], while in our experiments, the acetylated tubulin and Glu-tubulin levels moved in opposite directions with either short or long RECK knockdown.

3.3. Tubulin acetylation and detyrosination decrease fibroblast migration

Having demonstrated that both short and long RECK affect the levels of the acetylated and Glu-forms of tubulin, we next investigated the effect of these tubulin modifications on fibroblast motility. We modulated the levels of acetylated or Glu-tubulin forms by designing shRNAs against αTAT1 or TTL to decrease levels of acetylation and increase levels of Glu-tubulin, respectively (Fig. 2A). Knockdown of αTAT1 and TTL enzymes was confirmed through real-time RT-PCR (Fig. 2B). As expected, αTAT1 knockdown decreased levels of acetyl-tubulin, while TTL knockdown increased levels of Glu-tubulin (Fig. 2C). Neither αTAT1 nor TTL knockdown

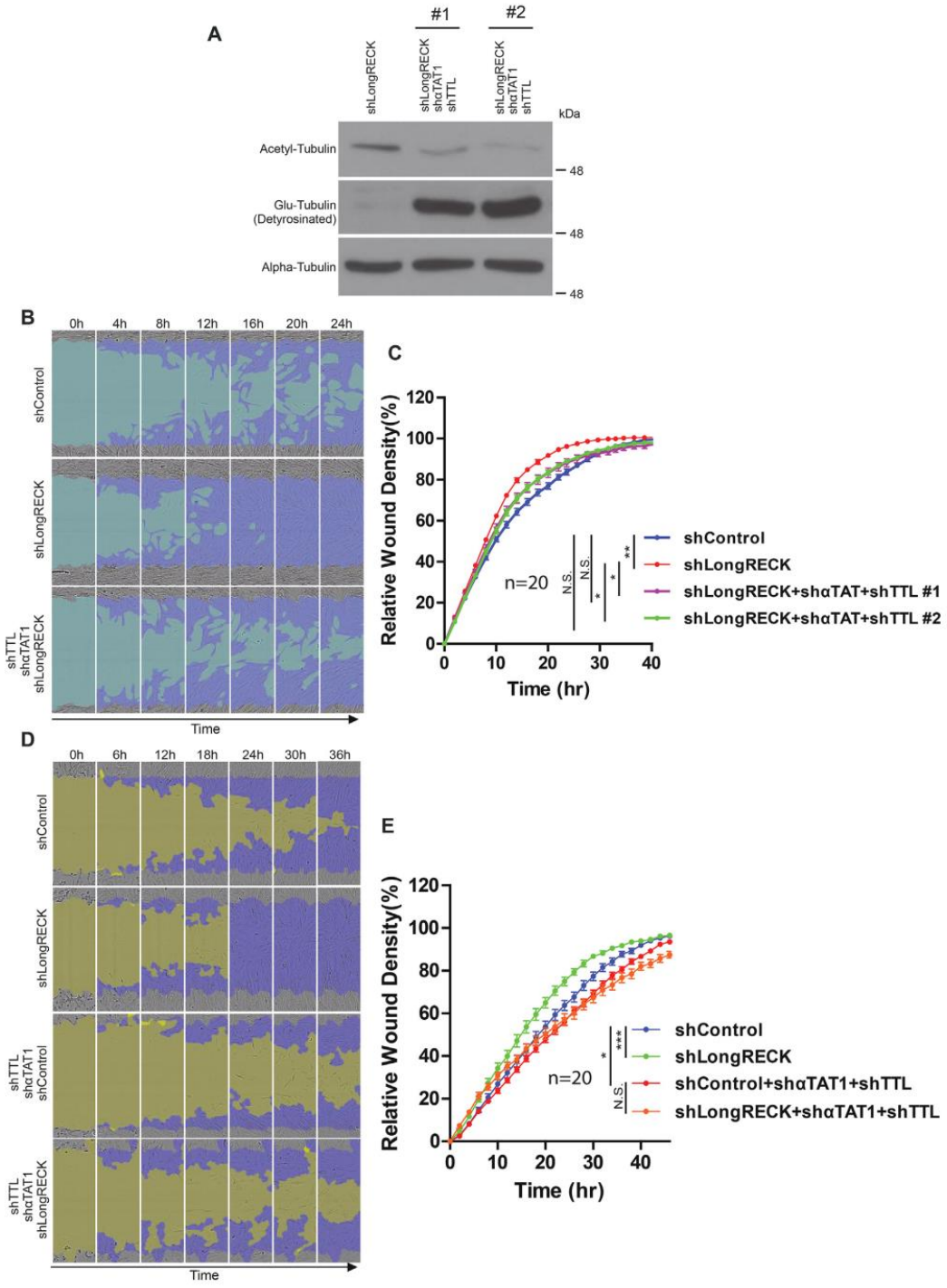


Fig. 3. Knockdown of αTAT1 and TTL reverts faster migration with long RECK knockdown. (A) Western blot of acetyl-tubulin and Glu-tubulin levels following shRNA knockdown of either the long RECK isoform alone or both long RECK and tubulin-modifying enzymes in immortalized fibroblasts. (B) Representative images of fibroblast migration after transfection with shRNAs targeting either long RECK or long RECK, αTAT1, and TTL. The light blue region depicts the initial wound created by IncuCyte WoundMaker, while the dark blue region depicts cell movement over a span of 24 h. (C) Quantification of migration assay. Data are shown as mean ± S.E. with 20 replicates. Cells only targeted for long RECK knockdown migrate further than control cells, as expected; however, knockdown of tubulin-modifying enzymes reverts this phenotype. Two independent experiments showed similar results. Data from one experiment is shown. (D) Representative images of fibroblast migration. Cells expressing the indicated combinations of shRNAs were monitored for migration rate. The dark yellow region depicts the initial wound created by IncuCyte WoundMaker, while the dark blue region resembles cell movement over a span of 36 h. (E) Quantification of migration assay. Data are shown as mean ± S.E. with 20 replicates. Two independent experiments were performed with similar results. Data from one experiment is presented. One asterisk indicates $p < 0.05$, two asterisks indicate $p < 0.01$, three asterisks indicates $p < 0.001$ based on ANOVA analysis. (For interpretation of the references to colour in this figure legend, the reader is referred to the Web version of this article.)

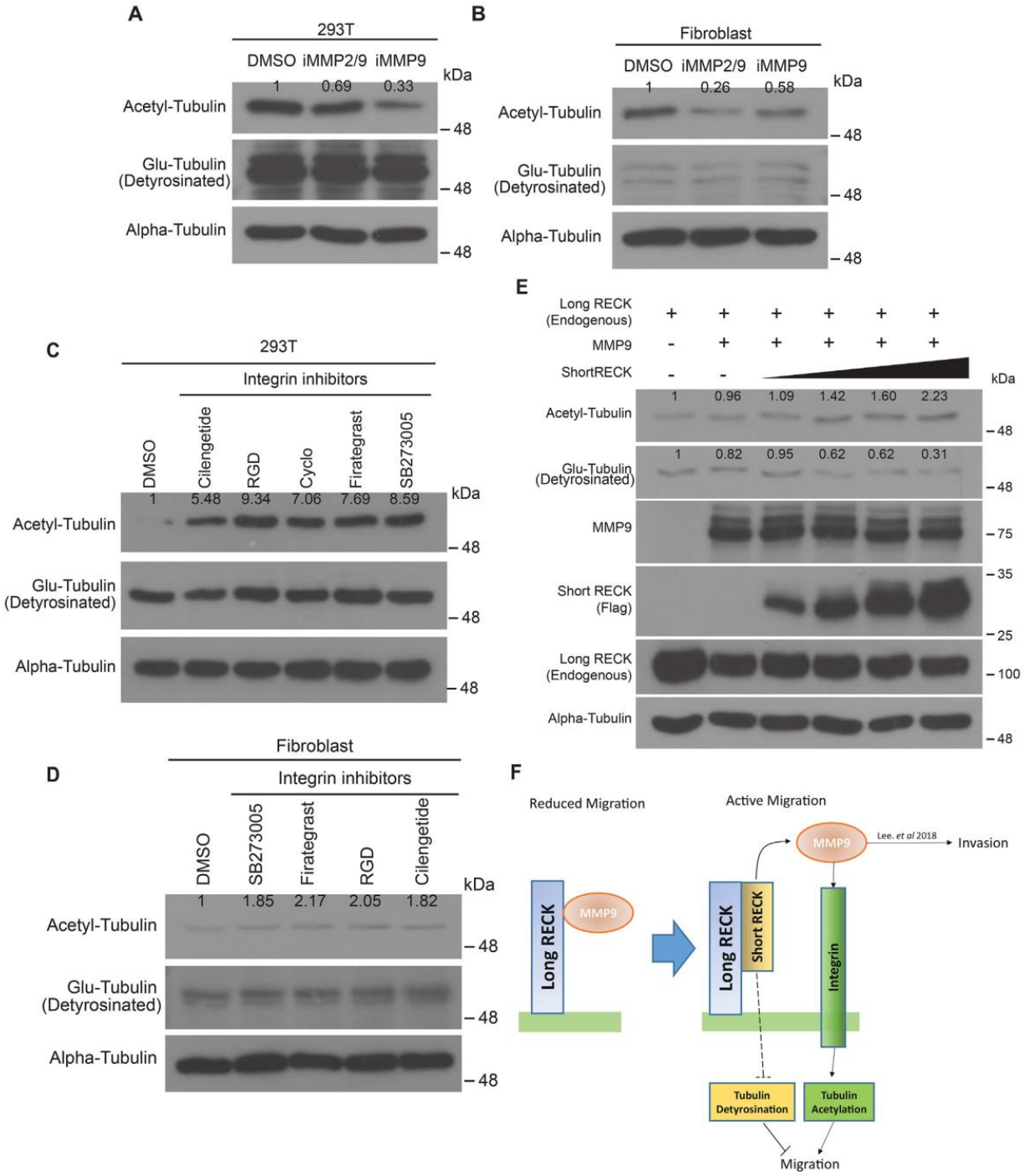


Fig. 4. MMP9 and the integrin signaling pathway regulate levels of acetyl-tubulin. (A and B) Western blots demonstrating acetylated tubulin levels, but not Glu-tubulin levels, are regulated by treating fibroblasts with the indicated MMP inhibitors. Two different cell lines show similar results. (C and D) Levels of acetyl-tubulin increase after treatment with integrin inhibitors. Acetyl-tubulin levels increase in the presence of integrin inhibitors in both 293T and fibroblasts. Glu-tubulin levels are constant and are not affected by treatment with any of these integrin inhibitors. (E) 293T cells overexpressing MMP9 were transfected with increasing levels of short RECK to release MMP9. Effects on tubulin acetylation and detyrosination were monitored with immunoblotting. As short RECK levels increased, acetyl-tubulin levels increased and Glu-tubulin levels decreased. Two independent experiments showed similar results. (F) Working model. In reduced cell migration conditions, the long RECK isoform interacts with MMP9 and suppresses MMP9 activity to inhibit cell migration. In contrast, when short RECK is generated under conditions of active cell migration, MMP9 liberated from long RECK by short RECK can affect tubulin acetylation levels, possibly through modulation of integrin activity. In addition, short RECK expression can also reduce tubulin detyrosination. Fibroblast migration is enhanced by tubulin PTMs modified by short RECK. Dashed lines show a pathway yet to be elucidated. Numbers on the western blots indicate relative protein expression level compared to control.

affected total tubulin levels (Fig. 2C). Fibroblasts transduced with either αTAT1-targeted or TTL-targeted shRNAs exhibited decreased cell migration (Fig. 2D and E). The findings show that altering tubulin PTMs can affect fibroblast cell migration. Furthermore, the directionality of the effects of these tubulin PTMs is consistent with tubulin PTMs mediating the effects of RECK isoforms on cell migration. Because long RECK knockdown results in faster migration, increased acetyl-tubulin and decreased Glu-tubulin due to long RECK knockdown would also be predicted to increase migration. Likewise, because short RECK knockdown resulted in slower migration, the decreased acetyl-tubulin and increased Glu-tubulin that follow short RECK knockdown would be predicted to decrease fibroblasts migration.

3.4. Knockdown of tubulin-modifying enzymes prevents increased fibroblast migration following long RECK knockdown

We monitored the effect of shRNA-mediated knockdown of long RECK and tubulin-modifying enzymes on fibroblast migration. We characterized levels of acetyl-tubulin and Glu-tubulin after shRNA-mediated knockdown of long RECK, αTAT1, and TTL. When compared to fibroblasts only expressing an shRNA against long RECK, fibroblasts expressing shRNAs to long RECK, αTAT1, and TTL saw a reversal in tubulin acetylation and detyrosination levels (Fig. 3A). We then tested whether reversing tubulin PTMs while knocking down long RECK would revert the migration-promoting effects of long RECK knockdown. Indeed, when long RECK was knocked down along with αTAT1 and TTL, the cells migrated similarly to the rate in cells without RECK knockdown (Fig. 3B and C). These results are consistent with tubulin PTMs playing a role in the change in migration rate mediated by RECK. To further explore this possibility, we monitored the migration of fibroblasts with knockdown of RECK or a control shRNA and knockdown of αTAT1 and TTL or control shRNAs. While fibroblasts without manipulation of tubulin PTMs migrated more rapidly when long RECK was knocked down, fibroblasts with a reversal of tubulin PTMs did not migrate more rapidly when long RECK was knocked down (Fig. 3D and E). We concluded that modulation of tubulin PTMs is important for the effects of long RECK on fibroblast migration.

3.5. MMP9 and integrin activation affect acetyl-tubulin but not Glu-tubulin levels

Knockdown of long RECK promotes ECM degradation by MMP9, which would be expected to clear a path for cells to move [15,19]. We hypothesized that RECK's effects on MMP9 might also contribute to changes in migration through tubulin PTMs. To test this hypothesis, we asked whether MMP9 activity can affect tubulin acetylation or detyrosination. 293T cells or fibroblasts were treated with either an MMP9 inhibitor or an inhibitor of MMP2/9, and the levels of tubulin PTMs were monitored. Treatment with any of the inhibitors resulted in decreased levels of acetyl-tubulin, with no effect on the levels of Glu-tubulin (Fig. 4A and B). The results show that MMP2/9 activity can affect tubulin acetylation but not detyrosination.

To further understand how MMP9 inhibition might affect tubulin PTMs, we considered integrin signaling. MMPs are expected to affect the amount and quality of ECM proteins, and these proteins signal through integrins [20]. We treated 293T cells or fibroblasts with integrin-specific inhibitors and monitored the levels of acetyl-tubulin and Glu-tubulin. Each of the different integrin inhibitors individually increased levels of acetylated tubulin but did not change levels of Glu-tubulin (Fig. 4C and D). These results are consistent with a model in which inhibiting MMP9 results in higher levels of ECM proteins, more integrin signaling, and reduced acetylated tubulin. In Fig. 1, we observed that RECK isoforms can regulate both acetylated tubulin and Glu-tubulin levels, but neither MMP9 nor integrin inhibitors affect Glu-tubulin levels. Thus, we hypothesize that in addition to MMP9 and integrins, there are also other pathways through which RECK isoforms regulate Glu-tubulin independent of MMP9-integrin pathways.

3.6. Short and long RECK have opposing effects on tubulin PTMs

In our previous study, we observed that increased expression levels of short RECK disrupted MMP9 binding to long RECK on the cell surface as a result of short RECK binding to long RECK and releasing MMP9 from long RECK [15]. To further understand the effects of short RECK on tubulin PTMs, we tested for changes in tubulin acetylation and Glu-tubulin levels when short RECK protein is induced. We transfected 293T cells with increasing concentrations of short RECK while also overexpressing MMP9 to induce MMP9 liberation from long RECK by short RECK. Increased short RECK resulted in an increase in tubulin acetylation and a decrease in tubulin detyrosination (Fig. 4E). While the changes in tubulin acetylation could result from its effects on MMP9, the changes in Glu-tubulin are expected to reflect additional roles of the short RECK. Further studies will be needed to clarify the pathway that results in changes in Glu-tubulin levels in response to RECK isoforms and the connection between integrins and tubulin acetylation state. Taken together, we propose a novel model of isoform-specific RECK-mediated migration through tubulin PTM modulation. We hypothesize that MMP9 released from long RECK by competition with short RECK digests ECM proteins and reduces integrin-ECM interaction. Changes in integrin signaling and other pathways can then modulate tubulin PTMs, which will, in turn, affect fibroblast migration rates (Fig. 4F).

Conflicts of interest

The authors declare no competing or financial interests.

Author contributions

Conceptualization: H.N.L., H.A.C.; Methodology: H.N.L., O.B.; Formal analysis: H.N.L., O.B., H.A.C.; Investigation: H.N.L., O.B.; Supervision: H.N.L., O.B., H.A.C.; Writing −original draft: H.N.L., O.B.; Writing-review & editing: H.L., O.B., H.A.C.; Project administration: H.N.L., O.B., H.A.C.; Funding acquisition: H.N.L., H.A.C.

Acknowledgments

We thank the Eli & Edythe Broad Center for Regenerative Medicine & Stem Cell Research for Core Facilities that house and Incucyte instrument. We acknowledge Jeff Long (UCLA) for sharing equipment for real-time RT-PCR. HAC was the Milton E. Cassel scholar of the Rita Allen Foundation (http://www.ritaallenfoundation.org). HNL acknowledges a Whitcome Fellowship from the UCLA Molecular Biology Institute and a dissertation year fellowship from the Graduate Program, UCLA. HAC acknowledges funding from the National Institute of General Medical Sciences R01 GM081686, National Institute of General Medical Sciences R01 GM0866465, the Eli & Edythe Broad Center for Regenerative Medicine & Stem Cell Research, the Iris Cantor Women's Health Center, the NIH/National Center for Advancing Translational Sciences UCLA Clinical and Translational Science Institute UL1TR000124 and the UCLA Life Science Innovation Fund. The authors thank Barry Coller, Luisa Iruela-Arispe, Tracy Johnson, William Lowry, Jorge Torres, and Jose Rodriguez for helpful input.

References

[1] D.D. Tang, B.D. Gerlach, The roles and regulation of the actin cytoskeleton, intermediate filaments and microtubules in smooth muscle cell migration, Respir. Res. 18 (2017) 54.

[2] Y. Wen, C.H. Eng, J. Schmoranzer, N. Cabrera-Poch, E.J. Morris, M. Chen, B.J. Wallar, A.S. Alberts, G.G. Gundersen, EB1 and APC bind to mDia to stabilize microtubules downstream of Rho and promote cell migration, Nat. Cell Biol. 6 (2004) 820–830.

[3] G.G. Gundersen, J.C. Bulinski, Selective stabilization of microtubules oriented toward the direction of cell migration, Proc. Natl. Acad. Sci. U. S. A. 85 (1988) 5946–5950.

[4] G.G. Gundersen, Y. Wen, C.H. Eng, J. Schmoranzer, N. Cabrera-Poch, E.J. Morris, M. Chen, E.R. Gomes, Regulation of microtubules by Rho GTPases in migrating cells, Novartis Found. Symp. 269 (2005) 106–116, discussion 116-126, 223-130.

[5] G.G. Gundersen, I. Kim, C.J. Chapin, Induction of stable microtubules in 3T3 fibroblasts by TGF-beta and serum, J. Cell Sci. 107 (Pt 3) (1994) 645–659.

[6] T.A. Cook, T. Nagasaki, G.G. Gundersen, Rho guanosine triphosphatase mediates the selective stabilization of microtubules induced by lysophosphatidic acid, J. Cell Biol. 141 (1998) 175–185.

[7] C. Janke, J.C. Bulinski, Post-translational regulation of the microtubule cytoskeleton: mechanisms and functions, Nat. Rev. Mol. Cell Biol. 12 (2011) 773–786.

[8] K. Ersfeld, J. Wehland, U. Plessmann, H. Dodemont, V. Gerke, K. Weber, Characterization of the tubulin-tyrosine ligase, J. Cell Biol. 120 (1993) 725–732.

[9] J. Nieuwenhuis, A. Adamopoulos, O.B. Bleijerveld, A. Mazouzi, E. Stickel, P. Celie, M. Altelaar, P. Knipscheer, A. Perrakis, V.A. Blomen, T.R. Brummelkamp, Vasohibins encode tubulin detyrosinating activity, Science 358 (2017) 1453–1456.

[10] J.S. Akella, D. Wloga, J. Kim, N.G. Starostina, S. Lyons-Abbott, N.S. Morrissette, S.T. Dougan, E.T. Kipreos, J. Gaertig, MEC-17 is an alpha-tubulin acetyltransferase, Nature 467 (2010) 218–222.

[11] C. Hubbert, A. Guardiola, R. Shao, Y. Kawaguchi, A. Ito, A. Nixon, M. Yoshida, X.F. Wang, T.P. Yao, HDAC6 is a microtubule-associated deacetylase, Nature 417 (2002) 455–458.

[12] B.J. North, B.L. Marshall, M.T. Borra, J.M. Denu, E. Verdin, The human Sir2 ortholog, SIRT2, is an NAD+-dependent tubulin deacetylase, Mol. Cell 11 (2003) 437–444.

[13] J. Oh, R. Takahashi, S. Kondo, A. Mizoguchi, E. Adachi, R.M. Sasahara, S. Nishimura, Y. Imamura, H. Kitayama, D.B. Alexander, C. Ide, T.P. Horan, T. Arakawa, H. Yoshida, S. Nishikawa, Y. Itoh, M. Seiki, S. Itohara, C. Takahashi, M. Noda, The membrane-anchored MMP inhibitor RECK is a key regulator of extracellular matrix integrity and angiogenesis, Cell 107 (2001) 789–800.

[14] Y. Morioka, J. Monypenny, T. Matsuzaki, S. Shi, D.B. Alexander, H. Kitayama, M. Noda, The membrane-anchored metalloproteinase regulator RECK stabilizes focal adhesions and anterior-posterior polarity in fibroblasts, Oncogene 28 (2009) 1454–1464.

[15] H.N. Lee, M. Mitra, O. Bosompra, D.C. Corney, E.L. Johnson, N. Rashed, L.D. Ho, H.A. Coller, RECK isoforms have opposing effects on cell migration, Mol. Biol. Cell 29 (2018) 1825–1838.

[16] A. Legesse-Miller, O. Elemento, S.J. Pfau, J.J. Forman, S. Tavazoie, H.A. Coller, let-7 Overexpression leads to an increased fraction of cells in G2/M, direct down-regulation of Cdc34, and stabilization of Wee1 kinase in primary fibroblasts, J. Biol. Chem. 284 (2009) 6605–6609.

[17] A.E. Boggs, M.I. Vitolo, R.A. Whipple, M.S. Charpentier, O.G. Goloubeva, O.B. Ioffe, K.C. Tuttle, J. Slovic, Y. Lu, G.B. Mills, S.S. Martin, alpha-Tubulin acetylation elevated in metastatic and basal-like breast cancer cells promotes microtentacle formation, adhesion, and invasive migration, Cancer Res. 75 (2015) 203–215.

[18] C. Janke, G. Montagnac, Causes and consequences of microtubule acetylation, Curr. Biol. : CB 27 (2017) R1287–R1292.

[19] C. Takahashi, Z.Q. Sheng, T.P. Horan, H. Kitayama, M. Maki, K. Hitomi, Y. Kitaura, S. Takai, R.M. Sasahara, A. Horimoto, Y. Ikawa, B.J. Ratzkin, T. Arakawa, M. Noda, Regulation of matrix metalloproteinase-9 and inhibition of tumor invasion by the membrane-anchored glycoprotein RECK, Proc. Natl. Acad. Sci. U. S. A. 95 (1998) 13221–13226.

[20] M. Stefanidakis, E. Koivunen, Cell-surface association between matrix metalloproteinases and integrins: role of the complexes in leukocyte migration and cancer progression, Blood 108 (2006) 1441–1450.

CHAPTER 4:

Conclusions and Future Studies

Cell migration is controlled in a variety of ways (Devreotes and Horwitz, 2015; Etienne-Manneville, 2013; Kaverina and Straube, 2011; Nabeshima et al., 2002; Yamaguchi and Condeelis, 2007). Cell migration-related gene expression can be controlled by the activity of signaling pathways associated with cell migration such as ERK, AKT, and JNK (Huang et al., 2004). On the cell surface, invasion can be regulated by controlling the activity of matrix metalloproteinases (Kessenbrock et al., 2010). In addition, cytoskeleton dynamics can regulate cell migration by controlling the formation of filopodia and lamellipodia (Arjonen et al., 2011). Recently, it has been reported that cell migration can be controlled by alternative polyadenlyation (Mitra et al., 2018) Therefore, understanding the different molecular mechanisms that control cell migration is crucial in the study of developmental biology and cell migration-related disease therapies. The data shown in this thesis represents my efforts to understand how a change in the expression of alternative isoforms in response to changes in a cell's environment can control cell migration by focusing on the RECK protein.

Studies describing changes in protein function by altering protein sequence through alternative polyadenylation have been reported previously (Vorlova et al., 2011), but studies to relate alternative polyadenylation to migration have been mostly unexplored. Our lab discovered that migration of quiescent fibroblasts is slower than proliferating cells. We observed that for some genes, alternative polyadenylation becomes more frequent at distal polyadenylation sites when cells become quiescent (Mitra et al., 2018). These observations from our study led to the hypothesis that cell migration can also be controlled through alternative polyadenylation. We were able to test this hypothesis by silencing polyadenylation factors, such as CstF64, and confirmed that cell migration was reduced when CstF64 levels were reduced. However, we were

not able to explain the specific molecular mechanism by which alternative polyadenylation regulates cell migration in our previous study.

In Chapter 2, I showed that a short form of RECK produced by APA in cell migratory conditions supports cell migration unlike canonical RECK. Based on RNA-Seq and polyA-Seq data, we observed that RECK undergoes APA and generates a short form of RECK that is more prevalent when the fibroblasts are proliferating. However, we have not yet understood the molecular mechanism of how short RECK is generated. We will continue to investigate which polyadenylation factors and splicing factors are involved in generating the short isoform of RECK. I would expect to obtain the answer if we look at the differential expression of short RECK after introducing mutations in the binding site of specific polyadenylation factors or splicing factors in genomic DNA using CRISPR / Cas9 technology.

In chapter 2, I characterized the role of short RECK by knockdown experiments and revealed that the short form of RECK supports cell invasion. The short form of RECK interacted with the canonical RECK and inhibited cell migration suppression activity of the canonical RECK similar to a dominant negative form. The short form of RECK binds to the MMP 9 binding region of canonical RECK and plays a role in interfering with the interaction between MMP9 and canonical RECK. We still wonder how short RECK competes with MMP9 and does not compete with MMP2. Since MMP9 forms a homodimer and MMP2 does not (Dufour et al., 2010), one possibility is that the difference in RECK binding can be explained by differences in the structure of the MMP. However, the protein structure of MMP2 (PDB: 1RTG) and MMP9 (PDB: 1ITV) has been studied, whereas the protein structure of RECK isoforms has not been available to date. To answer the question, a protein structure study of RECK isoforms should be performed.

Using bimolecular fluorescence complementation assay, I established a method to visualize the interaction between short RECK and long RECK. This method is expected to be useful for small molecule high throughput screening for molecules that interfere with the interaction between short RECK and long RECK. If we discover small molecules that regulate cell invasion, our results may suggest a therapeutic strategy for not only cancer metastasis, but also to other cell migration-related diseases.

The relationship between tubulin posttransalational modifications and cell migration is poorly understood. Based on a previous report that RECK induces glu-tubulin (detyrosinated tubulin) (Morioka et al., 2009), I studied whether short RECK is involved in tubulin PTM and also investigated whether RECK isoforms might affect fibroblast migration by alterating tubulin PTMs. In Chapter 3, I found that RECK can regulate cell migration through tubulin PTMs. Interestingly, knockdown experiments showed that RECK isoforms modulate tubulin PTM differently. My results showed that short RECK supports tubulin acetylation and inhibits detyrosination, which is the opposite of long RECK's role on tubulin PTMs. I was able to reveal that tubulin acetylation supports fibroblast migration and detyrosination inhibits fibroblast migration. Our lab will continue to explore how tubulin PTM affects the migration of fibroblasts. Previous studies have shown that tubulin PTMs affect tubulin dynamics (Magiera and Janke, 2014) and tubulin dynamics affects cell migration (Ganguly et al., 2013). We have successfully visualized tubulin dynamics in fibroblasts by introducing fluorescent protein conjugated EB1 into fibroblasts. We will investigate whether changes in tubulin PTMs in fibroblasts affect tubulin dynamics by introducing shRNAs against TTL or αTAT1, which can alter the tubulin PTM level, into the engineered fibroblast. I also explained the mechanism by which short RECK

regulates tubulin PTMs, by observing that MMP9 liberated from long RECK by short RECK can induce tubulin acetylation through integrin signaling. It will be interesting going forward to determine which integrin is important for tubulin PTMs and which signaling pathway, such as Rac/CDC42 or FAK/Src, is used for tubulin PTMs by the integrin. In sum, I showed through Chapter 3 that migration of fibroblasts can be regulated via tubulin PTMs and that RECK isoforms can regulate tubulin PTMs. This study suggests that RECK isoforms can regulate fibroblast migration by modulating tubulin PTMs in addition to digesting ECM proteins.

The studies covered in this dissertation show that cell migration is regulated through APA, which adds one explanation for understanding the complex mechanisms that control cell migration. At the same time, it shows the molecular mechanism of how the short form of RECK supports cell migration and provides important clues to understanding cell migration during development and wound healing. My research also provides a rationale for the treatment of diseases associated with fibroblast migration. For example, many diabetic patients suffer from chronic wounds due to slow migration of fibroblasts (Blakytny and Jude, 2006). It is possible that if we induce the expression level of short RECK in wounds of these chronic wound patients, we would improve wound healing by promoting the migration of fibroblasts.

REFERENCES

Arjonen, A., Kaukonen, R., and Ivaska, J. (2011). Filopodia and adhesion in cancer cell motility. Cell Adh Migr *5*, 421-430.

Blakytny, R., and Jude, E. (2006). The molecular biology of chronic wounds and delayed healing in diabetes. Diabet Med *23*, 594-608.

Devreotes, P., and Horwitz, A. R. (2015). Signaling networks that regulate cell migration. Cold Spring Harb Perspect Biol *7*, a005959.

Dufour, A., Zucker, S., Sampson, N. S., Kuscu, C., and Cao, J. (2010). Role of matrix metalloproteinase-9 dimers in cell migration: design of inhibitory peptides. J Biol Chem *285*, 35944-35956.

Etienne-Manneville, S. (2013). Microtubules in cell migration. Annu Rev Cell Dev Biol *29*, 471-499.

Ganguly, A., Yang, H., Zhang, H., Cabral, F., and Patel, K. D. (2013). Microtubule dynamics control tail retraction in migrating vascular endothelial cells. Mol Cancer Ther *12*, 2837-2846.

Huang, C., Jacobson, K., and Schaller, M. D. (2004). MAP kinases and cell migration. J Cell Sci *117*, 4619-4628.

Kaverina, I., and Straube, A. (2011). Regulation of cell migration by dynamic microtubules. Semin Cell Dev Biol *22*, 968-974.

Kessenbrock, K., Plaks, V., and Werb, Z. (2010). Matrix metalloproteinases: regulators of the tumor microenvironment. Cell *141*, 52-67.

Magiera, M. M., and Janke, C. (2014). Post-translational modifications of tubulin. Curr Biol *24*, R351-354.

Mitra, M., Johnson, E. L., Swamy, V. S., Nersesian, L. E., Corney, D. C., Robinson, D. G., Taylor, D. G., Ambrus, A. M., Jelinek, D., Wang, W., *et al.* (2018). Alternative polyadenylation factors link cell cycle to migration. Genome Biol *19*, 176.

Morioka, Y., Monypenny, J., Matsuzaki, T., Shi, S., Alexander, D. B., Kitayama, H., and Noda, M. (2009). The membrane-anchored metalloproteinase regulator RECK stabilizes focal adhesions and anterior-posterior polarity in fibroblasts. Oncogene *28*, 1454-1464.

Nabeshima, K., Inoue, T., Shimao, Y., and Sameshima, T. (2002). Matrix metalloproteinases in tumor invasion: role for cell migration. Pathol Int *52*, 255-264.

Vorlova, S., Rocco, G., Lefave, C. V., Jodelka, F. M., Hess, K., Hastings, M. L., Henke, E., and Cartegni, L. (2011). Induction of antagonistic soluble decoy receptor tyrosine kinases by intronic polyA activation. Mol Cell *43*, 927-939.

Yamaguchi, H., and Condeelis, J. (2007). Regulation of the actin cytoskeleton in cancer cell migration and invasion. Biochim Biophys Acta *1773*, 642-652.